NTNU – Trondheim
Norwegian University of
Science and Technology

Organic binder as a substitute for bentonite in ilmenite pelletization

Marius Sunde

Chemical Engineering and Biotechnology
Submission date: June 2012
Supervisor: Leiv Kolbeinsen, IMTE
Co-supervisor: Stian Seim, TiZir Titanium & Iron

Norwegian University of Science and Technology
Department of Materials Science and Engineering

Acknowledgements

This project was carried out at the Department of Material Science and Engineering, at the Norwegian University of Science and Technology (NTNU) during the spring of 2012. The work was done in collaboration with TiZir Titanium & Iron in Tyssedal, Norway, and is related to the research projects ROMA and Gasferrosil.

My supervisor Leiv Kolbeinsen and co-supervisor Stian Seim are gratefully acknowledged for their support and guidance throughout this project. I would also like to thank Edith Thomassen and Shawn Wilson at SINTEF and Kristin Syverud at PFI for their assistance.

Abstract

TiZir Titanium & Iron produces high titania slag and high purity pig iron from ilmenite in Tyssedal. The ilmenite is pelletized before smelting. Bentonite is added to the ilmenite concentrate as a binder to give the pellets strength and durability. Bentonite consists mainly of silica and alumina, which are considered as impurities in the high titania slag production. The use of organic binder has therefore been suggested as a substitute for bentonite.This work has focused on developing knowledge on the pelletization process and investigating various organic binders.

Two methods of agglomeration, pelletization and briquetting, have been used in this work. Three batches of pellets have been made using a laboratory scale pelletizing drum. Two organic binders, Peridur 300 and Peridur 330, have been tested and compared to pellets made with bentonite and without binder. Seven batches of briquettes have been made using a cylindrical mold and a piston. Three organic binders, Peridur 300, calcium lignosulfonate and a nano cellulose fibre have been tested and compared to briquettes made with bentonite and without binder. The characterization included drop number test (pellets only), compression strength and thermal treatment.

Briquettes were employed because using pellets yielded large deviations in the results. These deviations were believed to stem from the varying geometry of the pellets and were substantially mitigated by the use of cylindrical briquettes. It was found that Peridur 300 is a potential alternative to bentonite. The findings from thermal treatment suggest that above 500°C sintering takes over as the dominating binding mechanism. For green strength, increasing binder viscosity has a positive effect.

Samandrag på norsk

TiZir Titanium & Iron produserer høgverdig titanoksidslagg og veldig reint råjern frå ilmenitt i Tyssedal. Før smelting blir ilmenitten pelletisert. Bentonitt blir då tilsatt som bindemiddel for å gi pelletsane styrke. Bentonitt er hovudsakleg samansett av silika og alumina som blir sett på som ureinheitar i høgverdig titanoksidslaggproduksjon. Bruk av organisk bindemiddel er difor blitt føreslått som substitutt for bentonitt. Dette arbeidet har foksuert på å utvide kunnskapen om pelletiseringsprosessen og utforske ulike organiske bindemiddel.

To agglomereringsmetodar, pelletisering og brikettering, vart brukt i dette arbeidet. Tre grupper med pellets vart laga ved hjelp av ein labskala pelletiseringstrommel. To organiske bindemiddel, Peridur 300 og Peridur 330, vart testa og samanlikna med pellets laga utan bindemiddel og med bentonitt. Sju grupper med brikettar vart laga ved hjelp av ei sylindrisk form og eit stempel. Tre organiske bindemiddel, Peridur 300, calcium lignosulfonat og ein nano cellulose fiber vart testa og samanlikna med brikettar laga utan bindemiddel og med bentonitt. Karakteriseringa inkluderte dropnummer-test (berre pellets), kompresjonsstyrke og termisk behandling.

Brikettar vart nytta då bruk av pellets gav store standardavvik i resultata. Den varierande geometrien til pelletsane er truleg orsaken til desse avvika. Bruk av sylindriske brikettar reduserte avvika betrakteleg. Det vart funne at Peridur 300 er eit potensielt alternativ til bentonitt. Resultat frå termisk behandling viser at sintring er den dominerande bindingsmekanismen over 500°C. For grøn styrke har høg viskositet ein positiv effekt.

Contents

List of Figures

List of Tables

List of symbols

Symbol	Description
c_O	Concentration of reducible oxygen atoms in oxides [mol/cm^3]
$D_j^{(eff)}$	Effective diffusivity of species j [cm/s]
Δ_m	Mass change [g]
γ_{lv}	Interfacial tension of liquid/vapor
K_e	Equilibrium constant
$k_{m(i)}$	Mass transfer coefficient for species i [cm/s]
M_n	Molecular weight [g/mol]
$\dot{n}_i$	Molar flow of specie i [mol/s]
$p_j^{(0)}$	Partial pressure of species j at exterior surface [atm]
$p_j^{(b)}$	Partial pressure of species j in the bulk phase [atm]
$p_j^{(i)}$	Partial pressure of species j at interface [atm]
p_j	Partial pressure of specie j [atm]
R	Gas constant
r	Rate of reation [mol/cm^{2}s]
S_H	Spreading coefficient
T	Temperature
θ	Angle
t	Time
T_g	Glass transition temperature
T_g°	Limiting value of glass transition temperature
V	Volume
W_A	Work of adhesion
W_C	Work of cohesion
x_i	Core radius, distance form origin to reaction interface [cm]
x_0	External radius of oxide sphere [cm]

1 Introduction

Titanium is the fifth most abundant metal in the earth's crust and occurs mainly in the minerals rutile (TiO_2) and ilmenite ($FeTiO_3$). Rutile is only one tenth as abundant as ilmenite and the world production is thus limited [1]. Ilmenite is found and excavated worldwide and is often associated with magnetite (Fe_3O_4). The main impurities are magnesium and manganese. Other impurities include V_2O_5, Cr_2O_3, Al_2O_3, CaO, SiO_2 and P_2O_5 [1]. As a metal, titanium is used for applications requiring good corrosion resistance and high strength-to-weight ratio. However, over 90% of the world's consumption of titanium is related to the pigment industry where titanium dioxide (TiO_2) is used for its excellent optical properties.

TiZir Titanium & Iron in Tyssedal, Norway, upgrades ilmenite to high purity pig iron and high titania slag, which is used as a raw material for TiO_2 pigment production. The process they use is a two stage process in which ilmenite concentrate is first pelletized and pre-reduced in solid state, followed by smelting in an electric arc furnace. This is called the Tyssedal process [2] and a schematic overview of it is shown in Figure 1.1 on the next page.

The pelletized ilmenite serve as a feedstock to the arc furnace, but need to endure abrasion during processing before it reaches this step. A binder is therefore added to the ilmenite concentrate. Bentonite is the most common binder for this purpose and is used in Tyssedal as well. It holds the pellet together by forming a solid bridge of hardened gel, strengthening the particle contact points and increasing the van der Waals forces between the particles [3]. However, there are some disadvantages related to using bentonite. Since it is a clay mineral, consisting of silica and alumina amongst other species, it ends up in the final product as an impurity. It would therefore be favorable to substitute bentonite with an organic binder which burns off in the process, reducing impurities in the product. This is, however, not a straight forward undertaking. One of the great benefits of bentonite is its ability to sustain the pellet's mechanical strength until it starts to sinter, at about 500°C to 700°C. Most organic binders on the other hand, will burn off or disintegrate at about 300°C, leaving the pellet virtually unbonded before sintering begins. This can cause severe problems in terms of dust generation or at worst case disintegration of the pellets.

The aim of this study was to expand the knowledge on the pelletization process, explore the possibility of using an organic binder for ilmenite pelletization and develop a method for comparison of binders.

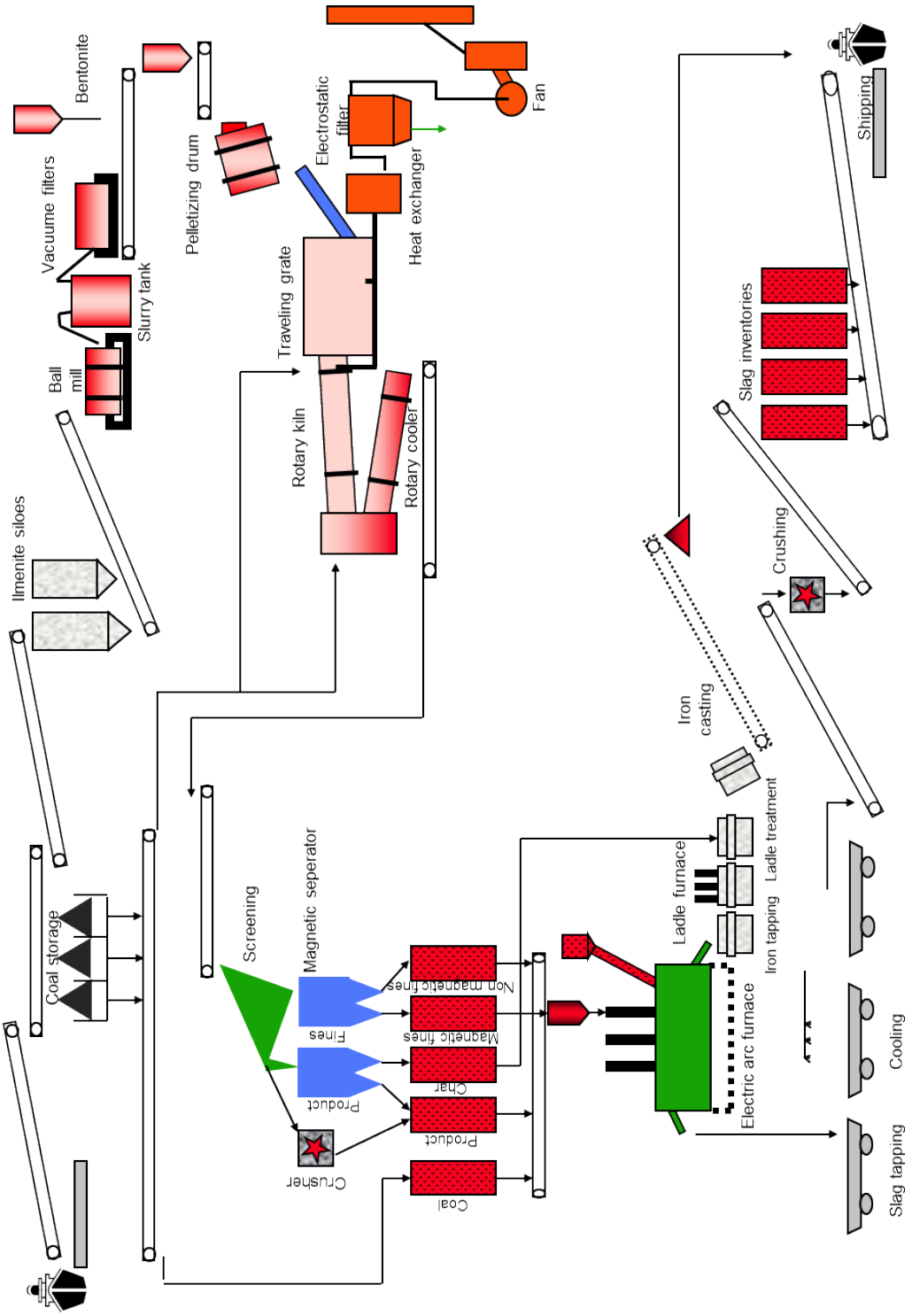

Figure 1.1: Schematic overview of the Tyssedal process [1].

2 Background

2.1 Agglomeration techniques

When ore is mined from the ground a large portion is considered to be gangue material. As a result of this the ore must be concentrated, which involves grinding it to very fine particles before it is shipped to a processing plant. This fine material is usually not suitable for further processing and needs to be agglomerated into larger particles in order to achieve required properties. Pelletization, sintering, nodulizing and briquetting are the most commonly used techniques. These techniques are presented below.

Pelletization

Pelletization is the process of rolling pulverized material into little balls using a drum or disc. A binder is usually mixed into the raw material to make the pellets strong and water is added to increase the capillary forces between the particles and bind them together. Pellets that have not been burnt are referred to as "green pellets". To obtain strength they are fired to form solid state bonds between the particles [3]. The process is applied in several streams of industries including mineral processing, agricultural products, detergents, pharmaceuticals and specialty chemicals to name a few [4]. The pelletization process is the main focus of this study and is therefore further discussed in Section 2.2.

Sintering

Sintering is done by mixing a solid fuel, such as coal, with fine particles and igniting the mixture on a travelling grate with air flowing from above. The fine particles are then bonded by partial melting into a porous material suitable for, amongst other things, blast [4] and arc [5] furnace feed. Due to breakage and abrasion during handling, sintering should be done close to the utilization point.

Nodulizing

This process involves feeding fine particles to a rotary kiln and heating to the point when melting starts to occur. Nodules are formed as the charge is tumbled in the kiln and bonded together by the liquefied portion of the partially melted fines. Advantages include insensitivity to feed moisture and particle size and high strength of nodules. Disadvantages include high operating cost, variable nodule size and poor chemical reactivity. This process is no longer in general use [4].

Briquetting

Briquetting is a cold bonding method which involves pressing mixtures of fine particles into lumps of composite particles using rolls, extruders or similar devices. To produce additional strength, the briquettes may be fired afterwards [3]. The technique is generally more expensive than other agglomeration techniques due to wear of equipment and energy consumption [4].

2.2 Pelletization and pellet processing

In many industries the pelletization process is a key step and problems here can cause serious errors in later stages of the process. It has therefore been a great incentive in the industry to advance the knowledge on the pelletization process. Over the last 50 years a great deal of research has been published on agglomeration methods and mechanisms [6], yet the process of pelletization has remained more of an art than a science, highly based on trial and error and experienced operators. However, during the last decade the qualitative understanding of the effects of different variables on the process has advanced rapidly. Nucleation, growth and breakage phenomena was recently reviewed by Iveson et al.[6]. Binder viscosity has been recognized as an important parameter in controlling granulation behaviour and agglomerate plasticity has been emphasized and intensively studied during recent years [7].

A rough scheme of the pre-reduction step in the Tyssedal process is illustrated in Figure 2.1. The process starts with wet grinding of ilmenite using a ball mill in order to make it suitable for pelletizing. The ilmenite slurry is then dewatered using a vacuum filter to obtain the proper water content, followed by addition of binder and recycled material. Pelletization is done in a balling drum, 10 meters long and 3 meters in diameter, rotating at 4-8 rpm [2]. Green pellets are screened to separate the production size fraction (8-12 mm) for further processing. Undersized pellets are returned directly to the balling drum while oversized are crushed before recycling. It is believed that each finished green pellet has been through the balling drum at least twice. The production rate of green pellets in Tyssedal is typically 60 t/h [8].

In order for the pellets to gain strength and enhance kinetic properties, they are pre-oxidized by firing them with a gas mixture of air and CO_2. This is done by distributing wet pellets onto a travelling grate with a bed height of about 30 cm. This travelling grate is made up of four different zones. In zone one and two, an updraft of gas at 150-200°C and downdraft at 250°C, respectively, removes water from the green pellets. When the pellets exit zone two, the upper part of the pellet bed is dry and warm while the bottom of the bed is still partly humid. In zone three, gas at 850-900°C flows through the bed from above to burn the pellet. In zone four the pellet bed is conditioned to obtain a uniform temperature. After this the pellets are transferred into a rotary kiln in which they are reduced at 1100-1200°C using coal to about 60% metallization [2]. This whole step is called

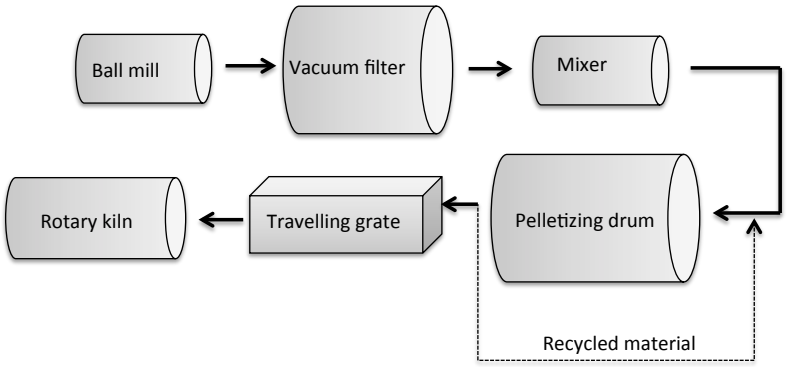

Figure 2.1: Process scheme of the pelletizing process in Tyssedal.

the pre-reduction. These pre-reduced pellets make up the feed for the electric arc furnace in which they are smelted and further reduced. Finally, the high titania slag and iron are separated and prepared for distribution.

2.3 Types of binders

The binder has two main objectives: Firstly, it has to make the ore plastic so it will nucleate seeds which will grow into well formed pellets. Secondly, it has to hold the pellet together during handling, drying and preheating or until it has been sufficiently strengthened by sintering. The optimum binder should produce high-quality pellets at a minimum cost and introduce as little contaminants as possible. It should also be non-toxic, easy to handle and not require an advanced feeding system. Hundreds of different materials have been suggested for this purpose. Eisele and Kawatra [4] recently reviewed alternative binders for pelletization of iron ore. Below is a brief synopsis of their review with a few additional contributions.

Organic polymers and fibres

Organic binders have been considered a substitute for bentonite. However, due to high cost and inferior thermal stability they have not been fully embraced in industry. A lot of research is being done to further develop organic binders ([9] [10] [11]). It is of great interest for a wide variety of industries that this research yield results. If bentonite can be substituted with an organic binder, contaminations in the products might be mitigated.

Peridur

Peridur is an organic binder produced by AkzoNobel that has been extensively tested and even applied at an industrial scale [4]. The chemical structure of Peridur

300 and 330 is shown in Figure 2.2. The molecule is called polyanionic cellulose (330) or sodium carboxymethyl cellulose (300), depending on the proportion of -CH_2COONa.

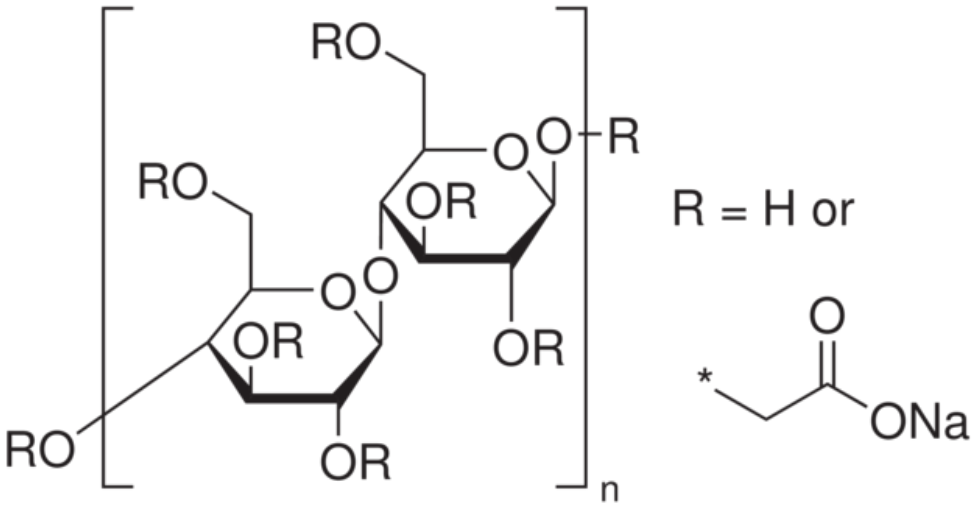

Figure 2.2: Chemical structure of polyanionic cellulose (PAC) and sodium carboxymethylcellulose (CMC)[12].

The strength of green pellets bonded with Peridur has shown to be comparable to pellets bonded with bentonite at low temperatures [4]. However, when the temperature exceeds about 300°C, Peridur starts to disintegrate, leaving the pellet very fragile [13]. The extent to which this is a problem depends on how roughly the pellets are treated during the preheat and firing stage [4].

Calcium Lignosulfonate

Borregaard Lignotech in Sarpsborg produce Calcium lignosulfonate ($C_{20}H_{24}CaO_{10}S_2$) (CaLS). This is an amorphous material derived from lignin, a highly polymerized material that makes up the middle lamella of woody fibers and holds the fibers together [14]. It has an average molecular weight in the range of 40 000 to 65 000 and is produced from softwood in the sulfite pulping method for manufacturing paper [14]. A proposed structure of a polymeric fraction of calcium lignosulfonate is shown in Figure 2.3.

Nano cellulose fibre

A nano cellulose fibre (NCF) has been developed at the Paper and Fibre Research Institute at NTNU. The material is derived from cellulose fibres which have been disintegrated into submicron- and nanofibrils [15]. A surface image, schematic representation and diameter distribution of a NCF sample are shown in Figure 2.4.

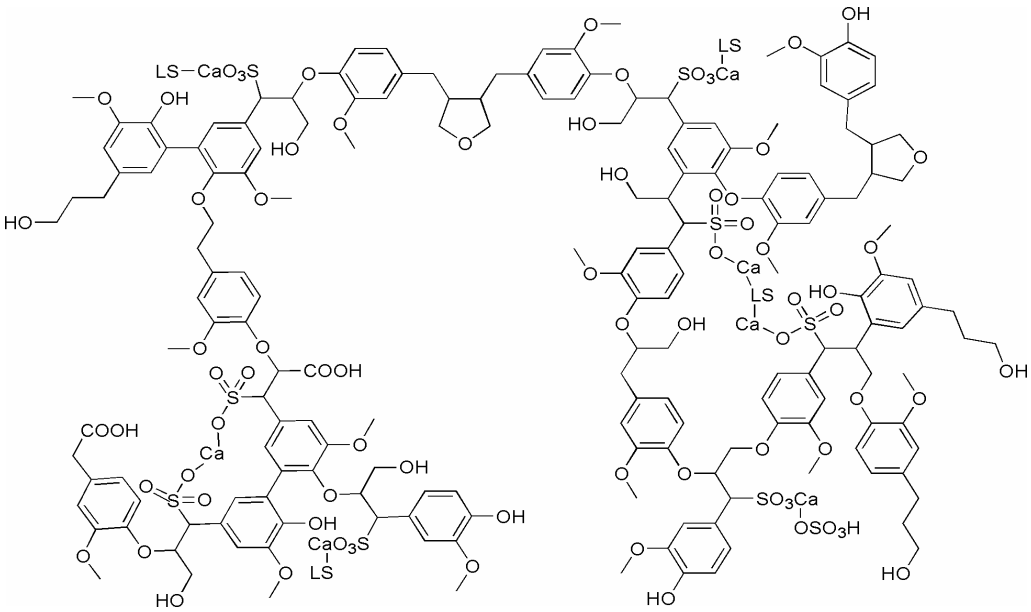

Figure 2.3: Polymeric fraction of calcium lignosulfonate [14].

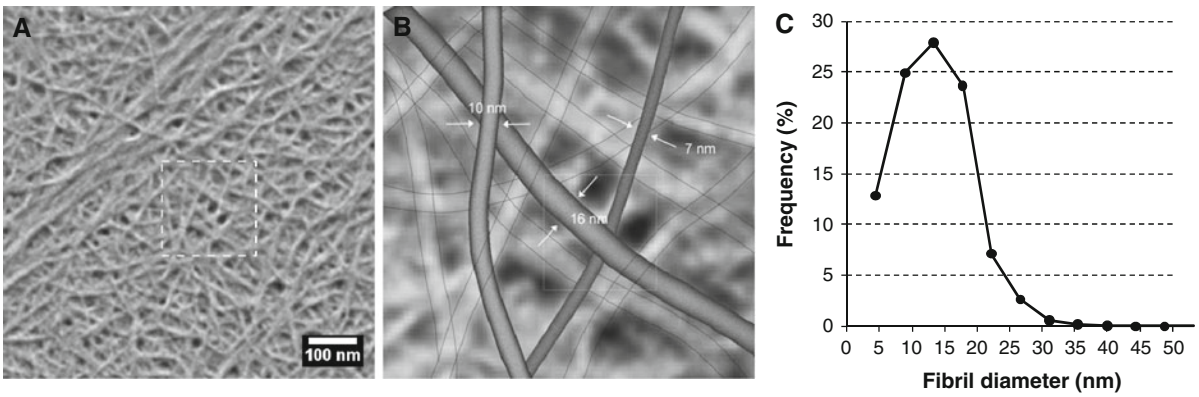

Figure 2.4: A) FE-SEM surface image. B) Schematic representation of the fibrils indicated in the area marked with a dashed rectangle in the left-image. C) Diameter distribution of a cellulose nanofibril sample [15].

Nano fibrils have a large length to width ratio and are highly crystalline giving them exceptionally good mechanical properties [15]. Being hydrophilic and with great ability to form interfibrillar hydrogen bonds, NCF form very strong thin films [15], which is a key binding mechanism in green ilmenite pellets. NCF also have a great capability to adsorb water. Today, the high cost of producing nano cellulose fibre severely limits the possibility of using it as a pellet binder on an industrial scale.

Cement and cementitious materials

Portland cement is a well known cementitious binder and is composed largely of CaO and SiO_2. These species are considered as impurities in high titania slag production and must separated out at a later stage. Portland cement works by reacting with water to form a hard, hydrated cement. The binding action is irreversible. In order to harden a pellet, a cementitious binder requires a substantial period of time, typically several hours. This makes it undesirable in many continuous processes.

Lime ($Ca(OH)_2$) is another cementitious material that hardens when mixed with water is and left to dry. It has been successfully used as a binder in a few cases and it has been reported that the performance of the pellet has been improved [4]. However, usage of this binder requires precise control of the physical properties of the concentrate and very rigorous plant procedures.

Bentonite

Bentonite is a clay consisting of a mixture of layered hydrated aluminosilicate primarily composed of montmorillonite with the ideal chemical formula $(Na,Ca)_{0.33}(Al_{1.67},Mg_{0.33})Si_4O_{10}(OH)_2$ x nH_2O [4]. The basic crystal structure is shown in Figure 2.5. Highly stable three-layer aluminosilicate platelets are loosely held together by electrostatic forces and make up the crystalline structure of bentonite. The lattice has a net negative charge due to isomorphic substitution of Al^{3+} with Mg^{2+} into the tetrahedral SiO_4 sheets which alters the crystal charge balance [4]. The net negative charge is balanced by surface adsorption of cations (commonly Na^+ and Ca^{2+}). Bentonite expands vastly upon wetting due to hydration of these exchangeable interlayer cations allowing water to be absorbed between the layers of the crystal [16]. Bentonite is the most common binder used for industrial ore pelletization [4]. Dry strength of ilmenite pellets is increased by bentonite in two ways. Firstly, it decreases interparticle distance by providing a colloidal material, thus increasing the van der Waals forces. Secondly, it forms a solid bridge of hardened gel that strengthens particle contact points. The binding mechanism of bentonite is illustrated in Figure 2.6.

Although bentonite has some very profound qualities as a binder for ilmenite pellets there are incentives to reduce the amount of bentonite used or find alternative

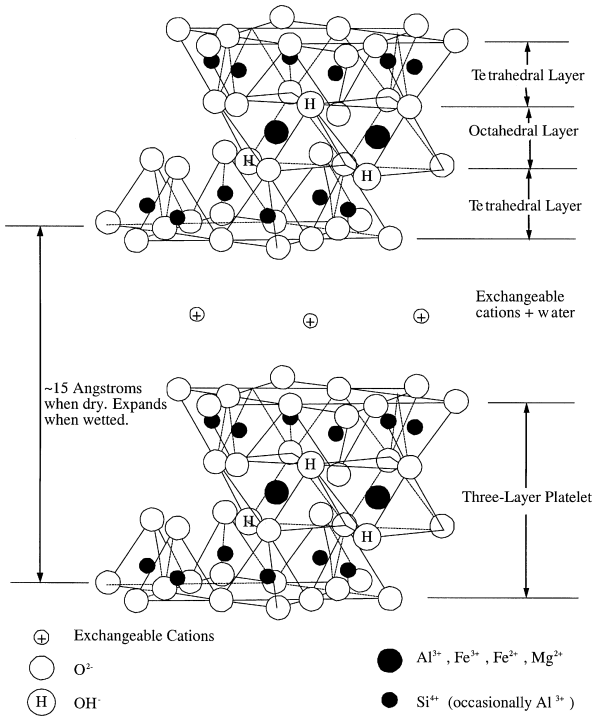

Figure 2.5: Structure of the smectite crystal. Each clay platelet consists of three layers. The platelets are loosely bonded by counterions (typically Na^+ or Ca^{2+}) between them [16].

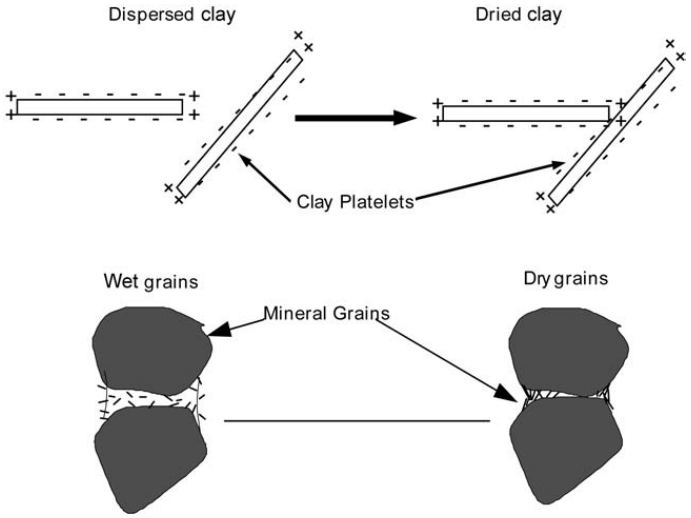

Figure 2.6: Traditional view of how bentonite platelets bind mineral grains in a pellet [4].

binders. Bentonite is challenging to handle and as mentioned before, contaminates the product.

Salts and precipitates

By dissolving salt in the water used for pelletization, the salt will crystallize and bind mineral grains as the water evaporates. Experiments have shown that the salt crystallizes on the pellet surface leaving the core of the pellet fragile [17]. This effect can be reduced by adding bentonite or another material that slows down the drying rate [17].

A precipitate that has been tested is urea ($CO(NH_2)_2$). This substance is completely dissolvable in water, but will solidify as the water evaporates. It has been shown to give good pellet strength up to about 150°C after which it burns off, leaving the pellet virtually unbonded [4]. Also, salts are known to cause refractory deterioration [18]. It is therefore not a desirable substance to use for high temperature processes.

Inorganic polymers

Sodium silicate is an example of an inorganic polymer which can form chains and cross-linked network and act as a binder. It is commonly used as binder for foundry sands, where it acts as a binder through its ability to form a bond consisting of precipitated silica gel, sodium silicate and silicic acids [19].

Binder combinations

There has been some investigation on the effects of mixing binders of different types [4]. However, the results have not shown any synergies. Binding properties have been intermediate between the two binders or even inferior to the use of the binders exclusively.

3 Theory

3.1 Important pellet properties

Pellets need to attain certain properties to allow for the process to run smoothly. These properties are presented in the next sections.

Green strength

The green pellets are handled quite roughly both in the pelletizing drum and during transport on conveyor belts. Elasticity is important for the green pellets' durability during handling, and is usually described by its drop number, which will be explained in Section 4.4. Adding more binder to the concentrate, generally increases elasticity and hence the drop number. Increasing the moisture content has the same effect.

Plasticity was recognized by Forsmo et al. [20] as a very important green pellet property. In order to enable growth, the plasticity needs to exceed a minimum level. The plasticity also affects the mechanical strength of green pellets. High plasticity makes the green pellets more resistant to rough handling. However, it is desirable to keep the plastic deformation at a lowest possible level [20]. In the pellet bed the load of above-lying pellets plastically deform the pellets underneath, which will decrease the permeability of the bed and is detrimental for drying, oxidation and burning. This property is largely controlled by moisture content [20].

Dry strength

Much of the consolidating forces disappear as the pellets are dried and water evaporates. The binder's main task is to hold the pellet intact until the particles start to sinter together. This is a very crucial part of the process and a successful outcome is very important. If the pellets are not sufficiently bonded, a great deal of dust will be generated and the pellet bed may collapse.

Burnt strength

The burnt pellets need to be robust in order to withstand the harsh treatment they receive in the rotary kiln. They are subjected to substantial abrasive wear and elevated temperatures. An illustration of the pellets' behaviour inside a rotary kiln is illustrated in Figure 3.1 on the next page. Insufficient pellet strength may result in substantial amount of fine dust being generated, or even total disintegration of the pellets.

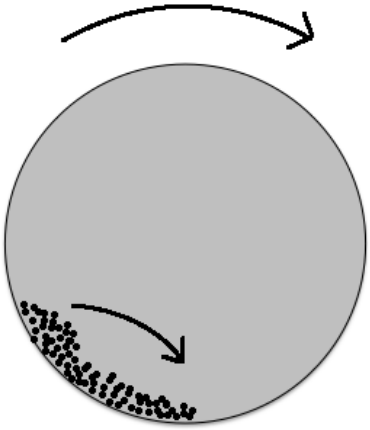

Figure 3.1: Pellet behaviour inside a rotary kiln.

Porosity

When the pellets reach the rotary kiln, they are reduced with CO as the reducing agent. CO-gas diffuse into the pellet, react with the ilmenite and leave as CO_2. Hence, it is important that the pellets are porous so gas can diffuse in and out. This will be described in more detail in Section 3.4. High porosity, however, leads to poor particle-particle contact, which decreases the mechanical strength of the pellet. A compromise between pellet strength and diffusivity must therefore be met.

3.2 Criteria for binders

The binder plays a very important role in the pelletization process and need to meet certain criteria. A brief discussion of these criteria is given in the paragraphs below.

Wettability

When a liquid comes in contact with a solid surface, it spreads like a drop. This process is called wettability and is illustrated in Figure 3.2. Good wettability (small θ) is important in order for maximum adhesion to occur. Qui et al.[10] say that in order for liquid to spread on a solid, the work of cohesion of the liquid must be less than the work the work of adhesion of the liquid on the solid. They defined the spreading coefficient (S_H) as the difference between work of adhesion (W_A) and work of cohesion (W_C), as given below.

$$S_H = W_A - W_C \tag{3.1}$$

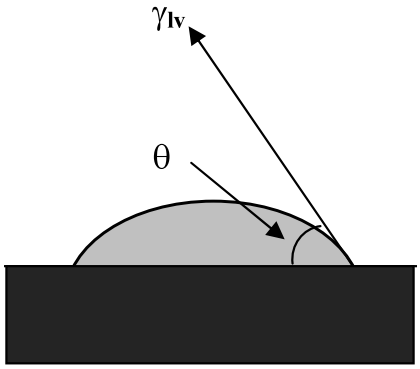

Figure 3.2: Contact angle of a liquid on a solid surface is often used as a measure for wettability [10].

As shown by Qui et al.[10], this coefficient can be expressed by the following equation:

$$S_H = \gamma_{lv}(\cos\theta - 1) \tag{3.2}$$

where S_H is the spreading coefficient, γ_{lv} is the interfacial tension of liquid/vapor, and θ is the contact angle. From this equation it can be seen that if γ_{lv} is kept constant, a smaller contact angle yields a greater spreading coefficient. For an organic binder, hydrophilic functional groups should be introduced into the binder molecules in order to obtain this property [10].

Adhesive force

The binding force at the interface between binder and ore particles is referred to as the adhesive force. The main attractive molecular force is chemical bonds, here mainly ionic bonds. Hydrogen bonds are also markedly stronger than van der Waals bonds, which are almost negligible due to the distance between particles within the pellet. To promote adhesive forces between binder molecules and ore particles, polar functional groups and hydrogen bond groups should be introduced into the molecule [10].

Cohesive force

The mechanical strength of the binder itself is referred to as cohesive force, which is the main binding force of the viscous binder. For an organic binder, this property depends on the chemical structure, molecular weight, crystallinity and the extent of cross-linking and branchin [10].

Thermal stability

When water has evaporated from the pellet it is mainly the binder that holds it together. It is therefore of paramount importance that the binder can withstand the temperatures the pellet is subjected to before it starts to sinter. Previous work has shown that use of organic binder yield good green pellet properties but insufficient dry strength [4]. This is because organic binders display good viscoelasticity at room temperature, but lose viscoelasticity and become more fragile at elevated temperatures. Upon heating, an organic polymer may undergo physical softening and melting, chemical oxidation, degradation and decomposition. Hence, the mechanical strength of the binder, and thus the pellets, is dramatically weakened. Good thermal stability is therefore essential when choosing an organic binder for ilmenite pelletization. This property will depend on the selection and design of the chain skeleton of the molecule, which will be discussed in Section 3.3.

Bentonite is thermally stable and will not burn off in the process. Even though this is negative for the final product it has a positive effect on the pellet strength. Sodium and calcium components in bentonite can act as fluxing agents during sintering and reduce the melting point of some minerals in the pellet [4]. A portion of the pellet will then melt before sintering temperature is reached, strengthening the pellet during preheating [4].

Binder viscosity

The binder viscosity has a great influence on both the growth rate and the strength of the pellets [20]. Low viscosity leads to surface water coalescing more quickly and can give uncontrollable growth. If the viscosity is increased the surface water coalesces more slowly and makes it easier to control the growth. The ideal viscosity is so that superficial water on the growing pellets and on the ore concentrate feed can coalesce within the time available during collision. Forsmo et al. [20] suggest that green pellets are over-saturated and viscous liquid form a ”network” at the surface. This ”network” makes up more than half of the total binding force due to its cohesive force.

3.3 Structure of organic binders

In the literature, many reports ([9] [11] [21]) on organic binders for agglomeration are based upon empirical research using different organic substances and varying the dosages. Very few reports have been made on the molecular structure of the binder, and this may be one of the reasons for the limited development and employment of organic binders in industry. Based on the principles of molecular design, interfacial chemistry and polymeric science, Qui et al. [10] investigated the functions and molecular structure for an ideal organic binder for iron ore pellets. They suggested a structure mold for an ideal organic binder. This structure mold is shown in Figure 3.3.

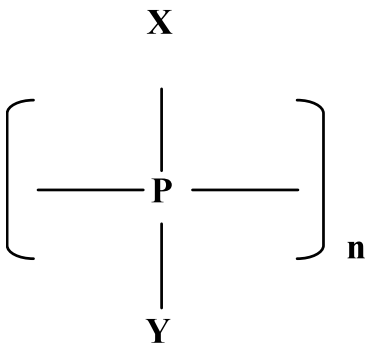

Figure 3.3: Molecular structure mold for organic binder for iron ore pelletisation. X = polar group; Y = hydrophilic group; P = organic chain skeleton; n = polymerization degree [10].

The chain skeleton, P, the different functional groups, X and Y, and the polymerization degree, n, are presented in more detail in the following sections.

Polar functional group, X

The main cations in an ilmenite pellet are Ti^{4+}, Fe^{3+} and Fe^{2+}. According to Lewis acid-base theory [22], the two former are classified as hard acids, and the latter as an intermediate acid. This means that the following polar groups will react with these ions: $-COO^-$, -OH, $-CONH_2$, $-NH_2$, $-NO_2$, =NH, $-N^+R_3$, $-PO_3H$, $-OSO_3H$, -SH, etc. However, polar groups containing sulphur and phosphorous should be avoided as these will result in impurities in the product. Qui, et al. [10] considered ionization potential, electronegativity and bond ionicity and concluded that $-COO^-$ is an ideal polar group.

Hydrophilic functional group, Y

Most of the polar groups also function as hydrophilic groups, but the type of hydrophilic groups will affect the affinity of polar groups. An electron-withdrawing group (e.g. SO_3H, NO_2, -COOH) will reduce the affinity of polar groups, while an electron-donating group (e.g., -OH, -SH) will enforce the affinity of polar groups. -OH is therefore a good candidate as the hydrophilic group [10].

Chain skeleton, P

In order to obtain good mechanical strength and thermal stability, the chain skeleton should have as many double and triple bonds in the molecules as possible. These bonds have much higher bond energies than single bonds and make the molecule more rigid. In general, decreasing flexibility of the polymer chain will

lead to an increase in both melting temperature (T_m) and glass transition temperature (T_g), which is the temperature at which an amorphous polymer goes from a rubbery and viscous liquid to a brittle and glassy solid. This can be achieved by increasing aromatic composition of the main chain or by incorporation of bulky substituents or non-rotational groups in the main chain [10].

Polymerization degree, n

The molecular weight of a polymer is determined by its degree of polymerization. Increased molecular weight results in greater chain interactions and improved mechanical strength. This is due to the neighboring binder molecules becoming more "wrapped" up in each other, allowing for more dissipation of stress forces. Such behaviour is illustrated in Figure 3.4. Entanglement also increases adhesion and improves the bond strength at the interface between particles.

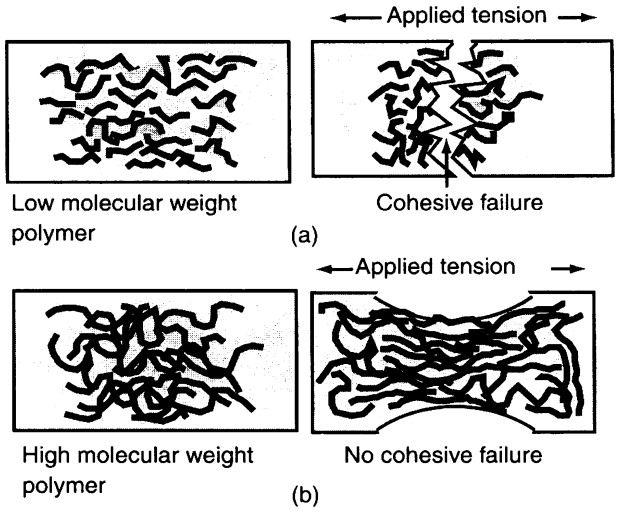

Figure 3.4: Effect of molecular weight of polymer on its cohesive strength [10].

The glass transition temperature increases with increasing molecular weight up to a moderate molecular weight. As shown by Qui, et al. [10], this can be expressed mathematically with the following expression:

$$T_g = T_g^\circ - \frac{K}{M_n} \tag{3.3}$$

where T_g° is the limiting value of T_g at high molecular weight, M_n the number-average molecular weight and K is a constant for a given polymer.

It is obvious that the higher the molecular weight, the better are the mechanical and thermal properties of a binder. However, the viscosity of the polymer solution will increase rapidly with increasing molecular weight, which in turn reduces the wettability. Thus, a compromise between viscosity, mechanical properties and thermal stability must be met.

3.4 Reduction of ilmenite pellets

The Fe-Ti-O system

The phase diagram for Fe-Ti_3O_5-TiO_2-Fe_2O_3 at 950°C, by Borowiec and Rosenqvist [23] is shown in Figure 3.5. The alpha-oxide (M_2O_3) varies from hematite (Fe_2O_3) to ilmenite ($FeTiO_3$). The spinell phase (M_3O_4) vary in composition from magnetite (Fe_3O_4) to ulvospinell (Fe_2TiO_4). Ferri-pseudobrookite (Fe_2TiO_5) and ferro-pseudobrookite ($FeTi_2O_5$), with respectively trivalent and divalent iron, form a solid solution with a M_3O_5 structure. The four numbered three phase areas in the diagram are:

1. Fe + Wustite ("FeO") + spinell
2. Fe + spinell + alpha-oxide
3. Fe + alpha-oxide + rutile
4. Alpha-oxide + rutile + pseudobrookite

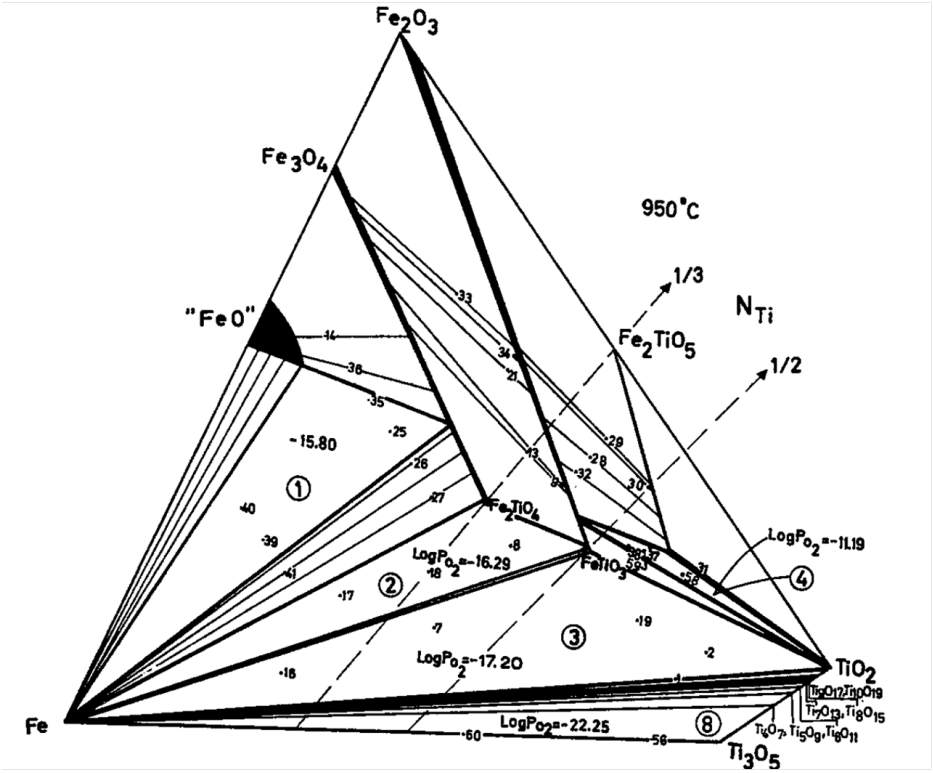

Figure 3.5: Equilibrium phase diagram for the system Fe-Fe_2O_3-TiO_2 at 950°C [23].

Reactions

Reduction of ilmenite with carbon at temperatures above 1000°C proceeds through carbon monoxide as a gaseous intermediate. Zhao [24] found that the following

reactions occur when using CO as reducing agent:

$$Fe_2TiO_5(s) + CO(g) + TiO_2(s) = 2FeTiO_3(s) + CO_2(g) \tag{3.4}$$

$$FeTiO_3(s) + CO(g) = Fe(s) + TiO_2(s) + CO_2(g) \tag{3.5}$$

$$Fe_2O_3(s) + 3CO(g) = 2Fe(s) + 3CO_2(g) \tag{3.6}$$

$$nTiO_2(s) + CO(g) = Ti_nO_{2n-1}(s) + CO_2(g) \tag{3.7}$$

Poggi et al. [25] showed that the reduction of iron oxides in ilmenite occur in two stages. First, hematite is reduced with CO as reducing agent by the following reaction:

$$Fe_2O_3 + CO(g) = 2Fe + 3CO_2(g) \tag{3.8}$$

Secondly, the ferrous iron in ilmenite is reduced to metallic iron as follows:

$$FeTiO_3 + CO(g) = Fe + TiO_2 + CO_2(g) \tag{3.9}$$

The two reactions have been shown to occur consecutively and independently of each other [25].

Depending on temperature and the CO/CO_2 ratio the reverse Boudouard reaction, given below may occur.

$$2CO(g) = C(s) + CO_2(g) \tag{3.10}$$

The reverse Boudouard reaction is catalyzed by metallic iron produced under reduction of ilmenite [26]. The composition of binary CO/CO_2 gas mixtures in equilibrium with solid carbon and ilmenite as a function of temperature is shown in Figure 3.6.

The top right corner of this diagram shows the temperatures and gas compositions at which reduction without carbon deposition is possible. The rate of carbon deposition is mainly affected by composition of reducing gases and the reducing temperature [26].

Reduction degree

By assuming that all iron in the ilmenite is in the form of Fe_2O_3, the reduction degree can be calculated using Equation 3.11

$$\text{Reduction degree} = \frac{\Delta m}{\%Fe \cdot m \cdot M_{Fe} \cdot \frac{3}{2} \cdot M_O} \tag{3.11}$$

where Δm is the mass change, %Fe is the weight percent iron in the sample, m is the sample mass and M_{Fe} and M_O are the molar mass of iron and oxygen, respectively.

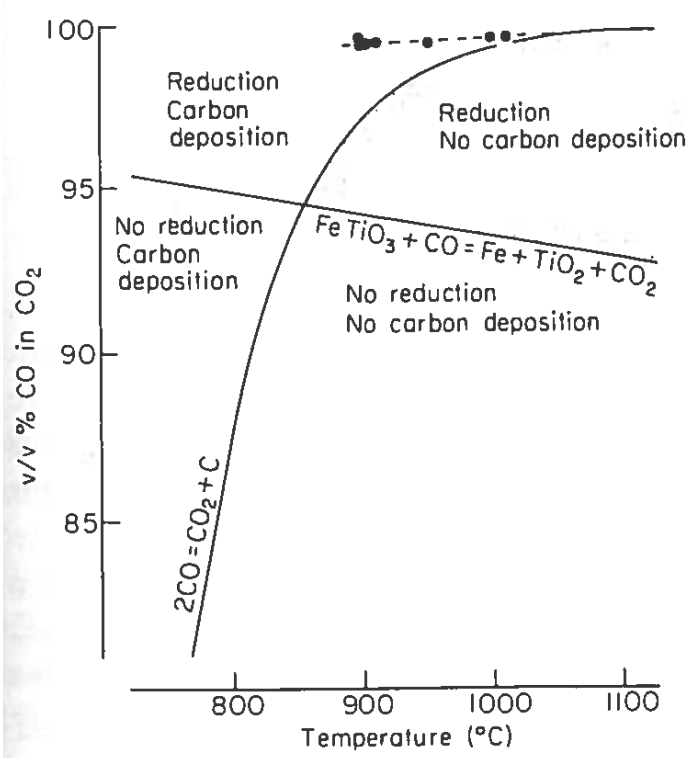

Figure 3.6: CO/CO_2 gas composition in equilibrium with carbon and ilmenite as a function of temperature. - - - • - - - , Observed disproportionation of CO over reduced ilmenite [26].

Kinetics of ilmenite reduction

Gas-solid reactions, see Equation 3.12, play an important role in the materials production industry and have been extensively studied in the past [27].

$$\mathrm{MO(s) + aA(g) = M(s) + bB(g)} \tag{3.12}$$

The reaction is a heterogeneous reaction occurring at phase boundaries accompanying mass and heat transfer between reaction interface and bulk phase. As this is a non-catalytic reaction of particles with surrounding gas, the shrinking core model can be used to illustrate what is occuring. This model assumes that the reaction first occur at the outer surface of the particle and then moves into the solid. As the core of unreacted material shrinks, an outer layer of completely converted and inert material is left behind. Spitzer et al. [28] developed a generalized mathematical model to describe the kinetics of gas-solid reactions of dense spheres. For analysis they identified five steps, as summarized below. The steps are illustrated in Figure 3.7 on the next page.

1. Transfer of gaseous reactant, A, from bulk gas through stagnant gas film to the external surface of the solid particle. (gas-film resistance)

2. Diffusion of gaseous reactant through a porous product layer into the interface of the unreacted core. (shell-layer resistance)

3. Chemical reaction between gaseous and solid reactants at reaction interface. (interface resistance)

4. Diffusion of gaseous product, B, through the porous product layer towards the outer surface of the particle. (shell-layer resistance)

5. Transport of gaseous product through the gas film and into the bulk phase. (gas-film resistance)

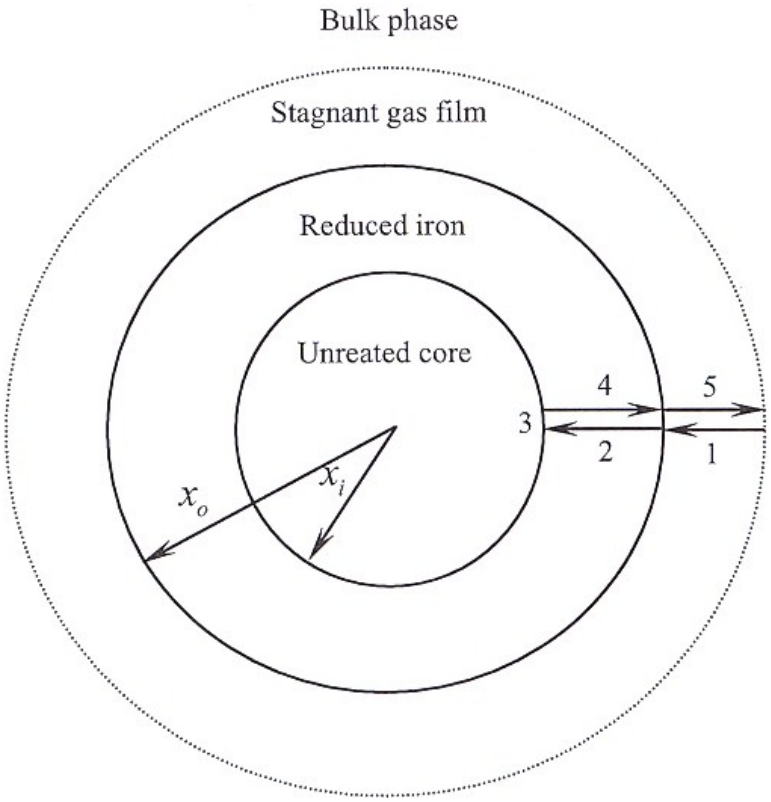

Figure 3.7: Generalized model for dense particle reduction under mixed control [28].

Using an electric analogy these steps offer resistance in series to the overall chemical reaction, driven by potential differences expressed as differences in partial pressure or consumption of gas species. The rate of transfer of oxygen and reaction rate is then the "current" referring to Ohm's law. The rate of removal of oxygen from a single oxide particle is equal to the molar oxygen density of the core times the rate of consumption of the core volume. Expressed mathematically for a sphere gives,

$$\dot{n}_O = c_O \frac{dV}{dt} = c_O 4\pi x_i^2 \frac{dx_i}{dt} \tag{3.13}$$

Since the pellet consists of different oxides that are reduced, the only mass transfer out of the pellet is that of oxygen. CO goes into the pellet and leaves as CO_2. This can be expressed mathematically as,

$$\dot{n}_O = \dot{n}_A = -\dot{n}_B \tag{3.14}$$

Resistances

Spitzer et al. [28] showed that an expression for the molar flow of gaseous reactant and product in the five diffusion steps can be obtained. Below is a brief summary of this.

i) Gas-film resistance

The molar flow of gaseous reactant from the bulk phase to the outer surface of the pellet is given by:

$$\dot{n}_A = -(\frac{k_{m(A)}}{RT} 4\pi x_0^2) \cdot (p_A^{(b)} - p_A^{(0)}) \tag{3.15}$$

The molar flow of gaseous product from the exterior of the pellet through the gas film to the bulk phase can be expressed similarly:

$$\dot{n}_B = +(\frac{k_{m(B)}}{RT} 4\pi x_0^2) \cdot (p_B^{(0)} - p_B^{(b)}) \tag{3.16}$$

ii) Shell-layer resistance

The molar current of gaseous reactant or product through the porous pellet at any time and position is:

$$\dot{n}_j|_{x,t} = -4\pi x^2 \frac{D_j^{(eff)}}{RT} (\frac{\partial p_j}{\partial x})_{x,t} \tag{3.17}$$

Integrating this equation across the shell layer at any time t between the external surface x_0 and the position of the unreacted core at x_i yields:

$$\dot{n}_A = -(\frac{4\pi x_i x_0}{x_0 - x_i} \cdot \frac{D_A^{(eff)}}{RT})(p_A^{(0)} - p_A^{(i)}) \tag{3.18}$$

$$\dot{n}_B = +(\frac{4\pi x_i x_0}{x_0 - x_i} \cdot \frac{D_B^{(eff)}}{RT})(p_B^{(i)} - p_A^{(0)}) \tag{3.19}$$

The effective diffusivity is less than the normal gas-phase diffusion coefficient because transport can only occur in the voids of the porous pellet and must follow a

tortuous path.[28]

iii) Interface resistance

The rate of the surface reaction is proportional to the area of the receding interface:

$$-\dot{n}_A = +\dot{n}_B = -\dot{n}_O = r_O 4\pi x_i^2 \tag{3.20}$$

It is assumed that the reaction follows first-order, reversible kinetics. The rate of the surface reaction is then given by:

$$r_O = \frac{k_r}{RT}(p_A^{(i)} - \frac{p_B^{(i)}}{K_e}) \tag{3.21}$$

iv) Generalized expression

Mass transfer or chemical reaction is driven by the partial pressure difference, which is proportional to the flow. The flow of gaseous reactant inward and gaseous product outward is described the molar current equations, i.e Eq. 3.15, 3.16, 3.18, 3.19 and 3.21. These equations may be converted into terms of oxygen removal and rearranged. Adding all these equations together and performing algebraic addition yields an Ohm's law type relation for the rate of reaction. The driving force is expressed in terms of bulk-phase concentration of reactant and product gas.

$$[\frac{1}{\alpha 4\pi x_0^2} + \frac{x_0 - x_i}{\beta 4\pi x_i x_0} + \frac{1}{k_r 4\pi x_i^2}] \cdot [-\dot{n}_O] = \frac{1}{RT}[p_A^{(b)} - \frac{p_B^{(b)}}{K_e}] \tag{3.22}$$

where

$$\alpha = \frac{K_e k_{m(A)} k_{m(B)}}{K_e k_{m(B)} + k_{m(A)}} \tag{3.23}$$

and

$$\beta = \frac{K_e D_A^{(eff)} D_B^{eff}}{K_e D_B^{(eff)} + D_A^{(eff)}} \tag{3.24}$$

The left hand term of Equation 3.22 expresses the total resistance to the overall reaction. These terms may be identified, from left to right, as gas-film, shell layer and interface resistance. The overall resistance tends toward infinity as the radius of the unreacted core approached zero. Thus the rate of oxygen removal approaches zero as the unreacted core is consumed.

The rate-determining step can depend on the reaction conditions and there may not be a single step determining the overall rate. It is therefore essential to know how the individual steps interact with each other when determining not only the rate-determining step but also when considering if other steps need to be taken into account.

Effect of temperature

Jones [26] studied the reaction rate of pre-oxidized Capel ilmenite at various temperatures in the range of 900-1200° C using CO gas as the reducing agent. The results are summarized in Figure 3.8 and 3.9. Figure 3.8 shows that the rate curves are displaced towards a faster reaction rate and higher peak values with increasing temperature. However, from Figure 3.9, on the next page, we see that this trend is reversed for temperatures above 1000°C, and at 1200°C there is no longer a two-peak behaviour. Jones [26] also observed that the reactivity curve for pre-oxidized ilmenite had a positive inflection at 930°C and peaked at approximately 1000°C. This can be explained by increasingly severe sintering of reaction mass when the temperature exceeds approximately 1000°C.

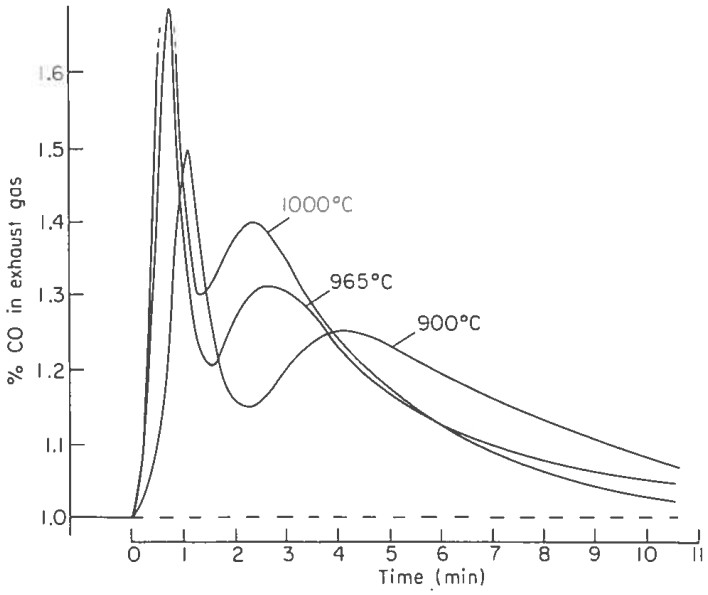

Figure 3.8: Rate curves at temperatures up to 1000°C for preoxidized Capel ilmenite [26]. (There is a misspelling in the original article. It should be "% CO_2" in the exhaust gas)

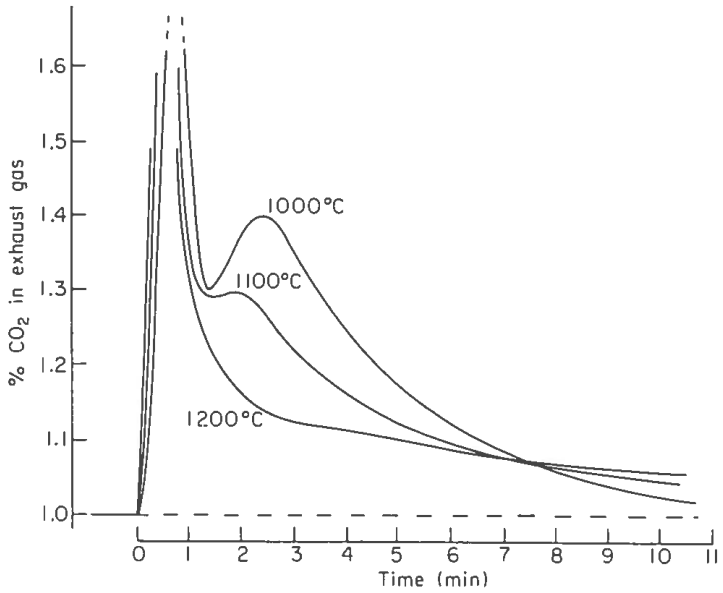

Figure 3.9: Rate curves at temperatures above 1000°C for preoxidized Capel ilmenite [26].

Merk and Pickles [29] studied the reduction of ilmenite by carbon monoxide in the temperature range 500-1000°C. They found that the rate and degree of reduction increased linearly with increasing temperature up to approximately 1000°C, as shown in Figure 3.10 on the next page.

Further increase in temperature resulted in an essentially constant reduction degree. This effect was attributed to shells of metallic iron precipitating at the ilmenite grain-boundaries. This reduces the permeability of gaseous reactant into the pellets, thus lowering the reduction rate. However, Merk and Pickels [29] found that this effect can be minimized by pre-oxidation.

Effect of pre-oxidation

The objective of pre-oxidation is making the pellet more susceptible to reduction. Basically, this is done by generating a phase transformation that "opens up" the structure in the pellet, making the diffusion of CO gas more fluent. Zhang and Ostrovski [30] and Chen [31] studied the reactions occurring during pre-oxidation. They found that $Fe_2Ti_3O_9$ (Fe_2O_3 x $3TiO_2$) was formed at 800°C. Increasing temperature led to Fe_2O_3 x $3TiO_2$ decomposing to Fe_2TiO_5 and TiO_2. Zhao [24] confirmed these results and also found that the optimum pre-oxidation temperature for ilmenite pellets is 800°C. Jones [26] and Merk and Pickels [29] suggested that pre-oxidation converts the large gains of ilmenite into a fine crystalline array of pseudobrookite containing a fine dispersion of rutile, as illustrated in Figure 3.11. Upon subsequent reduction ilmenite is regenerated, but the crystalline structure remains. Shells of metallic iron will then precipitate along sub-grain boundaries and not inhibit gas diffusion.

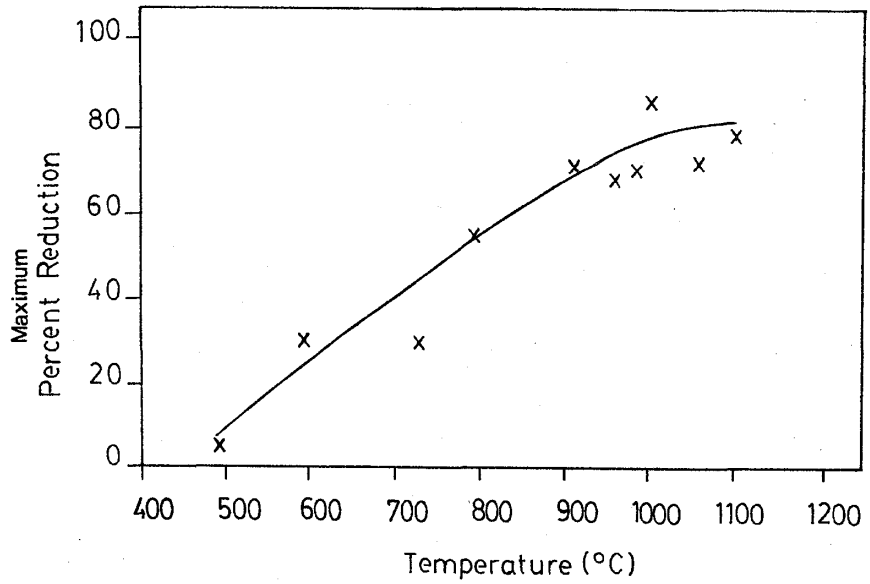

Figure 3.10: The effect of reduction temperature on the percent reduction for samples sintered in air at 540° C for 12 h [29].

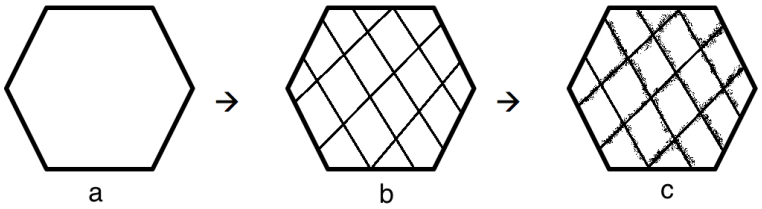

Figure 3.11: During pre-oxidation the large ilmenite grain (a) is converted into a fine crystalline array of pseudobrookite (b). Ilmenite is later reformed by reduction and metallic iron precipitates on the sub-grain boundaries (c).

Effect of particle size

In general, the reduction rate of ilmenite is increased with decreasing particle size. Smaller particles will give a greater surface area and more structural defects, which gives increased permeability of gas. However, too fine particles may cause severe dusting and lead to mass loss and impediments in process equipment.

4 Experimental

Two different methods of agglomeration were used in this work. These were pelletization and briquetting. In the following sections the materials and methods used for characterization of the pellets and briquettes are described in detail.

4.1 Materials

Ilmenite

The ilmenite concentrate used for this work was obtained from TiZir Titanium & Iron in Tyssedal, 16/11/11. The chemical composition is shown in Table 4.1.

Table 4.1: Analysis of ilmenite slurry, 16/11/11.

Specie	TiO_2	Fe_{tot}	MnO	CaO	MgO	SiO_2
Weight%	43.7	35.6	0.31	0.27	3.70	2.25
Specie	Al_2O_3	Cr_2O_3	V_2O_5	Nb	P_2O_5	ZrO_2
Weight%	0.56	0.096	0.19	0.005	0.016	0.05

A sieve analysis of the ilmenite concentrate is shown in Tabel 4.2

Table 4.2: Sieve analysis of the ilmenite concentrate.

Sieve [μm]	%
100	94.5
75	90.5
53	83.2
45	77.8

The ilmenite concentrate was dried at 105°C for 24 hours, broken up and screened through a 600 μm sieve in order to avoid lumpy material.

Binders

For pellets, three different binders were tested, namely bentonite, Peridur 300 (sodium carboxymethylcellulose) and Peridur 330 (polyanionic cellulose). A typical analysis of bentonite is shown in Table 4.3.

Table 4.3: Typical analysis of bentonite

Specie	SiO_2	Al_2O_3	Fe_2O_3	MgO	CaO
Weight%	53.0	20.0	4.6	3.7	4.9
Specie	Na_2O	K_2O	TiO_2	Cryst. water	
Weight%	3.4	0.6	0.6	5.2	

For briquettes, four different binders were tested, namely bentonite, Peridur 300, nano cellulose fibre (NCF) and calcium lignosulfonate (CaLS).

4.2 Pelletization

Ilmenite and binder were mixed by hand on a dry basis. Binder dosages were 0.8% bentonite and 0.08% Peridur 300 and 330. Pelletization was performed using a laboratory scale pelletizing drum (diameter = 80cm, depth = 15cm), shown in Figure 4.1. A very small amount of ore mixture (4-6 g) was added to the drum, rotating at about 30 rpm. The ore mixture was moistened with water using an atomizer to produce pellet "seeds". The seeds were enlarged by spraying water and adding ore mixture. As the pellets grew, they were screened to obtain a uniform size. The finished pellets were screened between 8 and 12 mm. Approximately 2.5 kg of pellets was produced per batch. The pelletization was performed by SINTEF Technician Edith Thomassen. A batch of industrially made pellets from Tyssedal was also investigated.

Figure 4.1: Laboratory size pelletization drum.

4.3 Briquetting

From the work of Sunde [32] it was found that variation in pellet shape lead to great standard deviations in the results. In order to reduce this uncertainty cylindrical briquettes were made.

Briquettes were made using four different binders, namely bentonite, Peridur 300, calcium lignosulfonate and a nano cellulose fibre (NCF). Peridur 300 and calcium lignosulfonate were tested with two different dosages. The binder dosages are shown in Table 4.4.

Table 4.4: Binder dosages.

Briquette type	Dosage [g]
No binder	-
0.8% Bentonite	3.2
0.1% Peridur 300	0.4
0.4% Peridur 300	1.6
0.1% CaLS	0.4
1% CaLS	4.0
NCF	0.2

400 g of ilmenite and 40 g of water were used per batch. The NCF was in the form of a 0.5% solution and 40 g of this solution was mixed with 400 g ilmenite. Briquettes (1 x 1.15 cm) were made using a steel mold and a piston, as shown in Figure 4.2. The ilmenite-binder mixture (3.0 g) was compressed at 0.2 kN/s up to 5 kN and held there for 2 s.

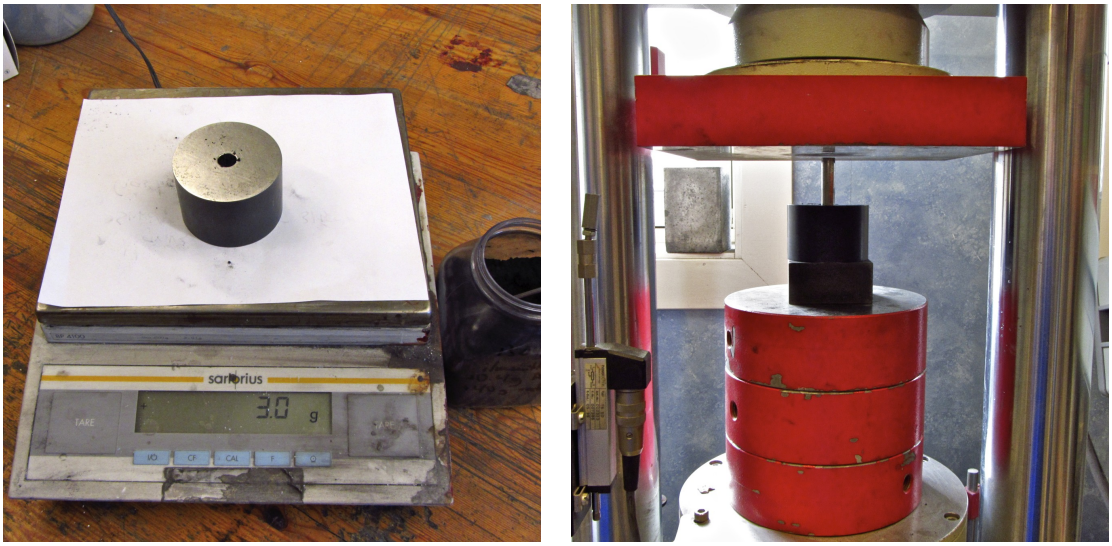

Figure 4.2: Briquetting equipment. Left: Steel mold filled with ilmenite-binder mixture. Right: Piston being pushed down into the steel mold.

4.4 Investigation of mechanical strength

Drop number and compression strength tests are widely used to assess the pellet strength. These are important properties as the pellets encounter frequent drops during balling and handling and compressive load from the weight of other pellets. The thermal shock test measures the pellets' ability to resist internal pressure created by sudden evaporation of water when the pellet is heated in a kiln. These three tests were employed in this work and are described below.

Drop number

Drop number was tested by dropping a green pellet freely from 46 cm down onto a hard surface until fracture was observed. The average value and standard deviation for 10 pellets were reported. This test was only performed on the pellet samples.

Thermal shock resistance

Thermal shock resistance was measured by firing groups of 15 randomly selected green pellets at 300°C, 500°C, 700°C and 900°C, for ten minutes. One group per

temperature. The number of pellets that cracked and/or exploded upon thermal treatment was recorded. The pellets were cooled to room temperature and subjected to a compression test, as described below. The same procedure was used for briquettes, except in groups of 10. Also, burning at 900°C was omitted, because the most interesting variations in compression strength happen before 700°C [32].

Compression strength

The compression strength of wet, dry and burnt pellets and briquettes was determined using an Instron 5543 compression and tensile strength tester. A picture of the equipment is shown in Figure 4.3. The pellets or briquettes were rendered broken if the stress-strain curve dropped 10% of the peak value. The average value and standard deviation of 15 pellets and 10 briquettes for load required to fracture a pellet or briquette (N/pellet or briquette) were reported.

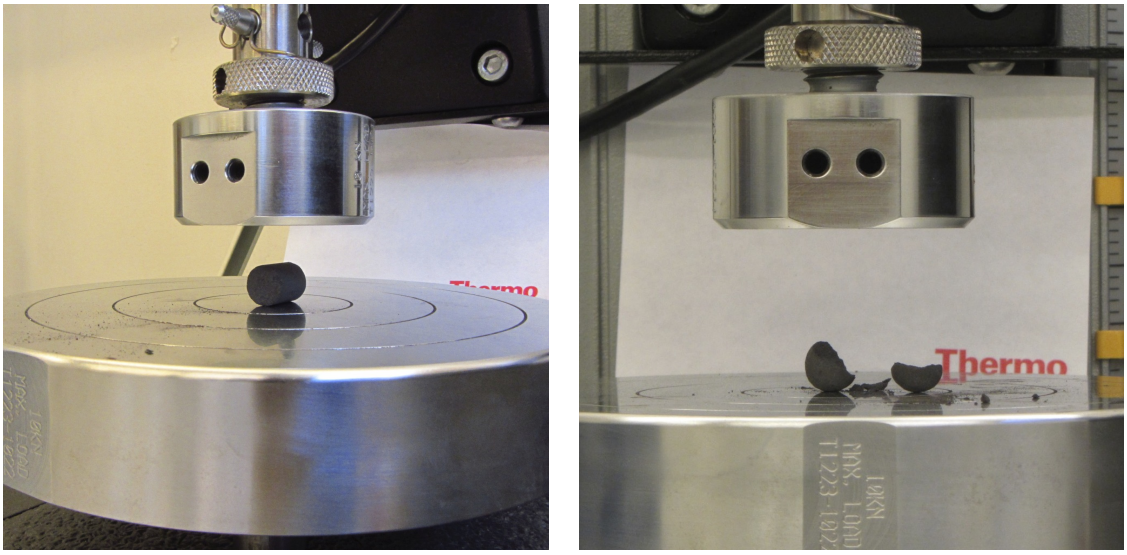

Figure 4.3: Compression test using an Instron 5543. Left: Briquette before compression test. Right: Pellet after compression test

4.5 Reduction of pellets in TGA

Three types of pellets were reduced in a thermogravimetric furnace apparatus (TGA). They were 0.8% bentonite, 0.08% Peridur 300 and no-binder pellets. A sketch showing the setup of the TGA is presented in Figure 4.4. Before reduction, all pellets were preoxidized. This was done by burning the pellets in a muffle furnace at 800°C in air atmosphere for 2 hours and letting them cool down in room temperature. About 200 grams of preoxidized pellets were used for each reduction experiment. The pellets were placed in the bottom of the crucible with a thermocouple in the center of the pellet bed. After the radiation sheet was placed

on top of the crucible, the thermocouple was raised halfway up the pellet bed to ensure correct temperature reading. The crucible was mounted to the weight and the gas tubes were connected. Once the weight had stabilized the furnace was raised to surround the crucible. The furnace and the pellets were heated to 1000°C while Ar gas 1 l/min was flowing through the system. Ar was replaced by CO gas and the reduction started immediately. A flow of CO gas, 5 l/min, was held for 4 hours. This was followed by a flow of Ar gas, 1 l/min, while the crucible and the pellets cooled down. Changes in weight, temperature and gas flow were logged every 2 seconds. This work was done in collaboration with Ph.D candidate Stephen Lobo at NTNU.

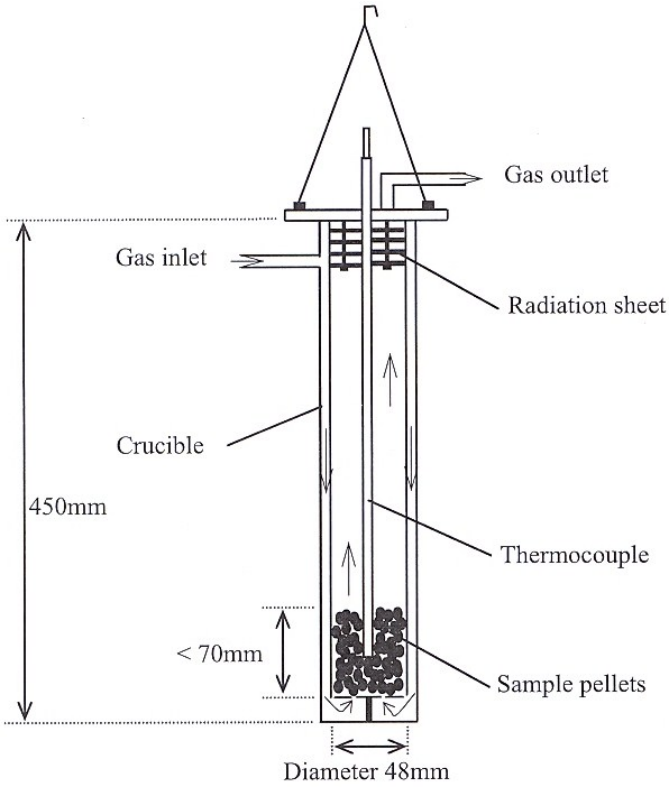

Figure 4.4: TGA crucible. [24]

4.6 Differential thermal analysis and mass spectrometry

Differential thermal analysis (DTA) and mass spectrometry (MS) was performed in synthetic air (21% O_2, 79% N_2), atmosphere on three different briquettes. These were 0.8% bentonite, 0.1% Peridur 300 and no-binder briquettes. They were heated from room temperature to 800°C at a rate of 9 °C/min. Temperature difference between the briquette sample and an alumina reference crucible was logged every 0.4 seconds. The off gas was analyzed for hydrogen, CH_4, CO, CO_2, and nitrogen using mass spectrometry. The apparatus was a Setaram SENSYS TG - DSC + MS Instrumentation and was operated by SINTEF Senior Engineer Shawn Wilson.

5 Results

The experimental results are presented in the following sections. First is a brief description of the pelletization process followed by the results from the characterization tests. Then comes a similar section on the briquettes. Finally the results from reduction in TGA and differential thermal analysis and mass spectrometry are presented.

5.1 Pellets

Four batches of pellets were successfully produced in the laboratory. A selection of pellets are shown in Figure 5.1.

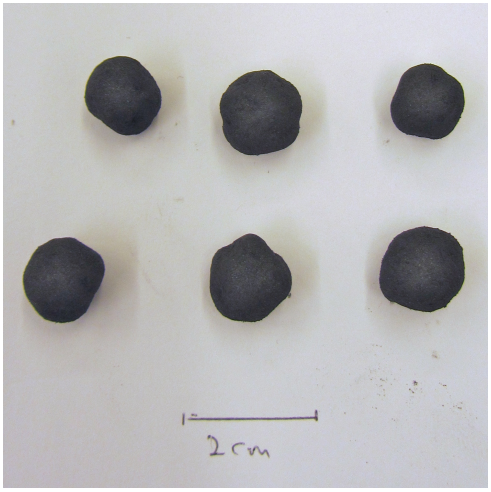

(a) Wet pellet, no binder.

(b) Wet, 0.08% Peridur 300.

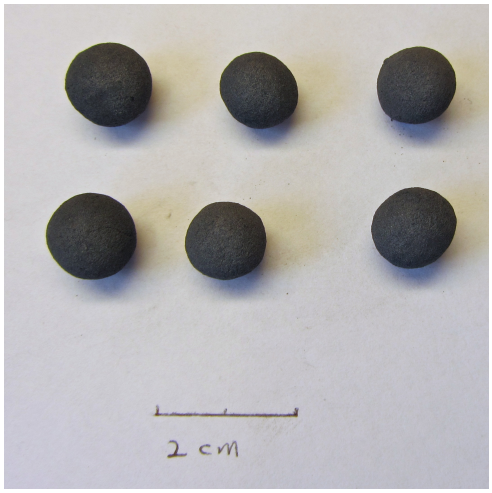

(c) Reduced bentonite pellet.

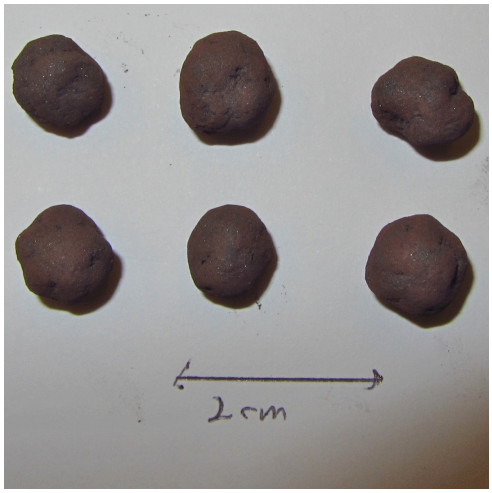

(d) Burnt 700°C, 0.08% Peridur 330.

Figure 5.1: A selection of the various pellets produced in the laboratory.

The pellets produced with bentonite had a relatively uniform size and spherical shape. The pellets produced with no binder or Peridur had a bulky shape and tended to be a bit smaller. A variation in how the pellets fractured under the compression test was observed. Some pellets cracked into pieces while others only had visible cracks, but were still in one piece. A few pellets did not have visible damage at the exterior at all. The general trend was that the wet and dry pellets did not break into pieces, but rather displayed exterior cracks or no damage at all. The burnt pellets usually cracked into two or several pieces. The bulk of the burnt Tyssedal pellets did not display any exterior cracks and very few of them cracked into pieces.

The results from the pellet experiments are summarized in Table 5.1. A graphic presentation of these numbers will be presented in the next sections.

No binder

Pellets made without binder had a bulky shape, as displayed in Figure 5.1 a). More dust was observed during handling of these pellets than others. The result from the compression test of pellets made without binder is shown in Figure 5.2.

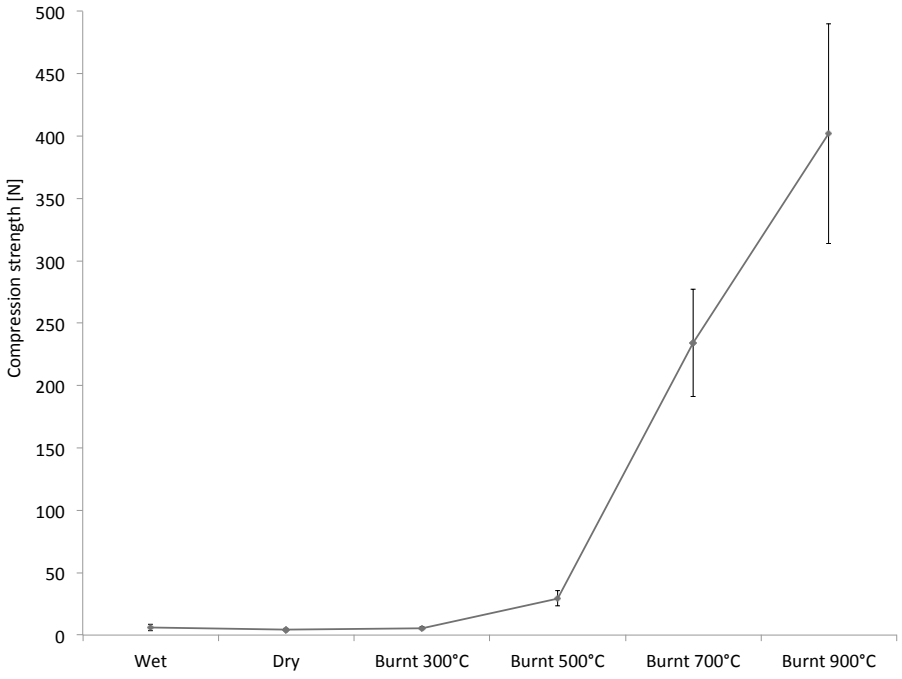

Figure 5.2: Compression strength of no-binder pellets.

The graph shows that the pellets are very fragile up to 300°C, but are strengthened by sintering at 500°C. None of the pellets displayed any visible damage after thermal treatment.

Table 5.1: Results from the pellet experiments.

	No binder	0.8% Bentonite	0.08% Peridur 300	0.08% Peridur 330	Tyssedal
Moisture, %	6.93	7.24	8.21	9.97	10.23
Drop number	2.60±0.52	2.1±0.32	4.60±0.84	2.50±0.71	12.4±1.51
Wet, [N]	5.88 ±2.58	9.52±1.74	6.41 ±1.35	6.94±1.55	3.90±1.17
Dry , [N]	4.39 ±1.05	24.19±2.75	9.49±1.97	6.97 ±1.60	21.14±3.17
Burnt 300°C, [N]	5.65 ±0.77	28.31±2.96	7.03 ±1.20	4.31±1.16	20.04±3.56
Burnt 500°C, [N]	29.43±6.06	99.45±11.45	35.00±7.28	31.10±10.69	40.95±12.73
Burnt 700°C, [N]	234.13±42.88	402.12±41.45	226.53±41.30	176.47±51.62	64.48±16.67
Burnt 900°C, [N]	401.86±87.99	507.10±84.73	312.69±72.31	286.17±84.96	112.54±26.26

Bentonite

The bentonite pellets obtained a nice spherical shape and a narrow size distribution. The ilmenite-bentonite mixture was easier to pelletize and led to somewhat bigger pellets compared to Peridur and no-binder pellets. The result from the compression test of bentonite pellets is shown in Figure 5.3.

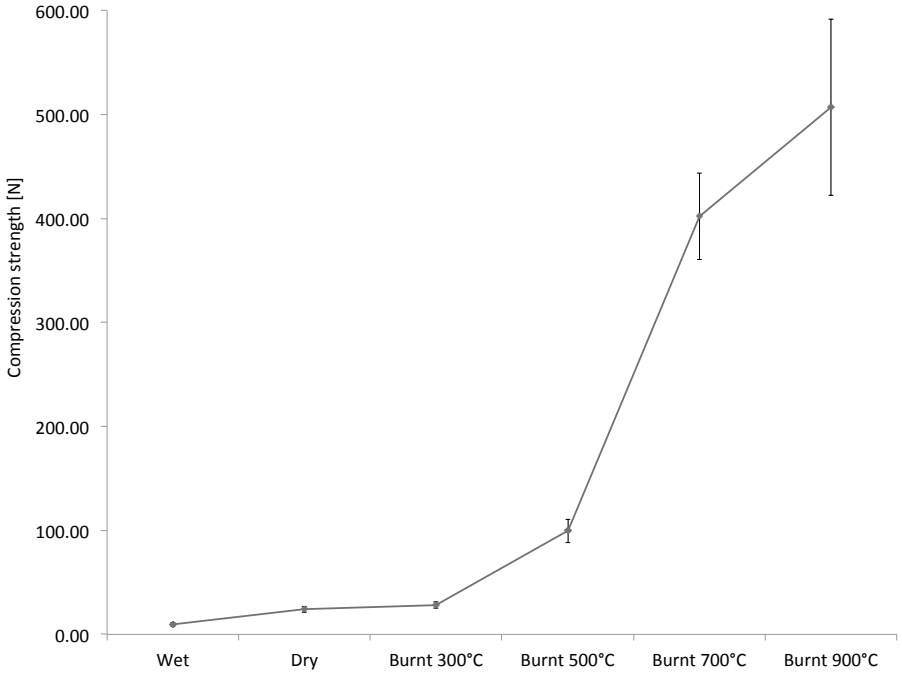

Figure 5.3: Compression strength of bentonite pellets.

The graph shows that there is a constant increase in strength as temperature increases. However, the most prominent strengthening occurs from 500°C when sintering starts. None of the pellets displayed any visible damage after thermal treatment.

Peridur

Both the Peridur 300 and 330 pellets obtained a bulky shape and a relatively wide size distribution. The result from the compression test of 0.08% Peridur 300 and Peridur 330 pellets are shown in Figure 5.4 and 5.5, respectively.

The graph for Peridur 300 shows that there is a slight increase in pellet strength from wet to dry, but it decreases after being burnt at 300°C. From 500°C and up sintering takes place, and the pellets are substantially strengthened. The graph for Peridur 330 shows that there is a slight decrease in pellet strength from wet to dry, and further decline after the pellets are burnt at 300°C. From 500°C the Peridur 330 pellets show a similar development as the Peridur 300 pellets. None of the pellets displayed any visible damage after thermal treatment.

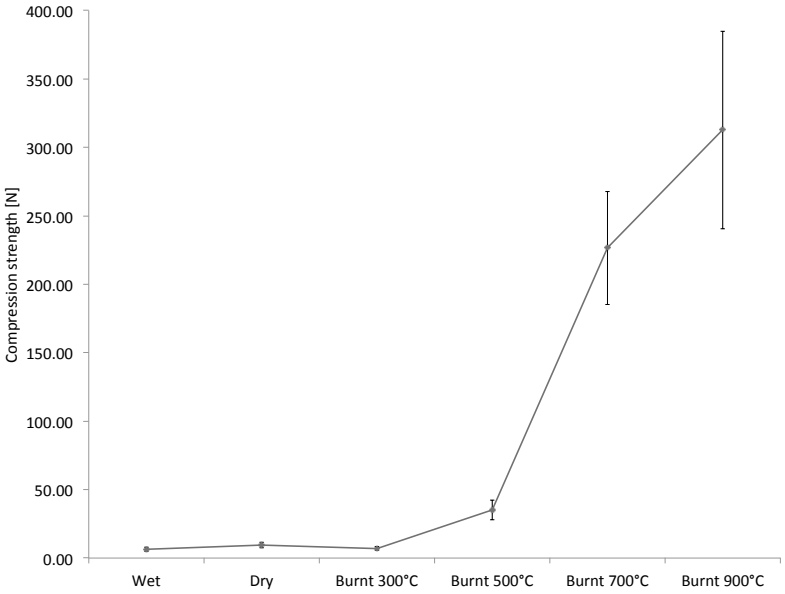

Figure 5.4: Compression strength of 0.08% Peridur 300 pellets.

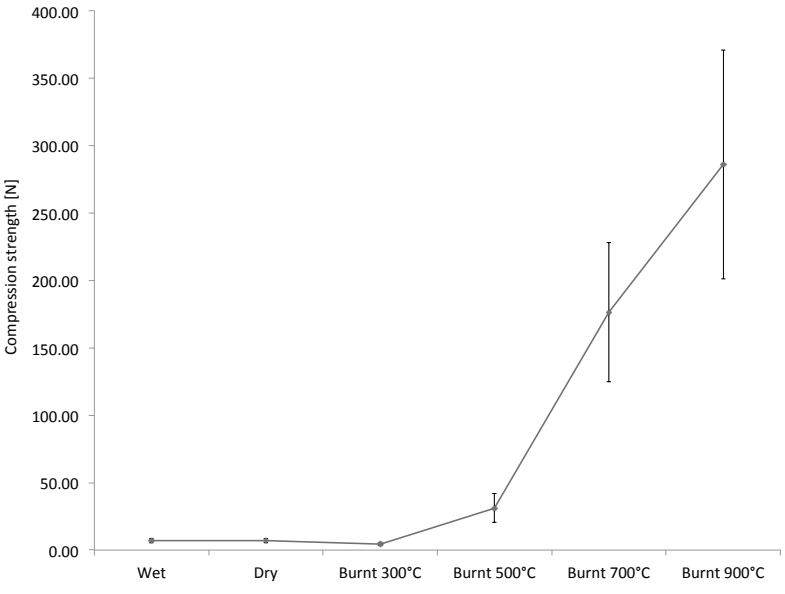

Figure 5.5: Compression strength of 0.08% Peridur 330 pellets.

Tyssedal

A selection of green pellets made industrially in Tyssedal are presented in Figure 5.6. The shape and size distribution of these differ substantially from those made in the laboratory. They are more bulky and less sphere shaped.

Figure 5.6: Green pellets made in Tyssedal.

The result from the compression test of Tyssedal pellets is shown in Figure 5.7.

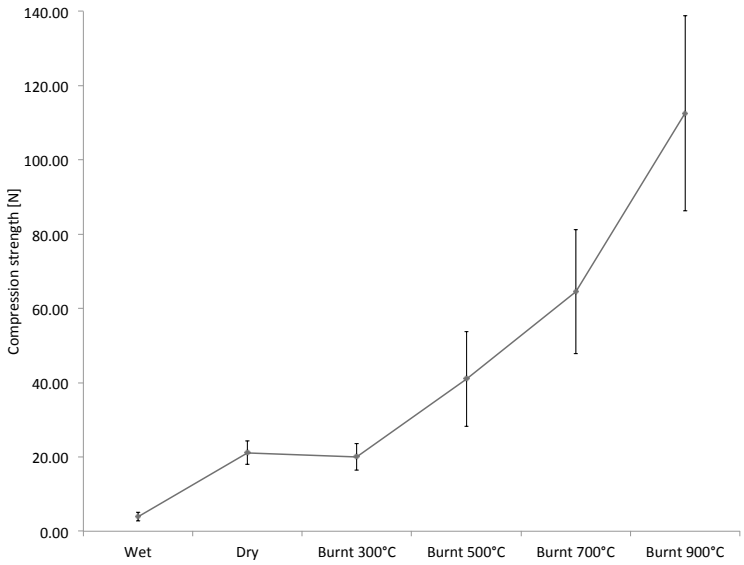

Figure 5.7: Compression strength of Tyssedal pellets.

The Tyssedal pellets show a solid increase in strength from dry to wet. After a small decline from dry to 300°C, they are strengthened by sintering from 500°C and up. One pellet disintegrated and three displayed visible damage after being burnt at 900°C.

5.2 Briquettes

Seven batches of briquettes were successfully produced in the laboratory. A selection of the briquettes are shown in Figure 5.8.

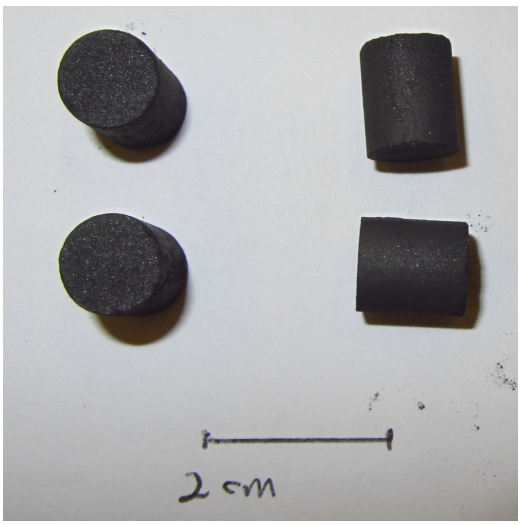

(a) Burnt 300°C, bentonite.

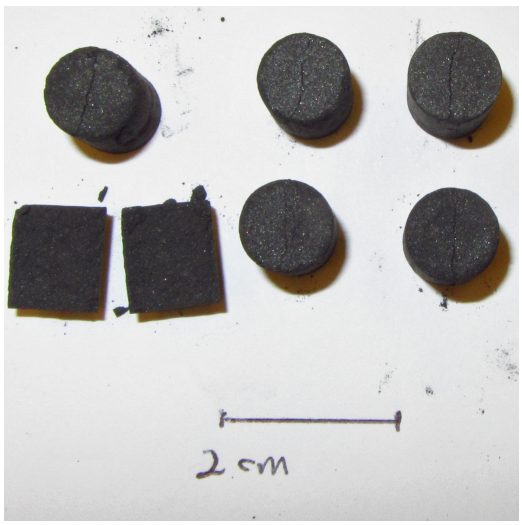

(b) Burnt 300°C, bentonite. After compression.

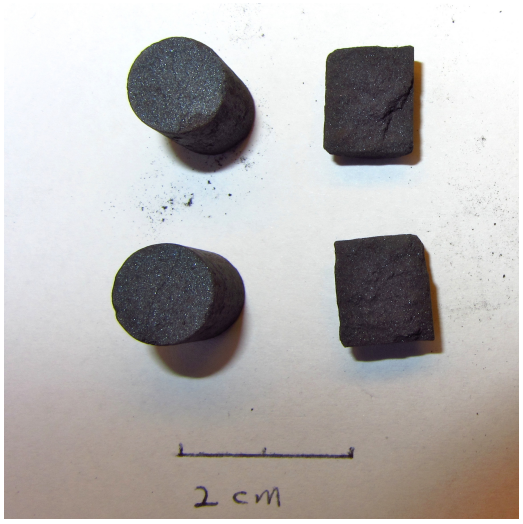

(c) Burnt 500°C, 0.4% Peridur 300. After compression.

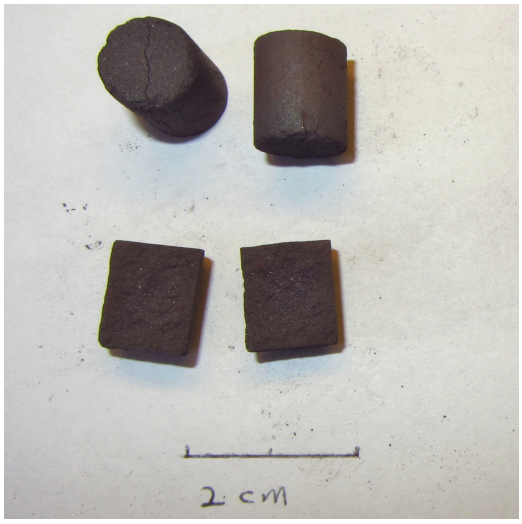

(d) Burnt 700°C, 0.4% Peridur 300. After compression.

Figure 5.8: A selection of the briquettes produced in the laboratory.

All briquettes had close to identical shape and size. The observed fracture pattern under compression was very similar for all briquettes, regardless of pre-treatment. The zigzag crack through the center of the briquette displayed in Figure 5.8 b) is a good representation of how most of the briquettes fractured. A few briquettes did not display any visible cracks upon compression and some broke into several

smaller pieces. The only easily observable difference between them was the amount of dust generated during handling.

The results from the briquette experiments are summarized in Table 5.2. A graphic presentation of these numbers follows in the next sections.

Table 5.2: Results from briquette experiments.

	No binder	0.8% Bentonite	0.1%Peridur 300	0.4% Peridur 300	0.1% Ca-LS	1% Ca-LS	NFC
Moisture, %	7.84	6.32	6.20	7.04	7.43	5.00	7.67
Wet, [N]	4.99 ±0.52	5.47 ±0.74	7.09 ±0.40	9.08±0.38	4.75 ±0.57	6.10 ±0.32	5.78 ±1.13
Dry , [N]	7.96 ±0.64	22.91 ±1.60	23.56±3.40	118.44±10.51	10.69±1.79	72.84 ±10.45	9.14 ±1.11
Burnt 300°C, [N]	9.11 ±1.64	21.38 ±1.85	13.30±1.80	73.90 ±14.12	11.917±2.02	68.41 ±11.87	8.43 ±1.17
Burnt 500°C, [N]	48.07 ±7.58	74.14 ±6.24	53.094±6.26	117.31 ±14.05	56.60±4.86	121.41 ±15.68	40.86 ±7.25
Burnt 700°C, [N]	279.76 ±32.86	312.34 ±22.37	245.708±21.27	261.04 ±35.58	247.25 ±32.90	345.60 ±38.09	263.16 ±41.89

Binder solutions

40 grams of water was mixed with a binder of varying type and/or dosage for each batch of briquette. Observations on the binder-water solution is presented in Table 5.3.

Table 5.3: Description of solutions of 40 g water mixed with various binders.

Dosage and type	Dissolving in water	Consistency	Comment
3.2 g Bentonite	Easy	Viscous, but running	Less viscous than 0.4 g Peridur 300
0.4 g Peridur 300	Hard	Viscous, but running	Left overnight for binder to dissolve
3.2 g Peridur 300	Hard	Firm gel, not running	Left overnight for binder to dissolve. Not useable
1.6 g Peridur 300	Hard	Soft gel, not running	Left overnight for binder to dissolve.
0.4 g Ca-LS	Very easy	Fluid	Strong smell
4.0 g Ca-LS	Very easy	Fluid	Strong smell
NCF gel	-	Soft gel, not running	Similar viscosity as 0.4 g Peridur 300

No binder

Briquettes made without binder generated more dust during handling than all the other. The result from the compression test of briquettes made without binder is shown in Figure 5.9. The graph shows that there is a slight increase in strength from wet to dry. From dry to 300°C the strength is marginally increased. At 500°C sintering starts and the briquettes are highly strengthened. None of the briquettes displayed any visible damage after thermal treatment.

Bentonite

The bentonite briquettes generated a moderate amount of dust compared to the others. The result from the compression test of briquettes made with bentonite is shown in Figure 5.10. It can be seen from the graph that there is a solid increase in strength from wet to dry and a marginal decline from dry to 300°C. The briquettes

are greatly strengthened from 500°C as a result of sintering. None of the briquettes displayed any visible damage after thermal treatment.

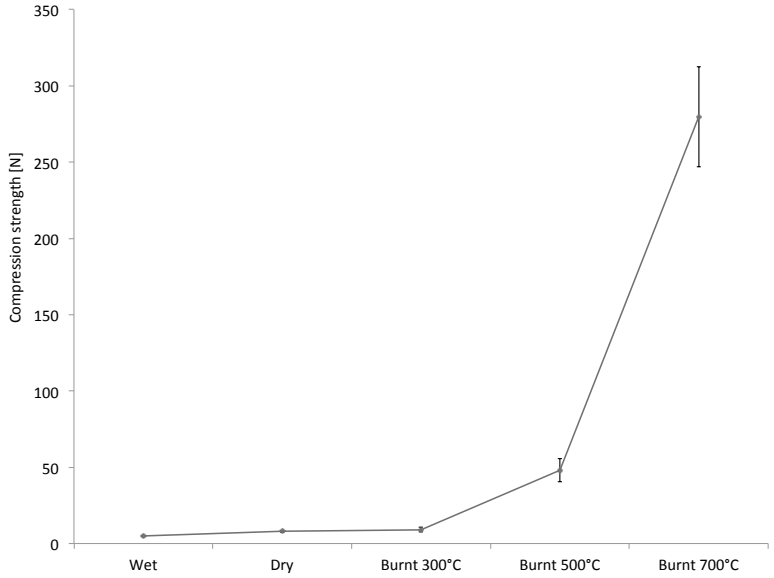

Figure 5.9: Compression strength of no-binder briquettes.

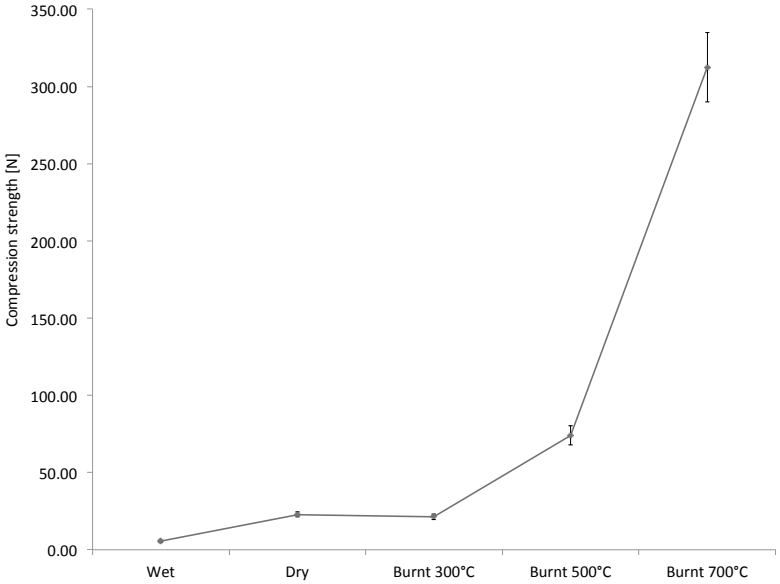

Figure 5.10: Compression strength of bentonite briquettes.

Peridur 300

The 0.1% Peridur 300 briquettes generated a moderate amount of dust, however a bit more than the bentonite briquettes. Briquettes made with 0.4% Peridur 300 generated very little dust during handling. The results from the compression test of briquettes made with 0.1% and 0.4% Peridur 300 are shown in Figure 5.11.

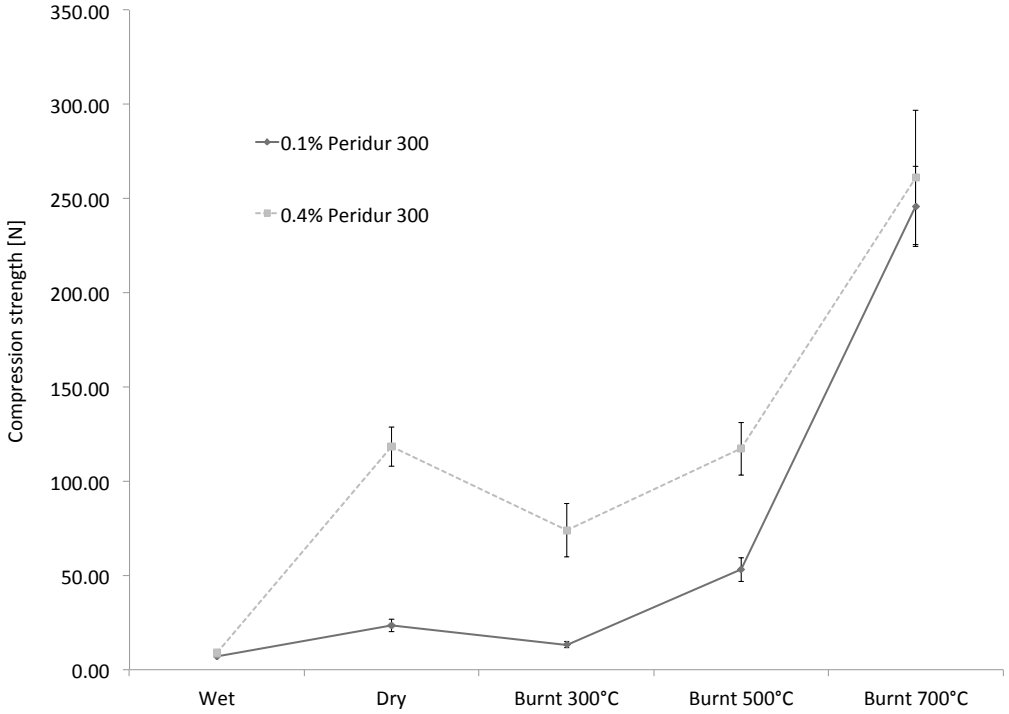

Figure 5.11: Compression strength of 0.1% and 0.4% Peridur 300 briquettes.

The graph shows that both dosages of Peridur 300 give similar strength development upon thermal treatment. The 0.4% Peridur 300 briquettes, however, show a remarkable increase in strength from wet to dry. From dry to 300°C both briquettes display a decrease in strength. From 300°C to 500°C both types are strengthened greatly. However, the 0.4% Peridur briquettes are stronger dry than at 500°C. The briquettes are further strengthened after being burnt at 700°C and end up with a fairly similar strength. None of the briquettes displayed any visible damage after thermal treatment.

Nano cellulose fibre

The NCF briquettes generated a moderate amount of dust during handling, though a little bit more than the bentonite and 0.1% Peridur briquettes. The result from the compression test of briquettes made with nano cellulose fibre is shown in Figure 5.12.

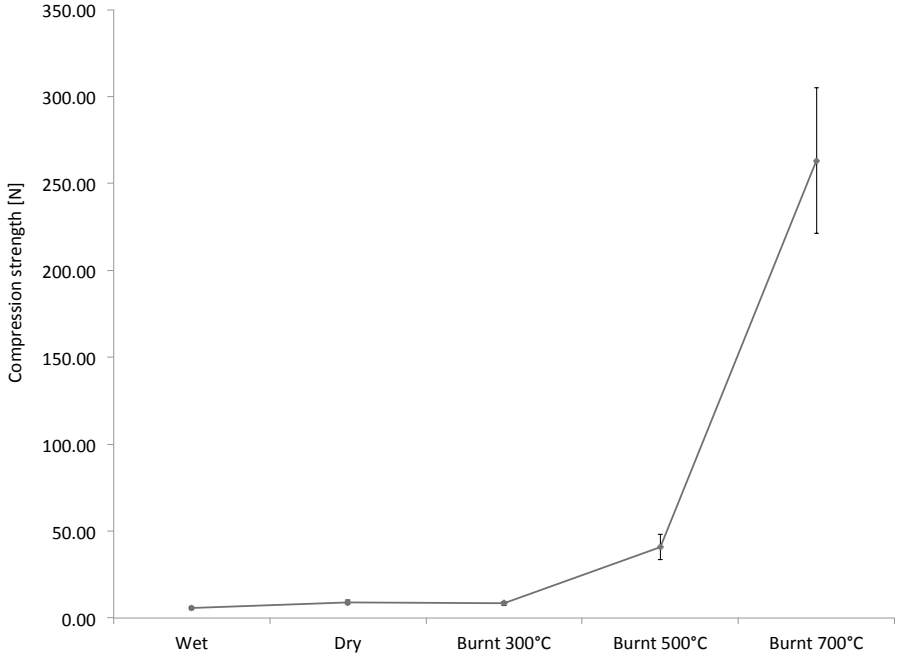

Figure 5.12: Compression strength of NCF briquettes.

The graph shows that the NCF is relatively weak up to 500°C. From this temperature they are strengthened by sintering. None of the briquettes displayed any visible damage after thermal treatment.

Calcium Lignosulfonate

Briquettes made with 0.1% calcium lignosulfonate generated a moderate amount of dust during handling. Briquettes made with 1% calcium lignosulfonate generated the least amount of dust of all the briquette types. A very unpleasant smell was released when they were burnt at 300°C and 500°C. At 700°C the smell was not as evident. The result from the compression test of briquettes made with 1% and 0.1% calcium lignosulfonate is shown in Figure 5.13 on the next page. The graph shows that the 1% CaLS briquettes have a much better strength development than the ones made with only 0.1% CaLS. The former show very good dry strength, but are slightly weakened at 300°C before sintering gives good strength at 500°C and 700°C. The 0.1% CaLS briquettes are relatively weak before sintering starts at 500°C. None of the briquettes displayed any visible damage after thermal treatment.

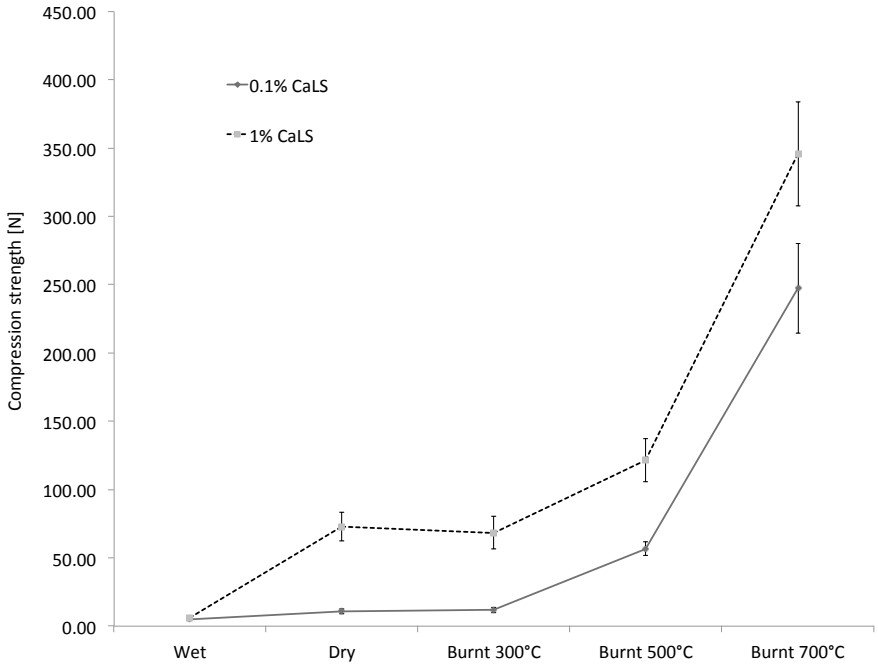

Figure 5.13: Compression strength of 0.1% and 1.0% Ca-LS briquettes.

5.3 Reduction in thermal gravimetric analyzer

Three different pellet types were reduced using a thermal gravimetric analyzer (TGA). The results from these experiments are shown in Table 5.4 and Figure 5.14. The reduction degree was calculated using Equation 3.11.

Table 5.4: Results from reduction experiment.

Type	Weight before	Weight after	Reduction degree	Comment
0.8% bentonite	201.68	172.89	0.7914	Bigger than the others
0.08% Peridur 300	200.53	169.49	0.8398	Bulky, varying size
No binder	200.21	171.43	0.8156	Bulky, varying size

From Figure 5.14 it is clear that the initial stage of reduction lasts for about 10 minutes. In this stage the Peridur pellets have a faster reduction rate than the others. The no-binder pellets are reduced marginally faster than the bentonite pellets during this stage. After this initial stage the reduction proceeds in a similar manner for all pellet types.

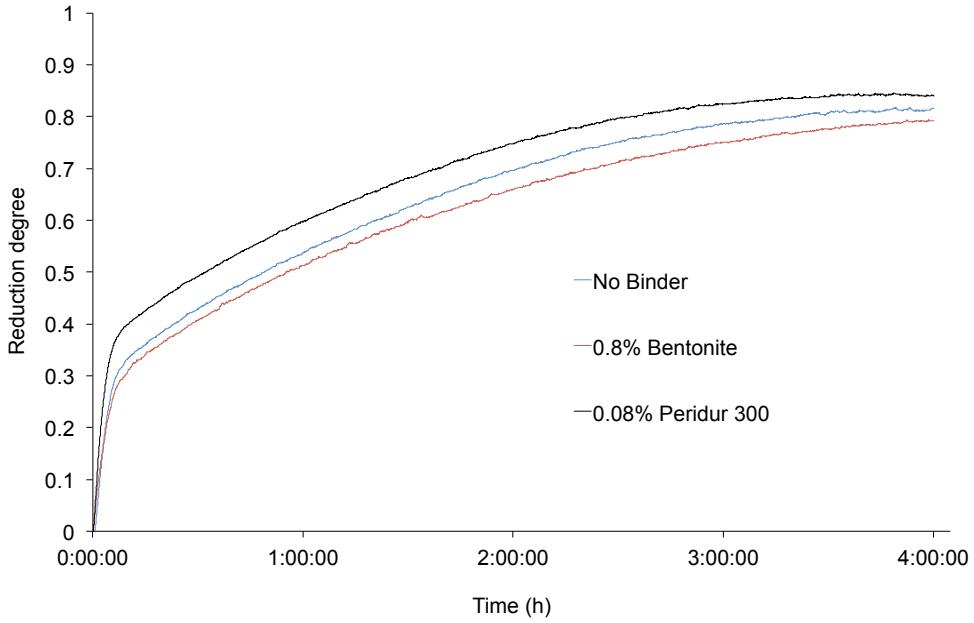

Figure 5.14: Conversion as a function of time for pre-oxidized pellets reduced with CO gas for four hours at 1000°C.

5.4 Differential thermal analysis and mass spectrometry

The results from the differential thermal analysis and mass spectrometry are presented in Figure 5.15 and 5.16 on page 50, and Figure 5.17 and 5.18 on page 51.

Figure 5.15 shows that there is a great weight loss up to about 110°C, especially for the no-binder briquette. This is water being removed and concur with relative concentration of water in the off-gas shown in Figure 5.17. At 300°C the weight starts to increase for all samples, indicating that oxidation has started. From Figure 5.16, which display the derivatives of the lines in Figure 5.15, it can be seen that after about 110°C the weight change is fairly constant and similar for all samples.

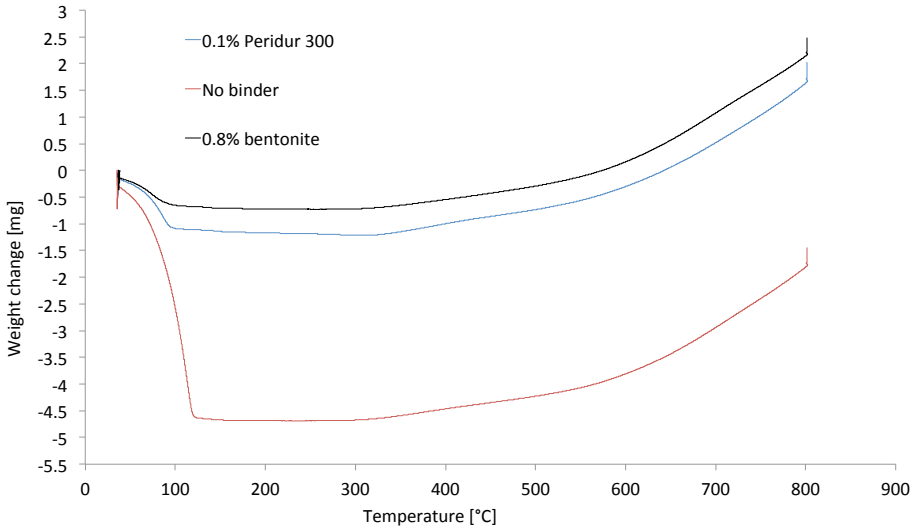

Figure 5.15: Weight change of matter from three different briquettes as a function of temperature.

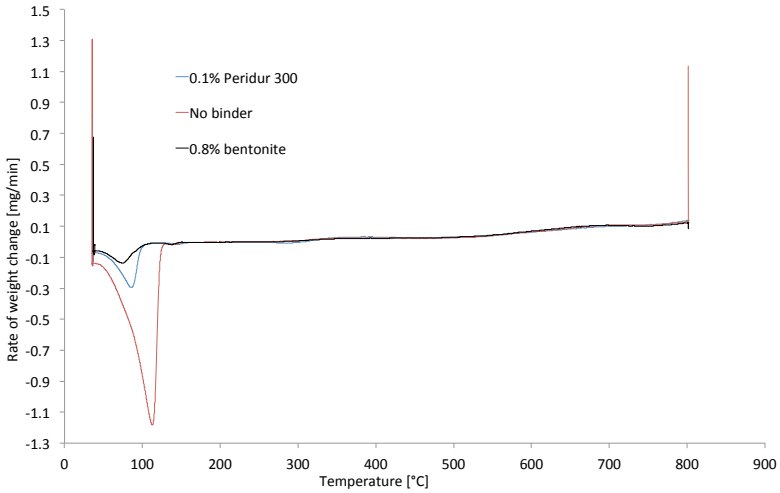

Figure 5.16: Weight change per minute of matter from three different briquettes as a function of temperature.

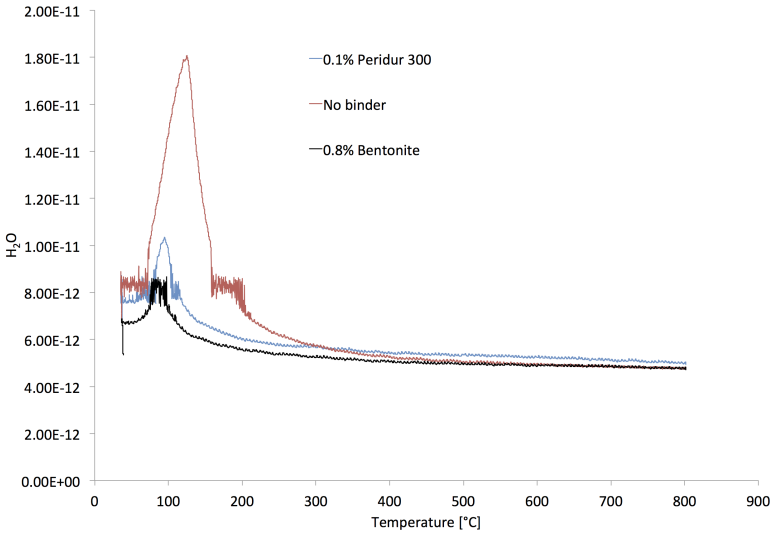

Figure 5.17: Relative concentration of water in the off-gas as temperature increases.

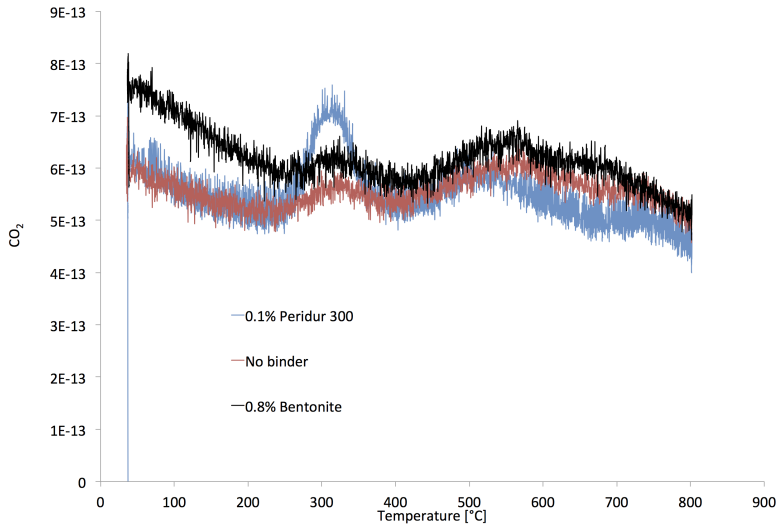

Figure 5.18: Relative concentration of CO_2 in the off-gas as temperature increases.

Figure 5.18 presents the relative concentration of CO_2 in the off-gas as temperature increases. All the curves show a similar form for the whole temperature range, but the peak at 300°C is considerably higher for the 0.1% Peridur 300 briquette.

6 Discussion

6.1 Pellets

This study aims to test the effect of different binders. It is therefore essential that the pellets' strength obtained from the pelletizing process itself is somewhat consistent from batch to batch. However, pelletization both on industrial and laboratory scale is a complex craft and challenging to standardize. Even though the procedure is the same for all batches there will always be variations from batch to batch. There are two main reasons for this. Firstly, generating "seeds" is the most difficult and also the most important part of labscale pelletization.This procedure is very difficult to repeat consistently. It is important to avoid agglomeration of the seeds, as this will yield pellets with bulky shape. The shape and size of the seeds will determine how the pellets grow, which directly affects their mechanical strength. This will be discussed further in the next section. Secondly, the amount of water added is based on how the agglomeration proceed and the considerations made during pelletization. This affects the drop number, wet compression strength and possibly how the pellets react to thermal treatment. Problems related to producing pellets with consistent shape and properties led to the decision of also using briquettes. This is further discussed in Section 6.2.

The thermal shock test showed an important difference between the laboratory and Tyssedal pellets. While one Tyssedal pellet exploded and several were fractured upon thermal shock of 900°C, none of the laboratory pellets suffered visible damage. This is believed to be attributed two things. Firstly, the Tyssedal pellets contains more moisture which can cause the pellet to rupture upon severe heating. Secondly, very fine recycled dust are added to the Tyssedal pellets, which may impair the diffusion of evaporated water out of the pellet. This will further contribute to a pressure build-up inside the pellet and can cause disintegration.

Shape and size

The selection of pellets presented in Figure 5.1 show that there were considerable variations in shape, especially for the Peridur and no-binder pellets. This will severely affect the measured compression strength value and is likely to be the major reason for the extensive standard deviation obtained in the compression strength results. A sphere-shaped pellet will yield a different fracture pattern than that of an irregular shaped pellet, as shown in Figure 6.1. For irregular pellets a small lump or protuberance may collapse before the pellet itself, giving an incorrect compression strength value.

It is worth mentioning that the compressive force experienced by the pellet when using the Instron 5543 is quite different from how the pellet would be compressed in a pellet bed. The Instron 5543 compresses the pellet between to flat surfaces

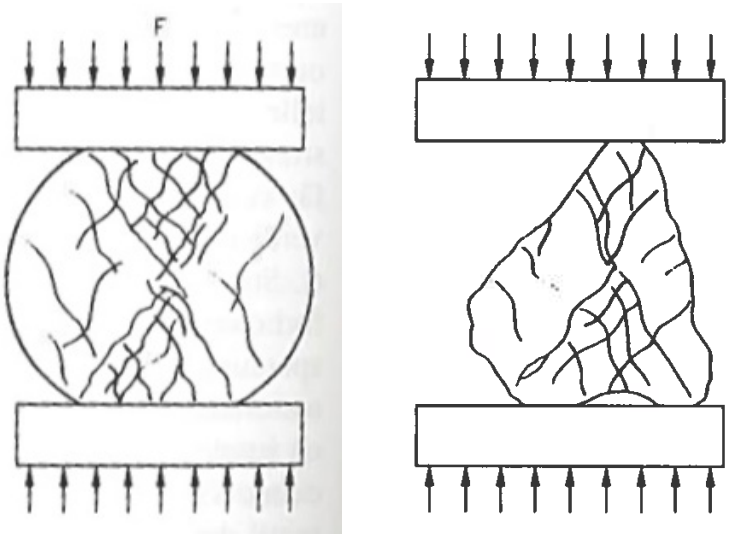

Figure 6.1: Fracture of a sphere-shaped and a non-symmetrical pellet. [33]

whereas in a pellet bed the compressive force would be imposed by adjacent pellets of various shape.

Compression strength

The compression strength for wet, dry and burnt pellets are shown in Figure 6.2. It is clear from this graph that the 0.8% bentonite pellets are stronger than the others. The Peridur and no-binder pellets do not show any significant strengthening before they are burnt at 500°C. For bentonite and Peridur pellets, there is an important difference in strength between dry and those burnt at 300°C. Bentonite pellets show a slight increase in strength while the Peridur pellets' strength decrease. From this it is clear that bentonite, as expected, is more capable of preserving the pellets strength at temperatures around 300°C. All pellets burnt at 500°C, 700°C and 900°C display increased compression strength. This indicates that the strengthening mechanism at these temperatures is less dependent on the binder. However, since the bentonite pellets are substantially stronger than the others, it must have an effect also at these temperatures.

It is noteworthy that the no-binder pellets show approximately the same strength up to 700°C and are stronger than Peridur pellets at 900°C. This was not expected and can imply that a dosage of 0.08% Peridur is too low.

From Figure 6.2 it seems the Tyssedal pellets are less susceptible to hardening by heat treatment than the laboratory pellets. This is, however, not necessarily the case. The shape of the Tyssedal pellets were significantly different than the laboratory pellets, which, as shown in Figure 6.1, results in a distinctively different fracture mechanisms. The compression strength of Tyssedal pellets is therefore not directly comparable to the laboratory pellets.

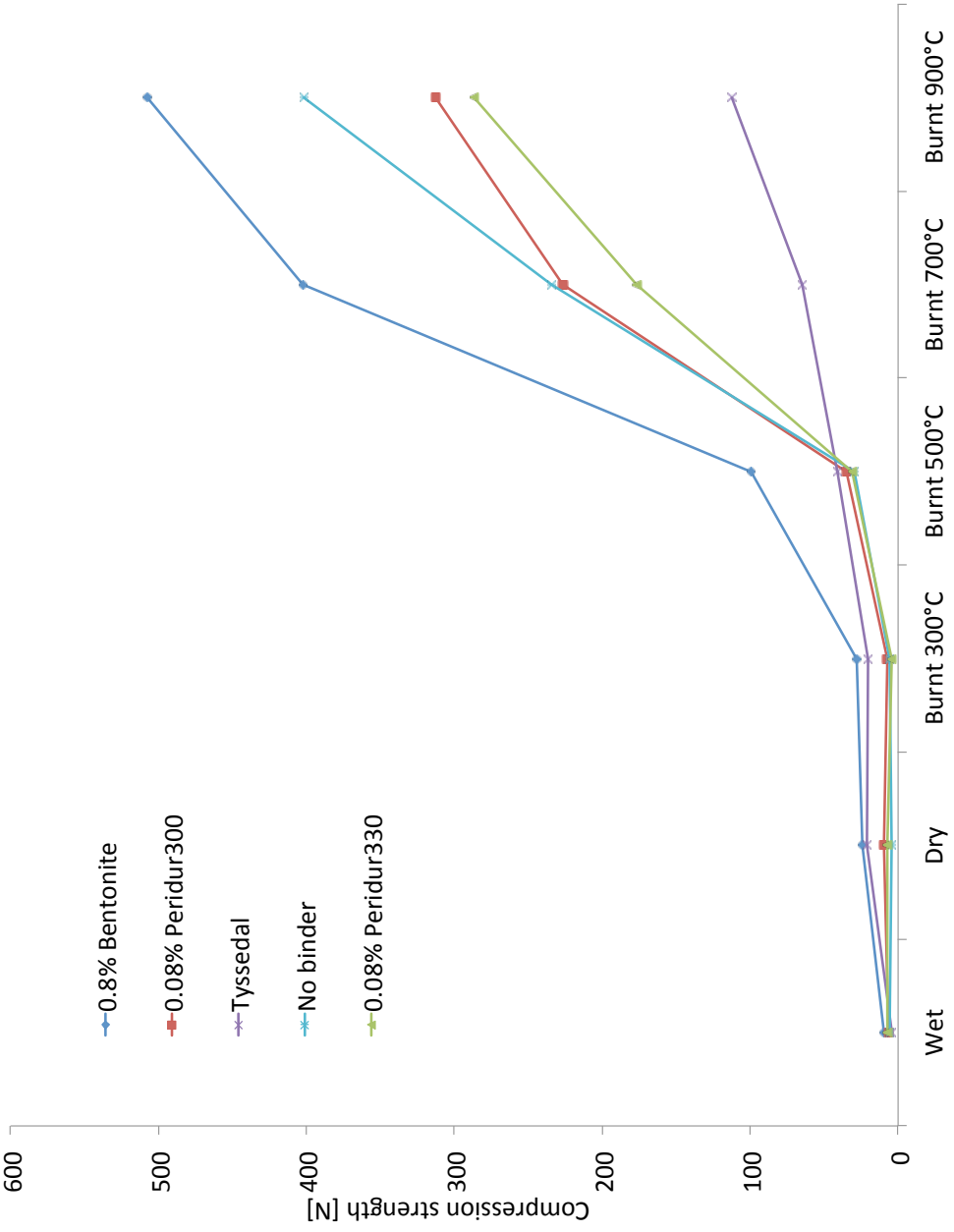

Figure 6.2: Pellet compression strength results.

Drop number

The pole diagram in Figure 6.3 shows the drop number for the different pellets. Generally, the drop number increases with increasing moisture content. This is because high moisture content in a pellet increases its elasticity making it more resistant to fracture. However, the water in the pellet needs to be evaporated, and more water consumes more energy. Also, as the water inside the pellet starts to evaporate, pressure builds up inside the pellet and may cause it to fracture or even explode. It is therefore important not to use more water than necessary.

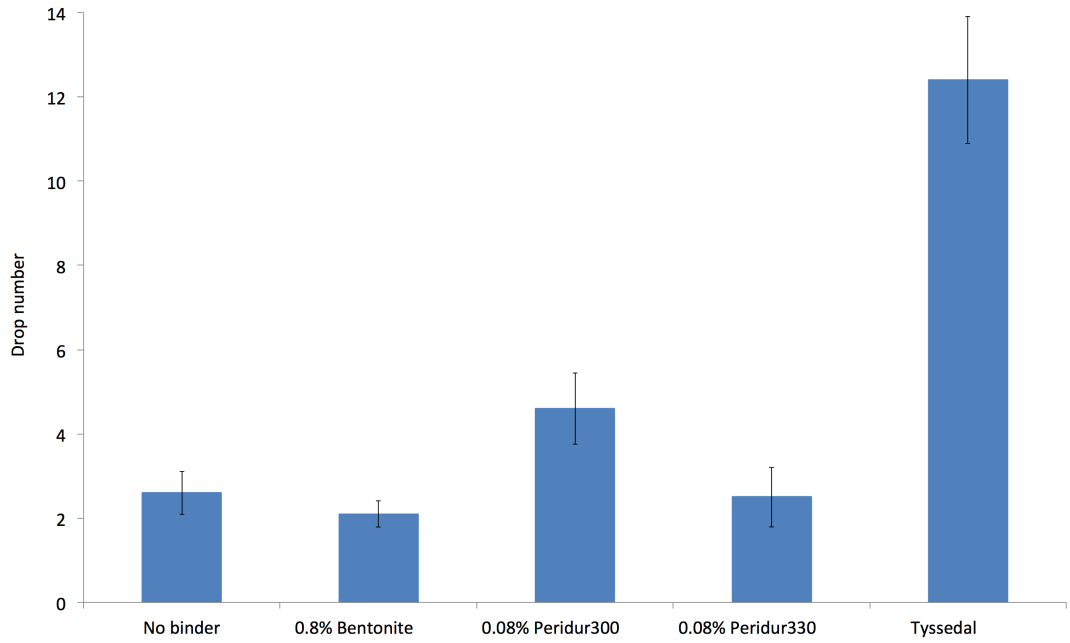

Figure 6.3: Pellet drop number.

The drop number for the pellets made in the lab did not exhibit a clear relation with the moisture content. Pellets made with 0.08% Peridur 300 stand out with a drop number of 4.6, which is about twice as much as the other laboratory pellets even though the moisture content was lower than for 0.08% Peridur 330 pellets. This result could be a consequence of how the pellets were made. As stated earlier, producing identical pellet batches is very difficult and unexpected drop numbers is a plausible outcome of this.

The Tyssedal pellets obtained a drop number of 10.23. They can however not be directly compared with the pellets made in the laboratory. These pellets are added recycled dust, contain more moisture, have a different shape and are not made in the same way.

Reduction

The three different pellet types used for the reduction experiments had different size and shape. The bentonite pellets had a size distribution closer to 12 mm than the Peridur 300 and no-binder pellets. They also had a nicer spherical shape, which can be seen in Figure 5.1. This is probably one of the major reasons why these pellets had a lower reduction degree. Looking at the shape of the curves in Figure 5.14 it seems that the binder has not played a vital role during reduction. The reduction starts fast as the oxygen atoms bonded more lightly are removed. After about ten minutes the reduction rate suddenly decreases and continues to gradually decrease. This behaviour is similar for all three pellet types.

From Figure 5.14 it can be seen that to reach 70% reduction degree, the Peridur 300 pellets only use about 2 hours, while the bentonite pellets use 3 hours. If this is a result of the binder and not the pellet size, it is a very good attribute of Peridur 300.

The 0.08% dosage of Peridur might be too low, as mentioned before. If the dosage of Peridur were to be increased, this should if anything affect the reduction degree in a positive way. The organic binders consist mostly of hydrogen and carbon which both act as reducing agents.

6.2 Briquettes

After several unsuccessful attempts to make uniformly shaped and sized pellets, a new procedure for testing binders was prompted. Instead of trying to reproduce the industrial pelletization process, an agglomeration technique which produced geometrically identical agglomerates showed promising aspects. Thus, it was decided to use cylindrical ilmenite briquettes for testing binders.

The procedure for making briquettes was very time consuming as it was only possible to make one at a time. They were, however, easily reproducible. The standard deviations for the compression test results presented in Table 5.2 are substantially lower than those for the pellets experiment. This is believed to be a direct consequence of the identical geometry of the briquettes. Figure 6.4 shows an illustration of how the briquettes fractured. A more or less clearly visible zigzag crack down the middle was observed on the bulk part of the briquettes.

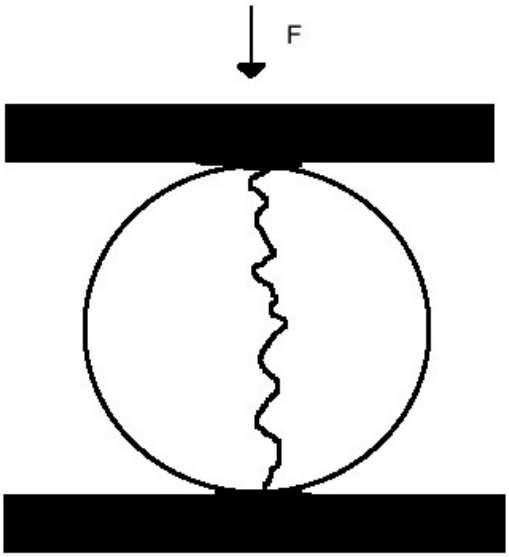

Figure 6.4: Illustration of the crack pattern in a cylindrical briquette.

When eliminating the uncertainty introduced by varying geometry and production procedure the results became more reliable. A diagram showing a comparison of the different briquette compression strengths is shown in Figure 6.5 on the next page.

Peridur 300

Increasing the Peridur 300 dosage from 0.1% to 0.4% yielded a remarkable strengthening effect. The green strength is in the same range as for the other binders, but the increase from wet to dry strength was much higher than expected. This could indicate that there is a dosage threshold which needs to be exceeded for Peridur 300 to take effect.

The drop in strength for 0.4% Peridur 300 briquettes from dry to 300°C coincide with the results for 0.1% Peridur 300. This is believed to happen due to crystal water being removed and binder burning off, as indicated by the DTA+MS experiment. Since the 0.4% Peridur 300 briquettes are much stronger than 0.1% Peridur 300 briquettes it is, however, likely that the binder still plays an important role at 300°C and 500°C. It is not before 700°C that the 0.1% and 0.4% Peridur 300 briquettes display strengths in the same range. This suggests that somewhere between 500°C and 700°C sintering becomes the more prominent binding mechanism.

The briquettes made with 0.4% Peridur 300 generated very little dust during handling. In industry this is an important property both in terms of operating conditions and economy, as lost material is lost revenue.

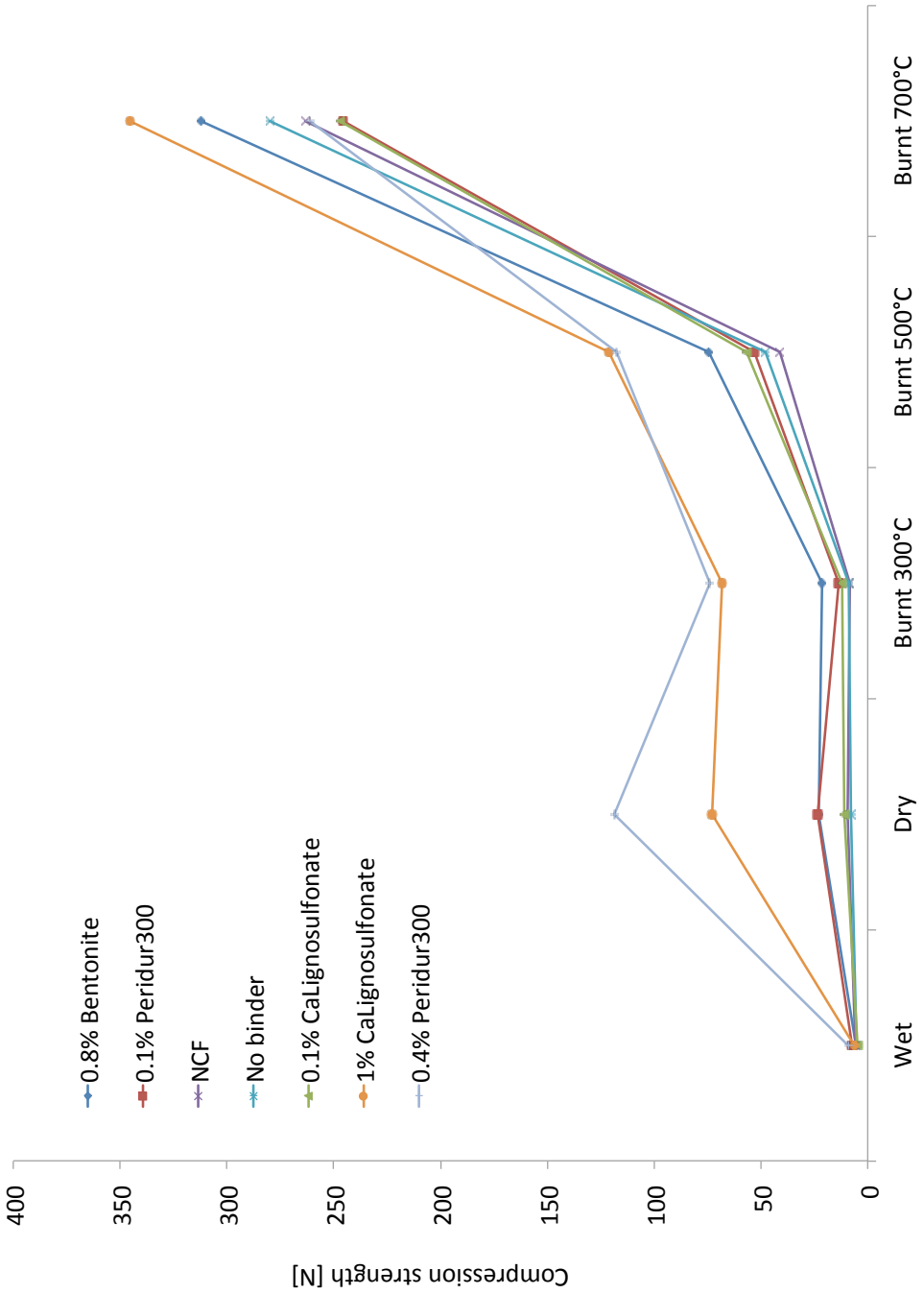

Figure 6.5: Comparison of briquette compression strength results.

No binder

When comparing the no-binder briquettes and those made with 0.1% organic binder or 0.5% solution NCF it seems that the binders have little or no effect. They show about the same or slightly better strength wet, dry (except Peridur 300, which has good dry strength) and burnt at 300°C and 500°C, and are inferior to the no-binder briquettes at 700°C. Even the 0.4% Peridur briquettes, which have almost fifteen times the dry strength are surpassed by the no-binder briquettes at 700°C. The good compression strength of no-binder briquettes at 500°C and 700°C supports the before mentioned assumption that sintering is the primary binding mechanism at these temperatures. It could be that the interparticle distance is smaller for the briquettes made without binder and that this makes them more susceptible to sintering. This would explain good strength they display at 700°C.

Bentonite

The bentonite briquettes show the same strength development as the other types, but decrease only marginally from dry to 300°C. Bentonite is known to be more temperature resistant than organic binders, so this was expected. Still, it was not expected that the 0.4% Peridur 300 briquettes are substantially superior to bentonite briquettes when dried and burnt at 300°C and 500°C. Considering that the dosage of bentonite is twice the dosage of 0.4% Peridur 300 it is clear that the efficiency per weight unit of Peridur 300 is much better than bentonite. This is of course a necessity for Peridur 300 to be economically appealing.

Between 500°C and 700°C a beneficial effect for bentonite compared to the 0.4% Peridur 300 briquettes is observed. A possible explanation is that small voids are left behind as the organic binder is completely burnt off, leaving the material more fragile. However, this effect is not observed when using 1% CaLS.

Calcium lignosulfonate

The 1% CaLS briquettes show very good strength overall and are by far the strongest at 700°C. As opposed to Peridur 300, the CaLS briquettes are only slightly weakened when going from dry to 300°C, which indicates that this binder is more temperature resistant.

The drawback with using calcium lignosulfonate industrially is that it contains calcium and sulphur. Calcium will eventually end up in the slag as a contamination and the sulphur will add to the sulphur emissions. Also, calcium lignosulfonate was the only binder which gave off a strong smell when burnt. This can have a negative effect on the working environment.

Nano cellulose fibre

The 0.5% nano cellulose fibre solution manufactured and supplied by the Paper and Fibre Research Institute in Trondheim gave briquettes which showed similar compression strength to 0.1% CaLS and no-binder briquettes. It is likely that the very low dosage of NCF, only 0.2 g NCF for 400 g ilmenite, is the reason for these results. It would have been interesting to test a more concentrated NCF gel, but this was unfortunately not feasible in this work.

For wet and dry briquettes, NCF are stronger than those made with only water. This is probably due to NCF's viscosity.

DTA

The incentive for performing a differential thermal analysis was to investigate if it was possible to observe when the organic binder burned off. In Figure 5.18 the graph for the 0.1% Peridur briquette has a peak around 300°C, which is the temperature organic binders are believed to burn off at. This is however not a confirmation of Peridur 300 burning off. The sample mass was only 125 mg and should contain about 0.1 mg Peridur 300. The peak could therefore also be a result of an impurity in the sample.

Binder viscosity

The binder's viscosity is an important strengthening mechanism for the green pellets, as mentioned in Section 3.2. Table 5.3 gives an overview of the observed properties of the different water-binder solutions. An interesting result is how the observed viscosity relates to the wet strength of the briquettes. The two least viscous binders, water and 0.1% CaLS, exhibit the lowest wet strength, while the two most viscous binder solutions 0.1% and 0.4% Peridur 300, exhibit the highest wet strength. This supports the previously mentioned influence of viscosity on green strength.

Load-strain curves

The load-strain curves from the compression test of briquettes and pellets are shown in Appendix A and B, respectively. These curves can give us information about how the briquettes/pellets behave under compression. This does, however, require detailed and systematic investigation and is not within the scope of this work.

Mixing

Mixing of binder and ilmenite was done differently for the two agglomeration methods. For pellets the binder was mixed with the ore on a dry basis. For briquettes the binder was dissolved in water and then mixed with ilmenite. Both methods introduced the challenge of knowing when proper mixing had been achieved. The reason for this was that the amount of binder in the ore mixture was extremely small compared to the bulk mass. The mixing procedure was done similar for the different batches, nevertheless, inconsistencies in mixing can have resulted in variations in the results which are not linked to the properties of the binder itself.

Pellets vs briquettes

The purpose of making briquettes was not to compare their performance quantitatively with pellets, but rather find an alternative method for comparing binders. The results obtained by using briquettes coincide qualitatively with the pellet results. The briquette results are, however, much more reliable since the uncertainty of varying geometry is eliminated. The use of briquettes makes it much simpler to test one factor at a time. These could be water content, binder dosage, dust additives or mixing, to mention a few. This enables a much more systematic investigation of the various parameters affecting the strength.

7 Conclusion

Two agglomeration methods were used to test the effect of various binders on ilmenite pellet strength. Pelletization proved to be an unsatisfactory method as it yielded substantial standard deviations. Briquettes yielded consistent results and were much easier to reproduce with identical shape and size for several bathes. The results for both methods coincide with each other, but are more sound for the briquettes.

- For labscale testing of binders, briquettes are better suited than pellets. They give more consistent results and are easily reproduced.

Three alternatives to bentonite as binder for ilmenite pellets were tested. Peridur 300 can work very well as a binder, but the dosage needs to be more than 0.1% by weight. A dosage of 0.4% Peridur 300 gave very strong briquettes, it is therefore believed that a dosage somewhere between 0.1% and 0.4% will work sufficiently. The 0.5% NCF gel is on par with bentonite in terms of wet strength, but did not contribute any additional strength upon thermal treatment. 1% calcium lignosulfonate gave very good strength at all temperatures. However, it contains unwanted elements, Ca and S, and gives off a strong smell when burnt. It is therefore not a very suitable alternative for bentonite.

- Peridur 300 is a potential alternative to bentonite.
- The 0.5% NCF gel does not provide adequate strength upon thermal treatment.
- Calcium lignosulfonate gives very good strength, however due to strong smell and unwanted elements it is not the most suitable alternative to bentonite.

All pellets and briquettes exhibit the same general trend in terms of strength development above 300°C - it increases. Briquettes made with Peridur 300, NCF and no binder end up with a fairly similar strength after being burnt at 700°C, regardless of binder dosage. This indicates that sintering is more prominent at this temperature.

- Above 500°C sintering is the dominating binding mechanism.

The observed viscosity of the different binders and their relation to green strength coincide with the accepted theory that more viscous binders (within limits) yield better green strength.

- Viscous binders give good green strength.

This work shows that there are possible alternatives to bentonite, but more research needs to be done before an organic binder can be utilized industrially for ilmenite pelletization.

8 Future work

This project does not conclude the matter at hand. More experiments need to be carried out in order to get an even better understanding of the binder's role in the pelletization process. Below are a few suggestion for future work.

- Asses several dosages of the same binders.
- Perform DTA and MS of dried briquettes with higher binder dosage.
- Investigate how the binders act at elevated temperatures.
- Look closer into what is happening in the dry-500°C interval.
- Test a more concentrated nano cellulose fibre gel.

It is of great interest to figure out how binders actually work at different temperatures and what specifically distinguish a good from a poor binder. This information is only obtainable through experiments and thorough investigation.

Bibliography

[1] Seim S. *Experimental Investigations and Phase Relations in the Liquid $FeTiO_3$-Ti_2O_3-TiO_2 Slag System*. PhD thesis, NTNU, 2011.

[2] Elstad H., K. Ure, and Ø. Tvedt. *Elektrokjemifaget karbotermiske prosesser - ilmenitt*. Tinfos Titan & Iron KS, Tyssedal, Norway, 1992.

[3] P.C. Hayes. *Process principles in minerals and materials production*. Hayes Publishing CO, Queensland, Australia, 2003.

[4] T.C. Eisele and S.K. Kawatra. A review of binders in iron ore pelletization. *Mineral Processing and Extractive Metallurgy Review*, 24(1):1–90, 2003.

[5] S.E. Olsen, T. Lindstad, and M. Tangstad. *Production of manganese ferroalloys*. Tapir Academic Press, 2007.

[6] S.M. Iveson, J.D. Litster, K. Hapgood, and B.J. Ennis. Nucleation, growth and breakage phenomena in agitated wet granulation processes: a review. *Powder Technology*, 117(1-2):3–39, 2001.

[7] Forsmo S.P.E., P.-O. Samskog, and B.M.T. Björkman. A study on plasticity and compression strength in wet iron ore green pellets related to real process variations in raw material fineness. *Powder Technology*, 181(3):321 – 330, 2008. URL: http://www.sciencedirect.com/science/article/pii/S003259100700280X, doi:10.1016/j.powtec.2007.05.023.

[8] Seim S. PhD Research Scientist TiZir Titanium & Iron. Personal communication, 2012.

[9] L. Haas. Effectiveness of organic binders for iron ore pelletization. *US Bur. Mines Rep. Invest.,*, page 21, 1989.

[10] Guanzhou Qiu, Tao Jiang, Hongxu Li, and Dianzuo Wang. Functions and molecular structure of organic binders for iron ore pelletization. *Colloids and Surfaces A: Physicochemical and Engineering Aspects*, 224(1-3):11 – 22, 2003. URL: http://www.sciencedirect.com/science/article/pii/S0927775703002644, doi:DOI:10.1016/S0927-7757(03)00264-4.

[11] O. Sivrikaya and A.I. Arol. Pelletization of magnetite ore with colemanite added organic binders. *Powder Technology*, 210(1):23 – 28, 2011. URL: http://www.sciencedirect.com/science/article/pii/S0032591011000623, doi:DOI:10.1016/j.powtec.2011.02.007.

[12] Sodium carboxymethyl cellulose [online]. Desember 2011. URL: http://www.sigmaaldrich.com/catalog/ProductDetail.do?N4=419273|ALDRICH&N5=SEARCH_CONCAT_PNO|BRAND_KEY&F=SPEC.

[13] Kater T. and H.R.G Steeghs. Organic binders for iron ore pelletization. *Proceedings of the 57th Annual Meeting of the Minnesota Section of AIME*, (MN):13.1–13.29, 1984.

[14] Calcium lignosulfonate (40-65) [online]. May 2011. URL: `http://www.fao.org/ag/agn/jecfa-additives/specs/monograph5/additive-505-m5.pdf`.

[15] K. Syverud, K. Xhanari, G. Chinga-Carrasco, Y. Yu, and P. Stenius. Films made of cellulose nanofibrils: surface modification by adsorption of a cationic surfactant and characterization by computer-assisted electron microscopy. *J Nanopart Res*, 13:773–782, 2011.

[16] Kawatra S.K. and S. J. Ripke. Laboratory studies for improving green ball strength in bentonite-bonded magnetite concentrate pellets. *International Journal of Mineral Processing*, 72(1-4):429 – 441, 2003. Special Issue To Honor Professor Douglas W. Fuerstenau. URL: `http://www.sciencedirect.com/science/article/pii/S0301751603001170`, `doi:10.1016/S0301-7516(03)00117-0`.

[17] P. Ayers. Development of dry strength in pellets made with soluble salt binders. *Transactions of the Institution of Mining and Metallurgy*, 85:177–183, 1976.

[18] Refractory inspection [online]. Desember 2011. URL: `http://constructionmanuals.tpub.com/14259/css/14259_225.htm`.

[19] Y.A. Owusu. Physical chemistry study of sodium silicate as a foundry sand binder. *Advances in Colloid and Interface Science*, 18(1-2):57–91, 1982.

[20] Forsmo S.P.E., A.J. Apelqvist, B.M.T. Björkman, and P.-O. Samskog. Binding mechanisms in wet iron ore green pellets with a bentonite binder. *Powder Technology*, 169(3):147 – 158, 2006. URL: `http://www.sciencedirect.com/science/article/pii/S003259100600338X`, `doi:DOI:10.1016/j.powtec.2006.08.008`.

[21] S. L. de Moraes and S. K. Kawatra. Laboratory study of an organic binder for pelletization of a magnetite concentrate. *Minerals & Metallurgical Processing*, 27(3):148–153, 2010.

[22] Lewis concept of acids and bases [online]. Desember 2011. URL: `http://chemwiki.ucdavis.edu/Physical_Chemistry/Acids_and_Bases/Acid/Lewis_Concept_of_Acids_and_Bases`.

[23] K. Borowiec and T. Rosenqvist. Phase relations and oxidation studies in the system Fe - Fe_2O_3 - TiO_2 at 700-1100°C. *Scandinavian Journal of Metallurgy*, 10(5):217–224, 1981.

[24] Zhao D. *Processing and Properties of Direct Reduced Iron Pellets Containing Material for Control of Steel Structure*. PhD thesis, NTNU, 2010.

[25] D. Poggi, GG Charette, and M. Rigaud. Reduction of ilmenite and ilmenite ores. *Titanium Science and Technology*, 1, 1973.

[26] Jones D.G. Kinetics of gaseous reduction of ilmenite. *J. appl. Chem. Biotech.*, 25:561–582, 1975.

[27] Szekely J., J. W. Evans, and H. Y. Sohn. *Gas-solid Reactions*. Academic Press, New York, 1976.

[28] Spitzer R.H., F.S Manning, and W.O Philbrook. Mixed-control reaction kinetics in the gaseous reduction of hematite. *Transaction of the Metallurgical Society of AIME*, 236(5):726–742, 1966.

[29] R. Merk and CA. Pickles. Reduction of ilmenite by carbon monoxide. *Canadian Metallurgical Quarterly*, 27(3):179–185, 1988.

[30] Zhang G. and O. Ostrovski. Effect of preoxidation and sintering on properties of ilmenite concentrates. *International Journal of Mineral Processing*, 64(4):201 – 218, 2002. URL: `http://www.sciencedirect.com/science/article/pii/S0301751601000552`, `doi:10.1016/S0301-7516(01)00055-2`.

[31] Chen Y. Different oxidation reactions of ilmenite induced by high energy ball milling. *Journal of Alloys and Compounds*, 266:150–154, 1998.

[32] M. Sunde. Organic binder as a substitute for bentonite in ilmenite pelletization. *Department of Material Science and Engineering, NTNU*, 2011.

[33] Sandvik K. L., M. Digre, and T. Malvik. *Oppredning av primære materialer of sekundære råstoffer*. Tapir, Trondheim, 1999.

A Briquettes

The load-strain curves obtained from compression test of briquettes using an Instron 5543 are presented in the following sections.

A.1 No binder

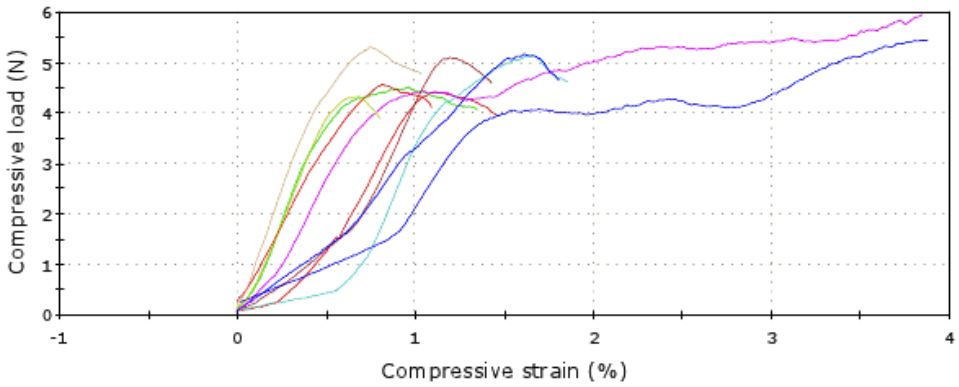

Figure A.1: Load-strain curves from compression test of wet briquettes made without binder.

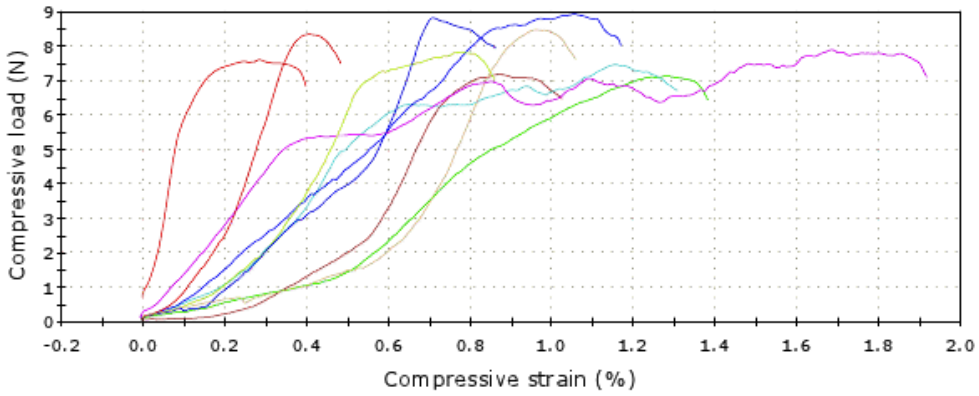

Figure A.2: Load-strain curves from compression test of dry briquettes made without binder.

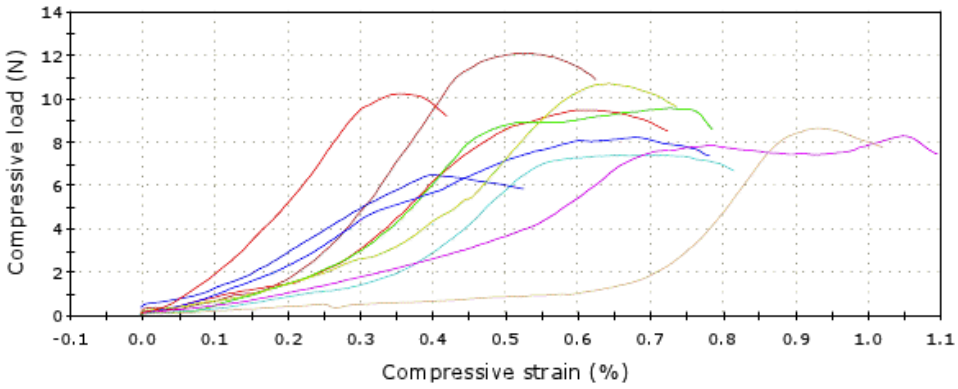

Figure A.3: Load-strain curves from compression test of briquettes made without binder and burnt at 300°C.

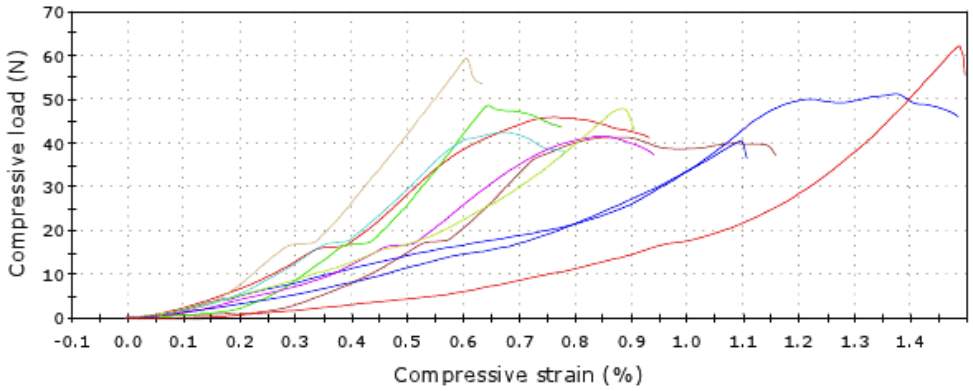

Figure A.4: Load-strain curves from compression test of briquettes made without binder and burnt at 500°C.

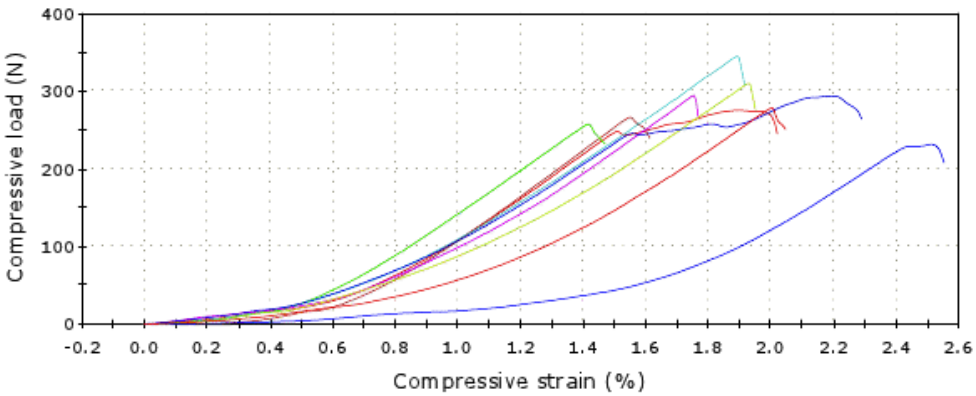

Figure A.5: Load-strain curves from compression test of briquettes made without binder and burnt at 700°C.

A.2 0.1% Peridur 300

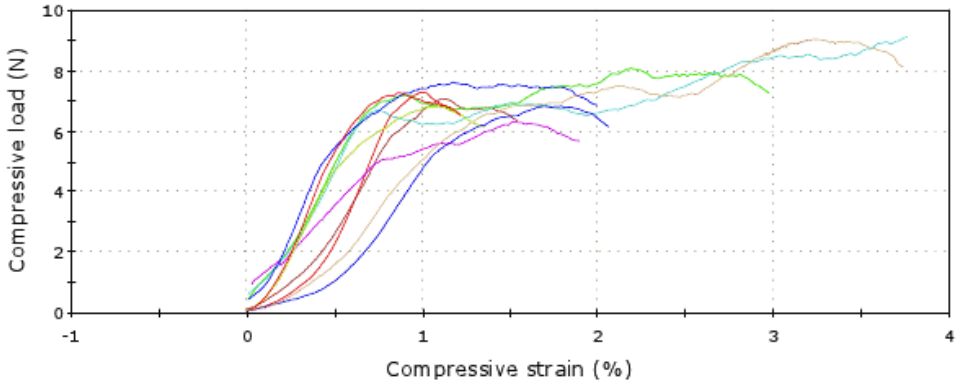

Figure A.6: Load-strain curves from compression test of wet 0.1% Peridur 300 briquttes.

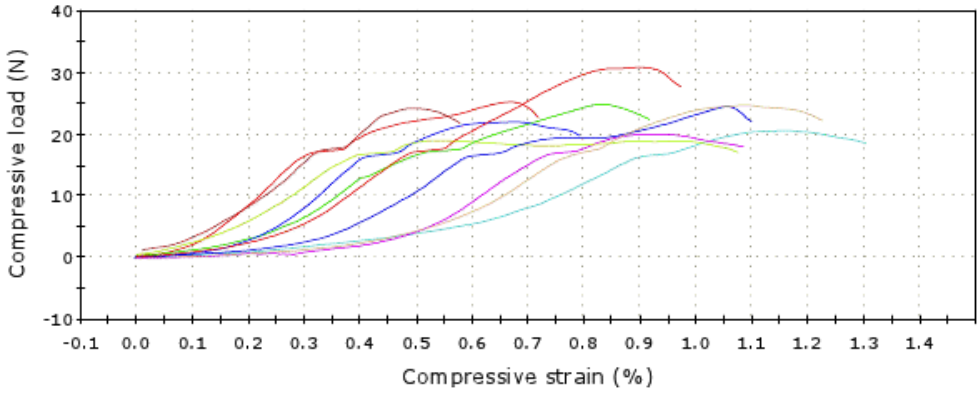

Figure A.7: Load-strain curves from compression test of dry 0.1% Peridur 300 briquttes.

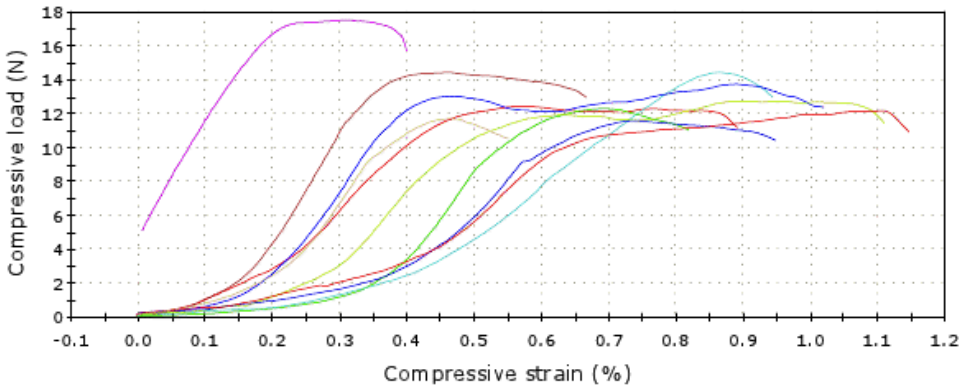

Figure A.8: Load-strain curves from compression test of 0.1% Peridur 300 briquettes burnt at 300°C.

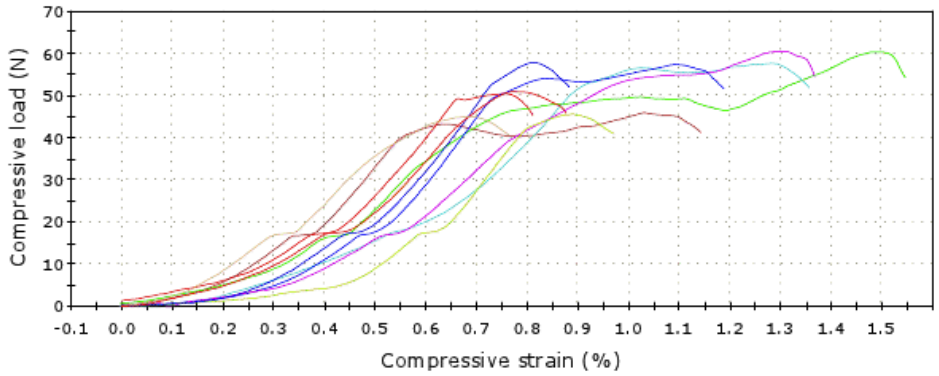

Figure A.9: Load-strain curves from compression test of 0.1% Peridur 300 briquettes burnt at 500°C.

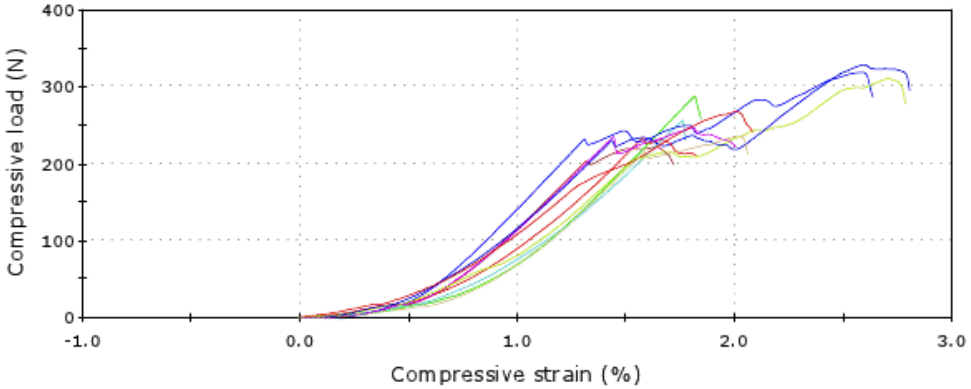

Figure A.10: Load-strain curves from compression test of 0.1% Peridur 300 briquettes burnt at 700°C.

A.3 0.4% Peridur 300

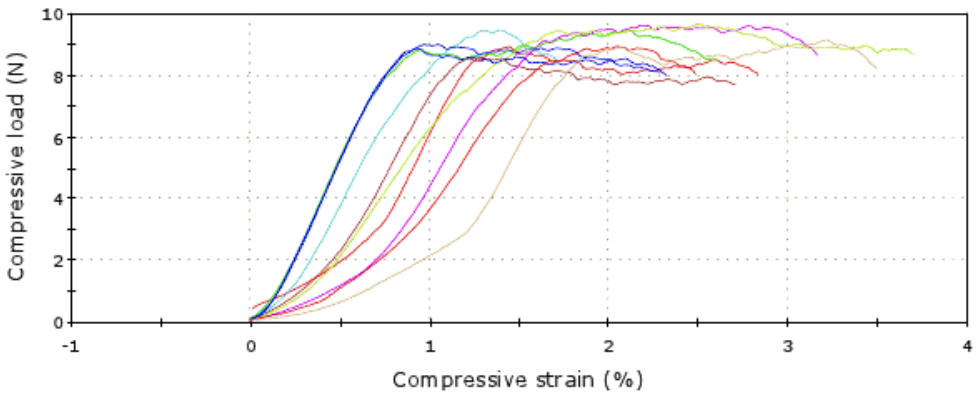

Figure A.11: Load-strain curves from compression test of wet 0.4% Peridur 300 briquettes.

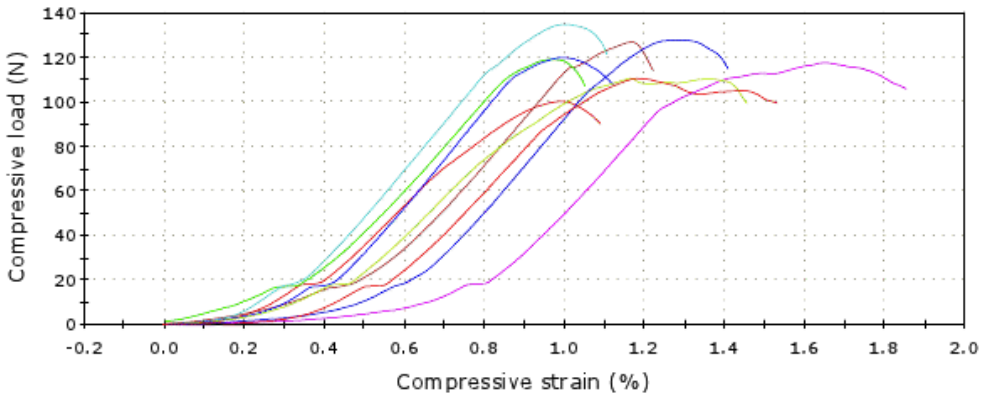

Figure A.12: Load-strain curves from compression test of dry 0.4% Peridur 300 briquettes.

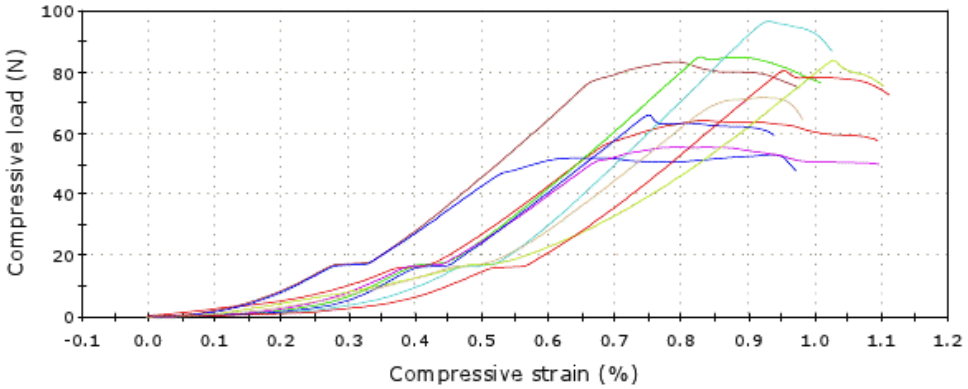

Figure A.13: Load-strain curves from compression test of 0.4% Peridur 300 briquettes burnt at 300°C.

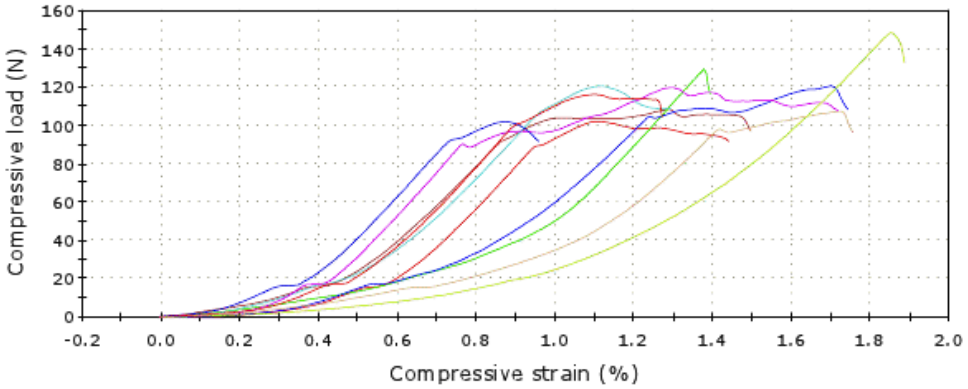

Figure A.14: Load-strain curves from compression test of 0.4% Peridur 300 briquettes burnt at 500°C.

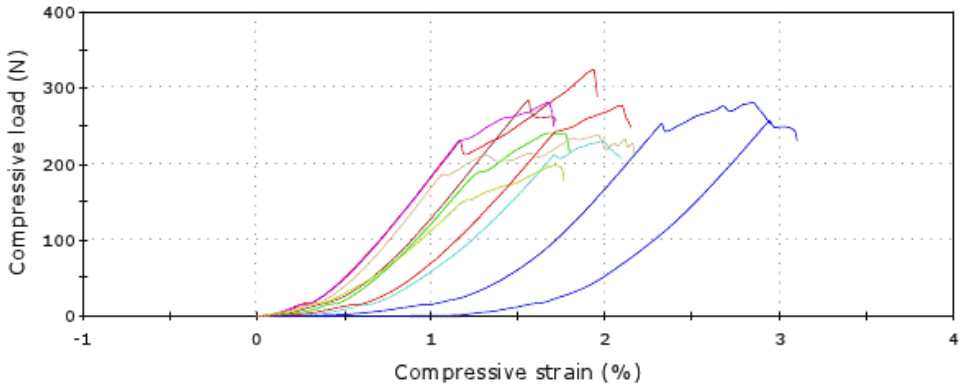

Figure A.15: Load-strain curves from compression test of 0.4% Peridur 300 briquettes burnt at 700°C.

A.4 Bentonite

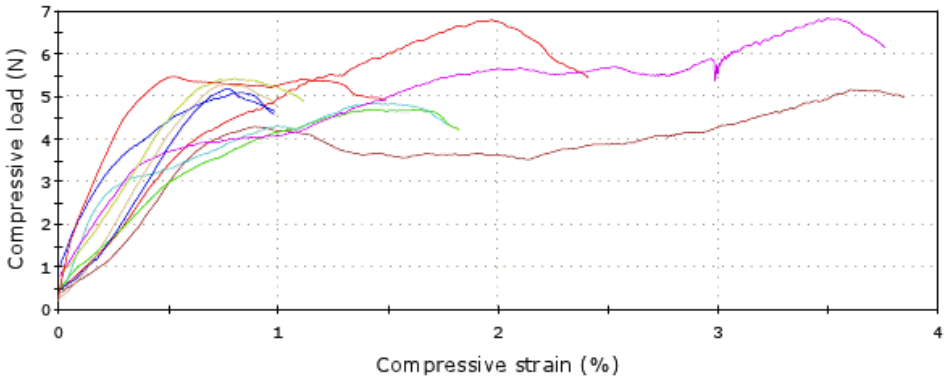

Figure A.16: Load-strain curves from compression test of wet 0.8% bentonite briquettes.

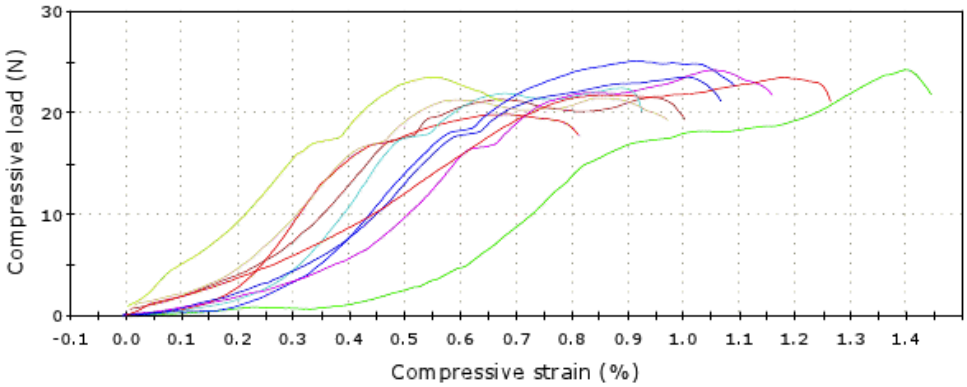

Figure A.17: Load-strain curves from compression test of dry 0.8% bentonite briquettes.

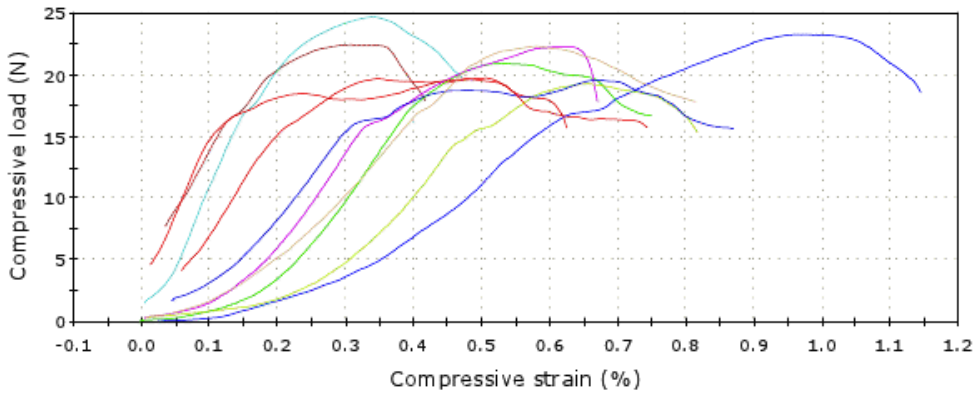

Figure A.18: Load-strain curves from compression test of 0.8% bentonite briquettes burnt at 300°C.

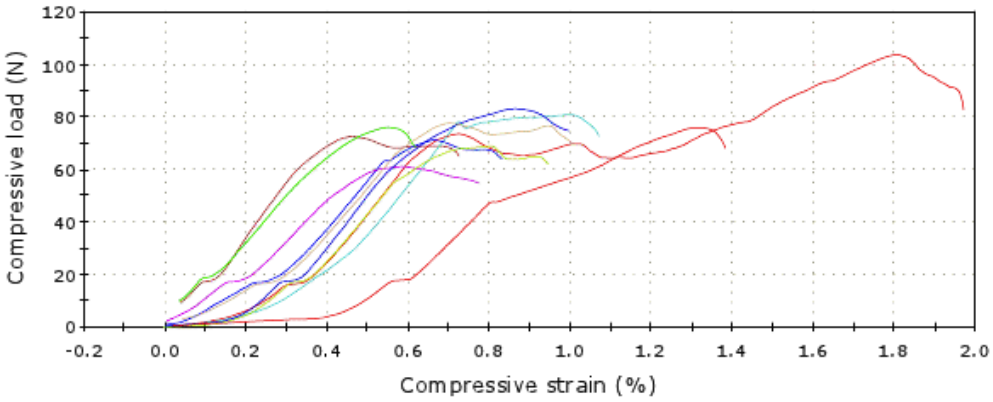

Figure A.19: Load-strain curves from compression test of 0.8% bentonite briquettes burnt at 500°C.

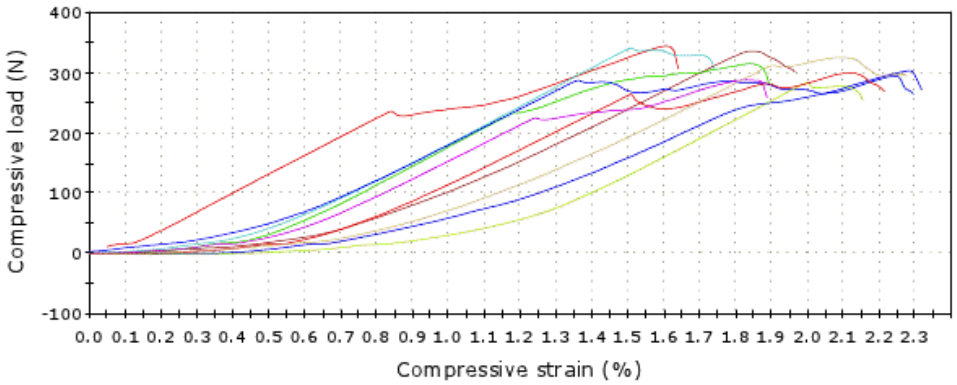

Figure A.20: Load-strain curves from compression test of 0.8% bentonite briquettes burnt at 700°C.

A.5 0.1% Calcium Lignosulfonate

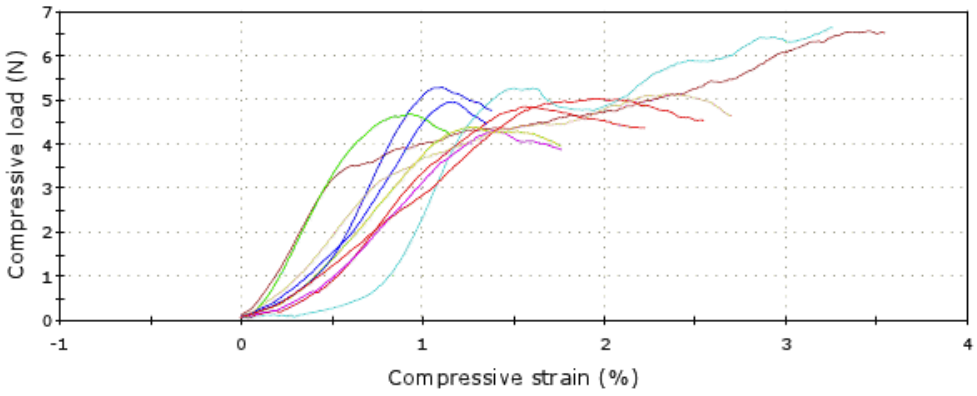

Figure A.21: Load-strain curves from compression test of wet 0.1% calcium lignosulfonate briquettes.

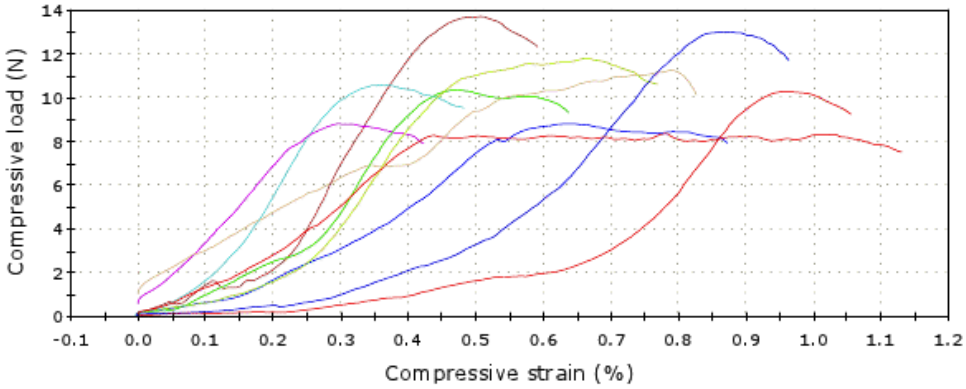

Figure A.22: Load-strain curves from compression test of dry 0.1% calcium lignosulfonate briquettes.

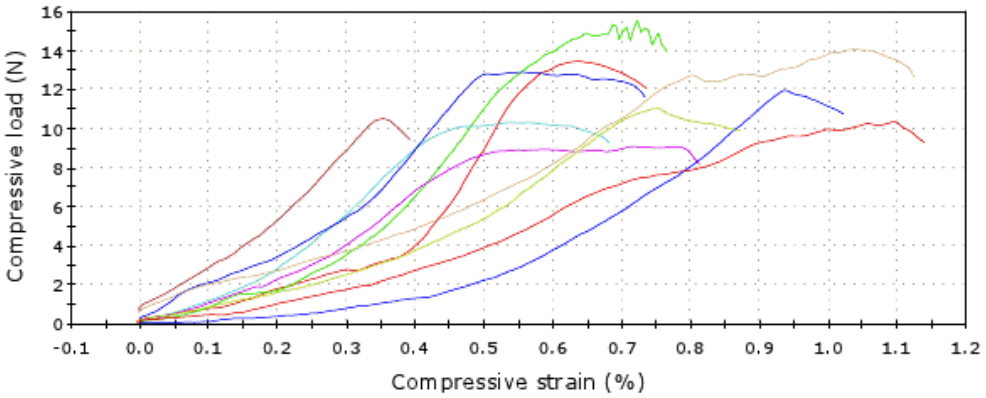

Figure A.23: Load-strain curves from compression test of 0.1% calcium lignosulfonate briquettes burnt at 300°C.

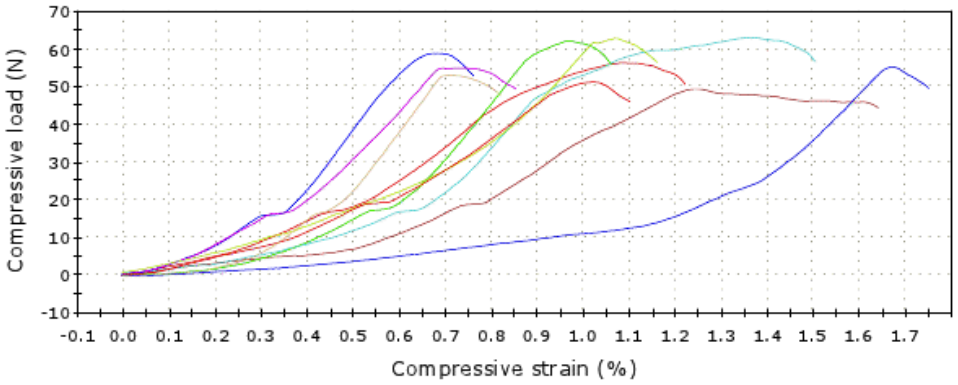

Figure A.24: Load-strain curves from compression test of 0.1% calcium lignosulfonate briquettes burnt at 500°C.

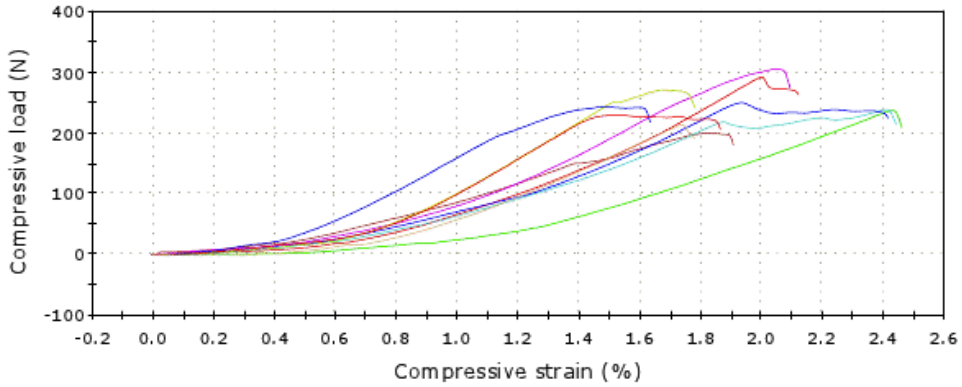

Figure A.25: Load-strain curves from compression test of 0.1% calcium lignosulfonate briquettes burnt at 700°C.

A.6 1% Calcium Lignosulfonate

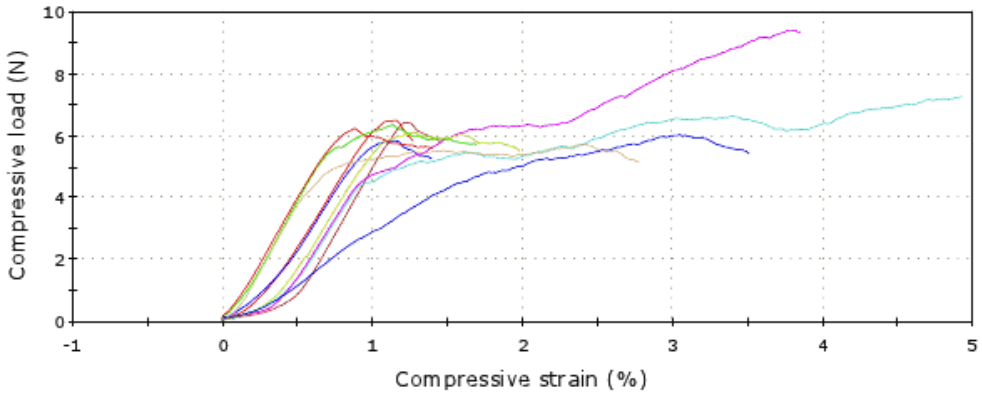

Figure A.26: Load-strain curves from compression test of wet 1% calcium lignosulfonate briquettes.

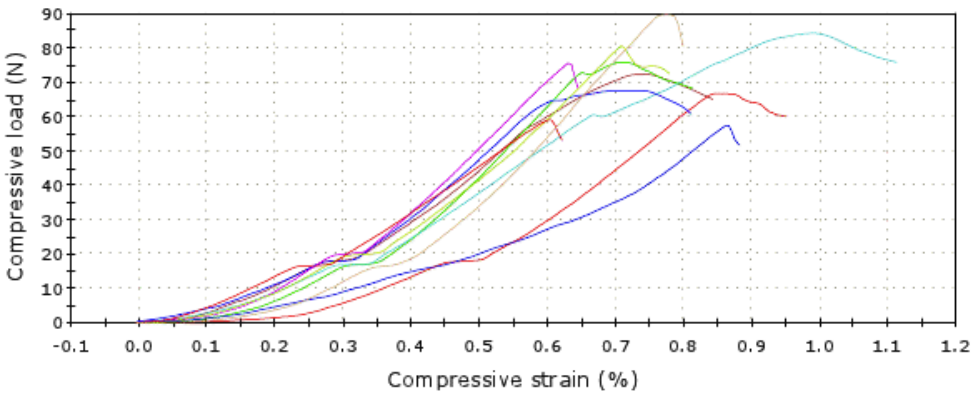

Figure A.27: Load-strain curves from compression test of dry 1% calcium lignosulfonate briquettes.

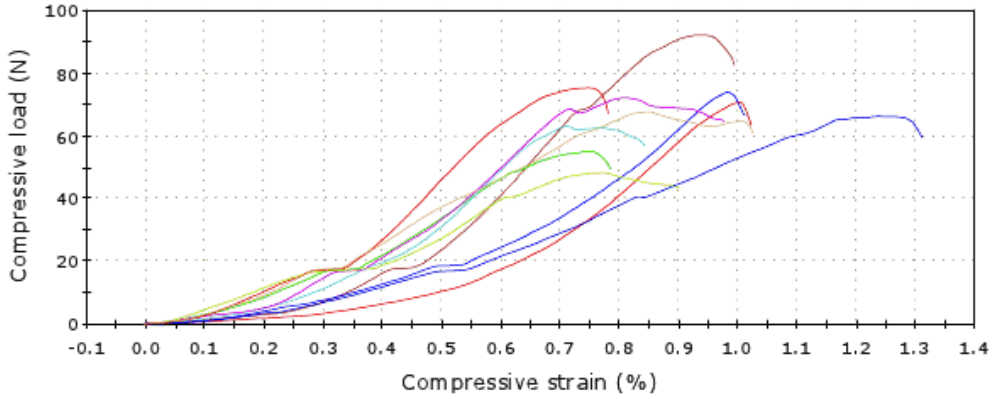

Figure A.28: Load-strain curves from compression test of 1% calcium lignosulfonate briquettes burnt at 300°C.

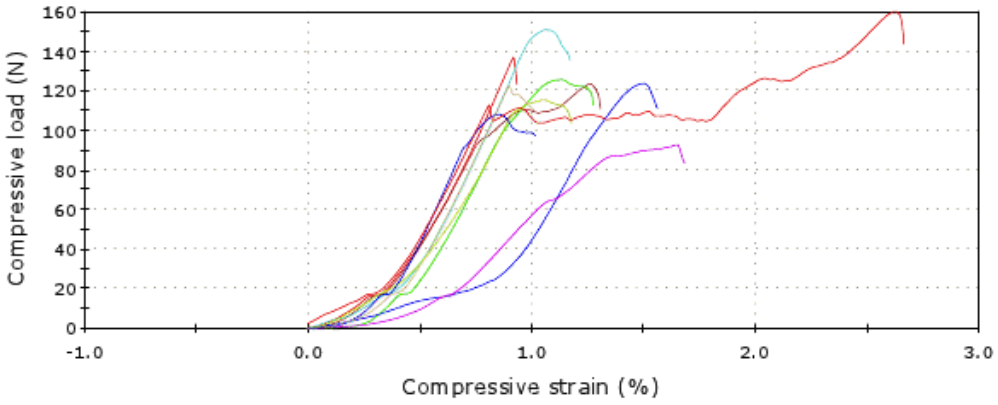

Figure A.29: Load-strain curves from compression test of 1% calcium lignosulfonate briquettes burnt at 500°C.

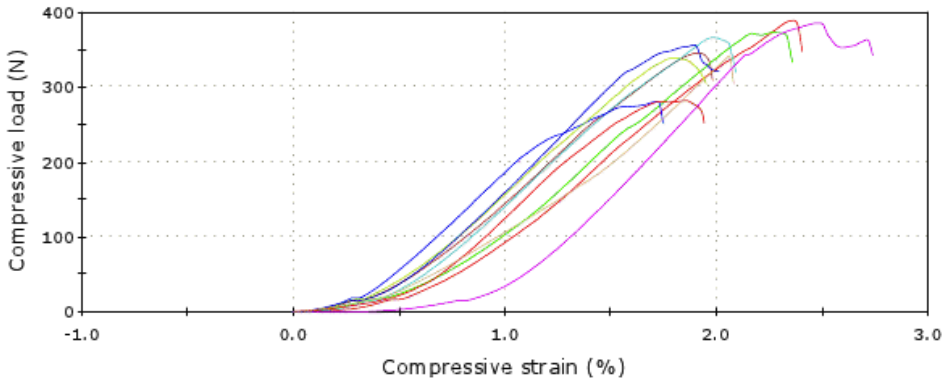

Figure A.30: Load-strain curves from compression test of 1% calcium lignosulfonate briquettes burnt at 700°C.

A.7 Nano cellulose fibre

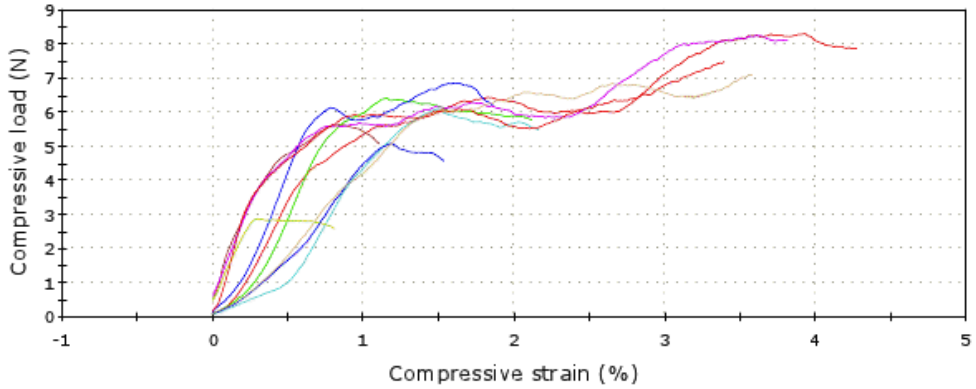

Figure A.31: Load-strain curves from compression test of wet nano cellulose fibre briquettes.

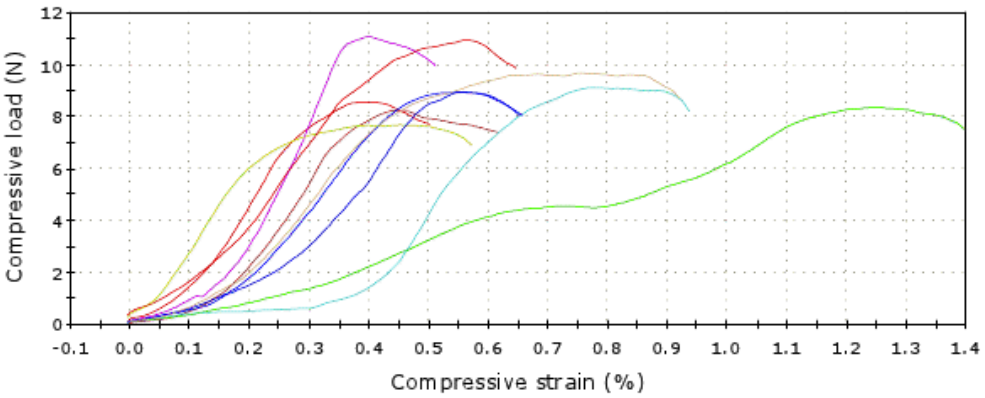

Figure A.32: Load-strain curves from compression test of dry nano cellulose fibre briquettes.

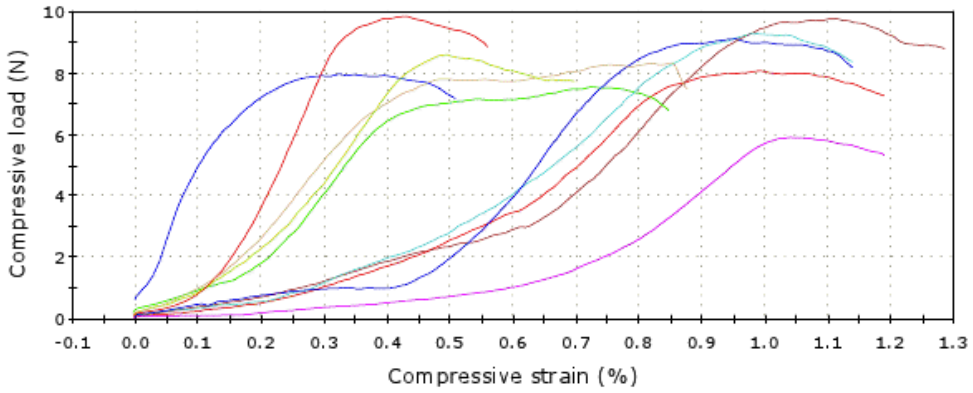

Figure A.33: Load-strain curves from compression test of nano cellulose fibre briquettes burnt at 300°C.

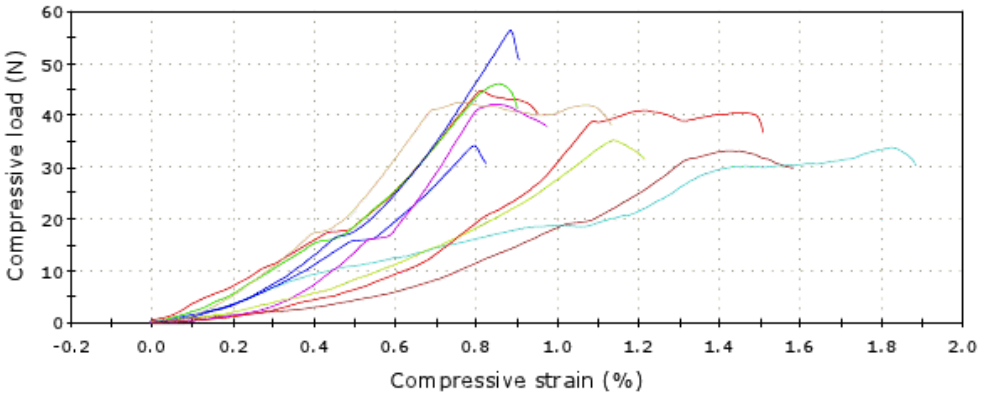

Figure A.34: Load-strain curves from compression test of nano cellulose fibre briquettes burnt at 500°C.

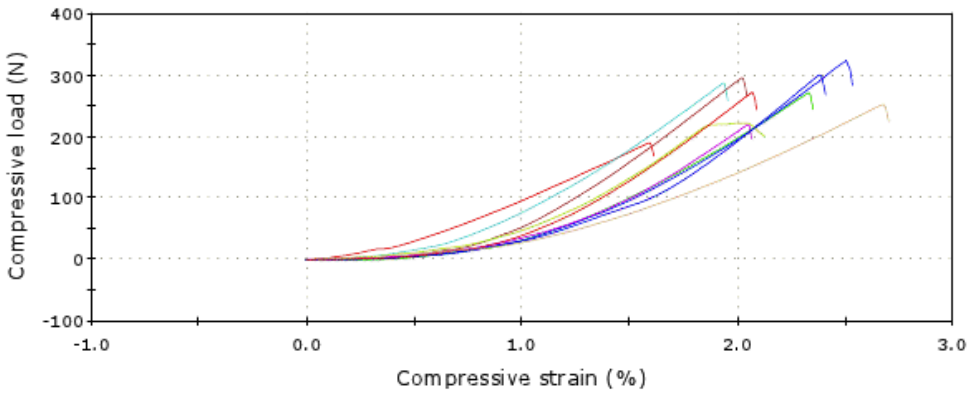

Figure A.35: Load-strain curves from compression test of nano cellulose fibre briquettes burnt at 700°C.

B Pellets

The following sections presents the load-strain graphs obtained from compression test of pellets using an Instron 5543.

B.1 No binder

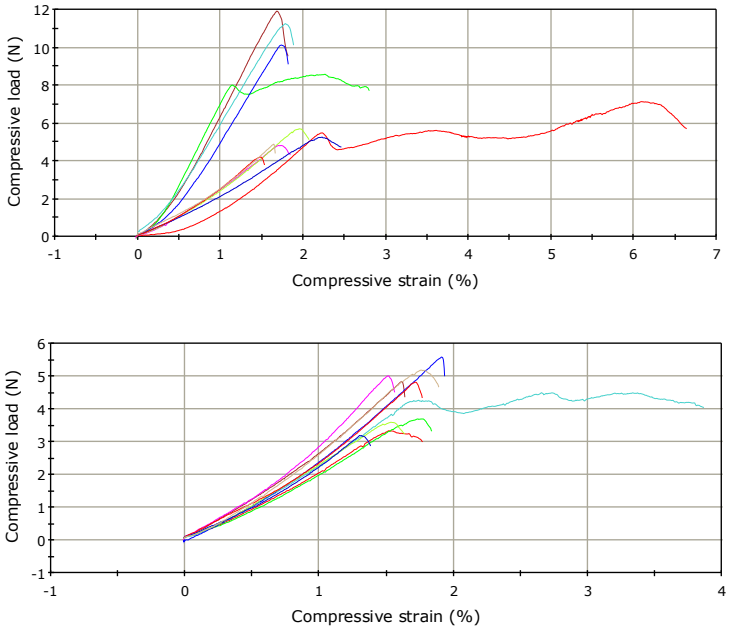

Figure B.1: Load-strain curves from compression test of wet pellets made without binder.

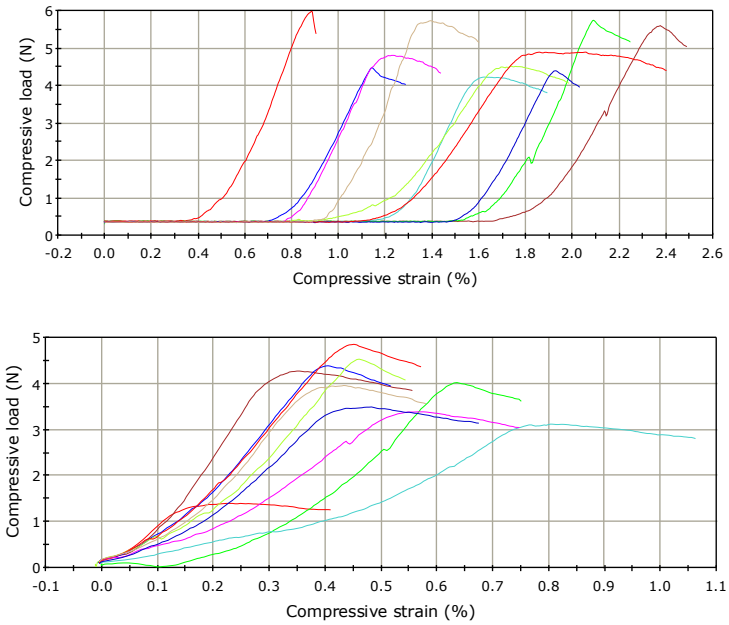

Figure B.2: Load-strain curves from compression test of dry pellets made without binder.

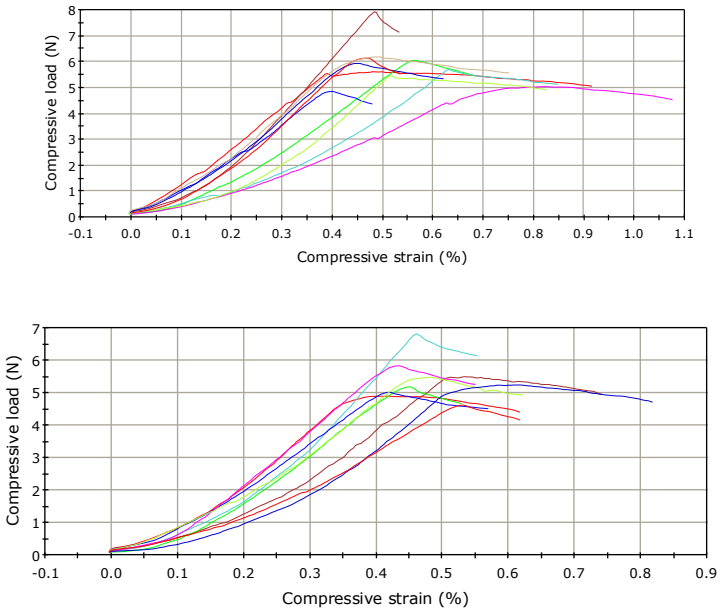

Figure B.3: Load-strain curves from compression test of pellets made without binder burnt at 300°C.

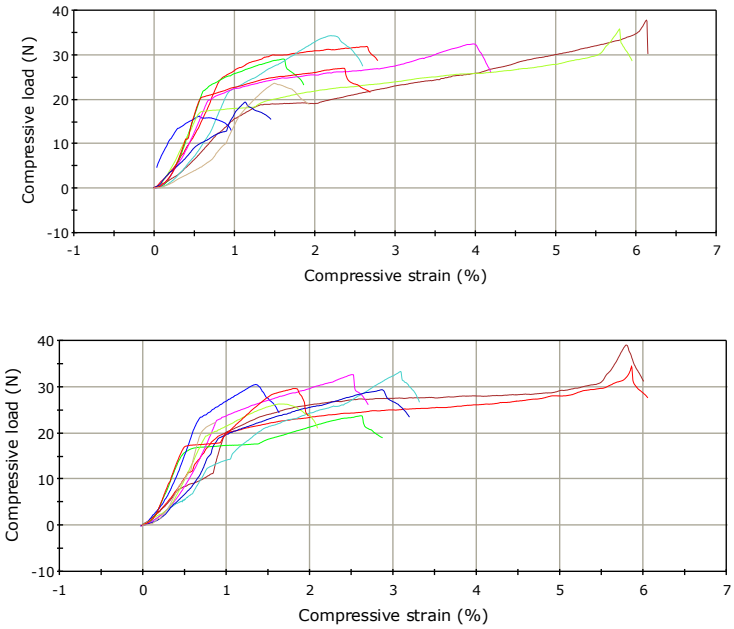

Figure B.4: Load-strain curves from compression test of pellets made without binder burnt at 500°C.

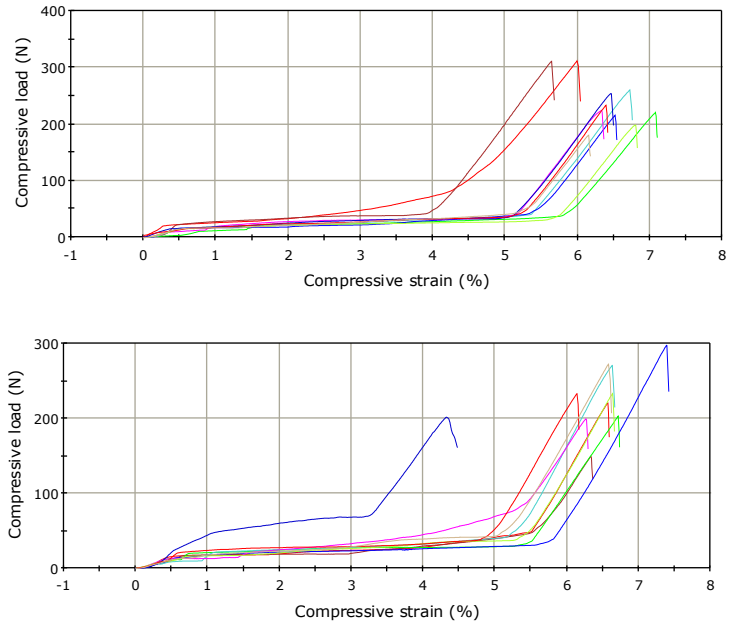

Figure B.5: Load-strain curves from compression test of pellets made without binder burnt at 700°C.

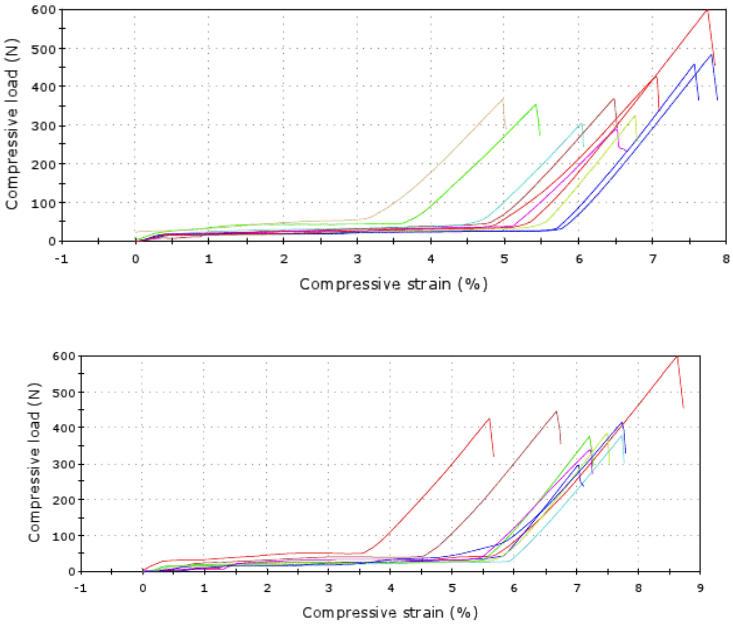

Figure B.6: Load-strain curves from compression test of pellets made without binder burnt at 900°C.

B.2 Peridur 330

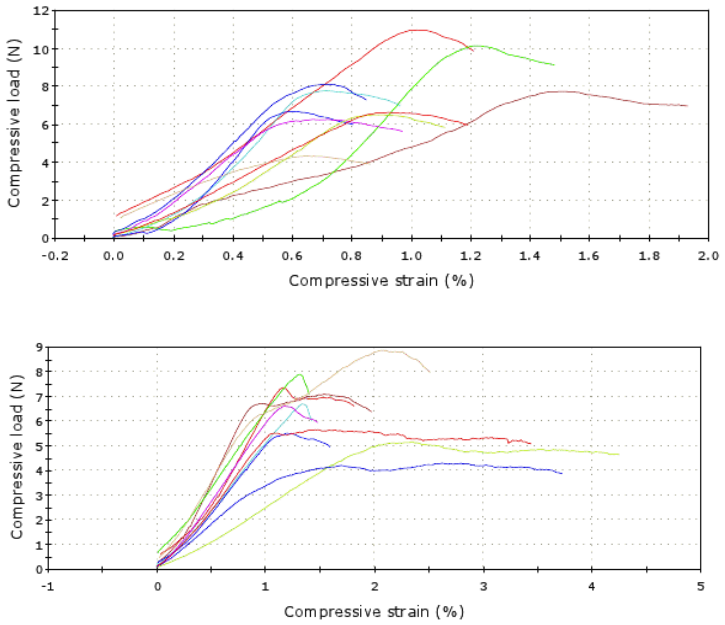

Figure B.7: Load-strain curves from compression test of wet 0.08% Peridur 330 pellets.

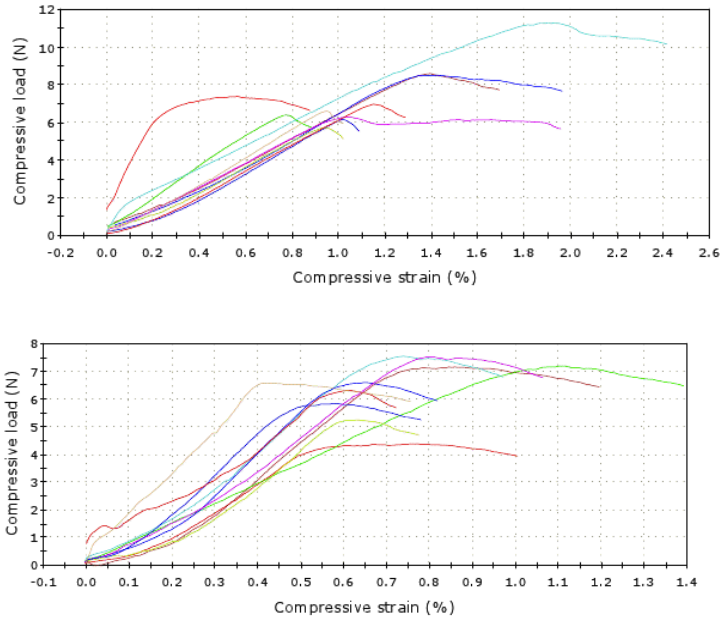

Figure B.8: Load-strain curves from compression test of dry 0.08% Peridur 330 pellets.

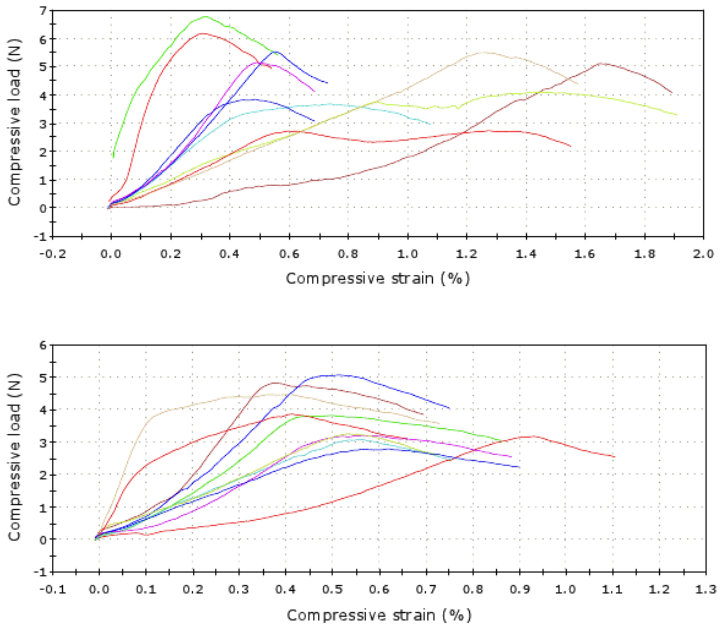

Figure B.9: Load-strain curves from compression test of 0.08% Peridur 330 pellets burnt at 300°C.

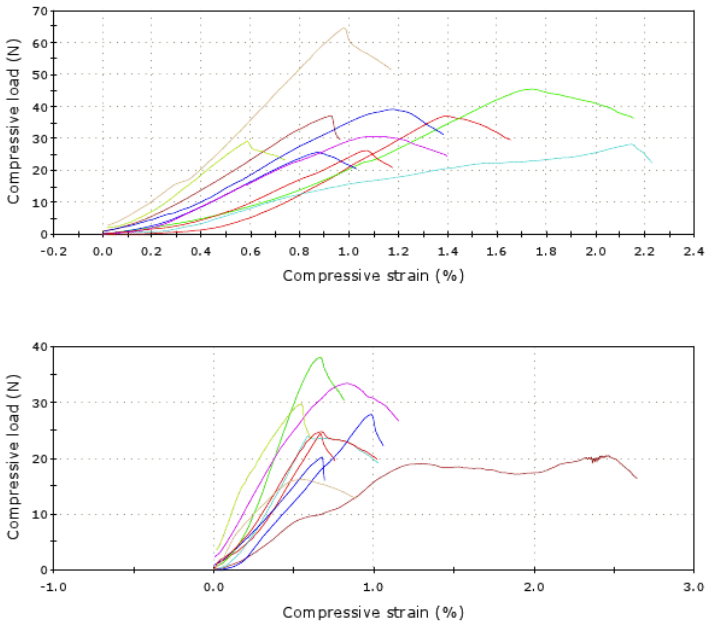

Figure B.10: Load-strain curves from compression test of 0.08% Peridur 330 pellets burnt at 500°C.

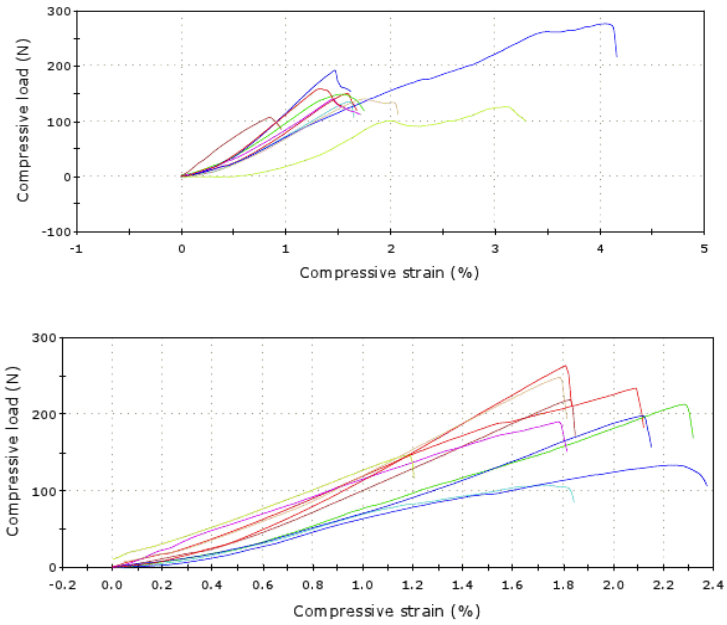

Figure B.11: Load-strain curves from compression test of 0.08% Peridur 330 pellets burnt at 700°C.

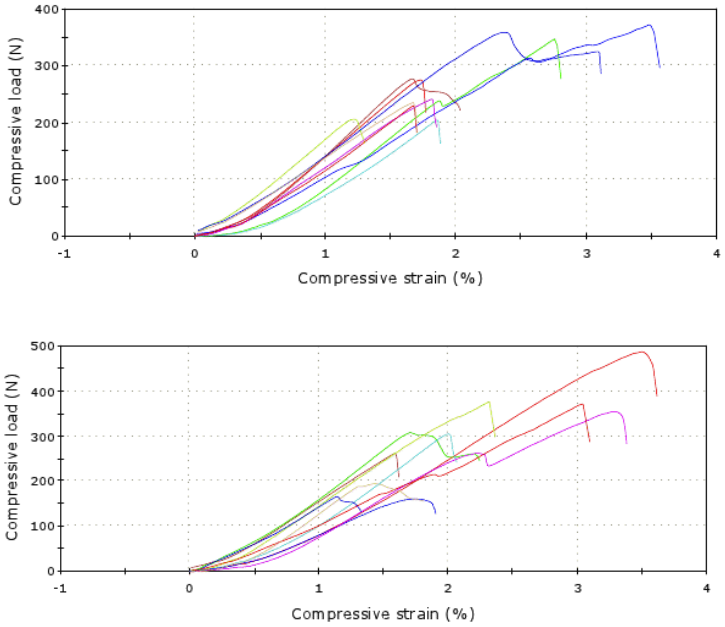

Figure B.12: Load-strain curves from compression test of 0.08% Peridur 330 pellets burnt at 900°C.

B.3 Peridur 300

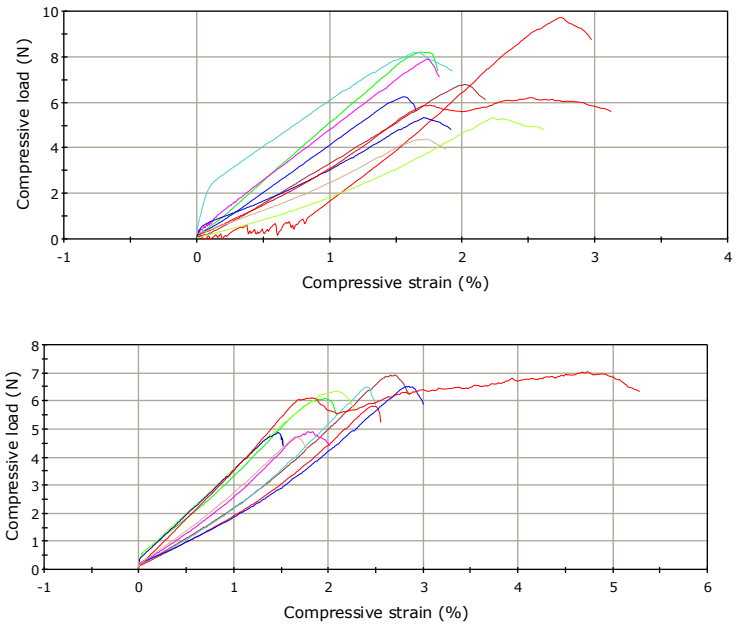

Figure B.13: Load-strain curves from compression test of wet 0.08% Peridur 300 pellets.

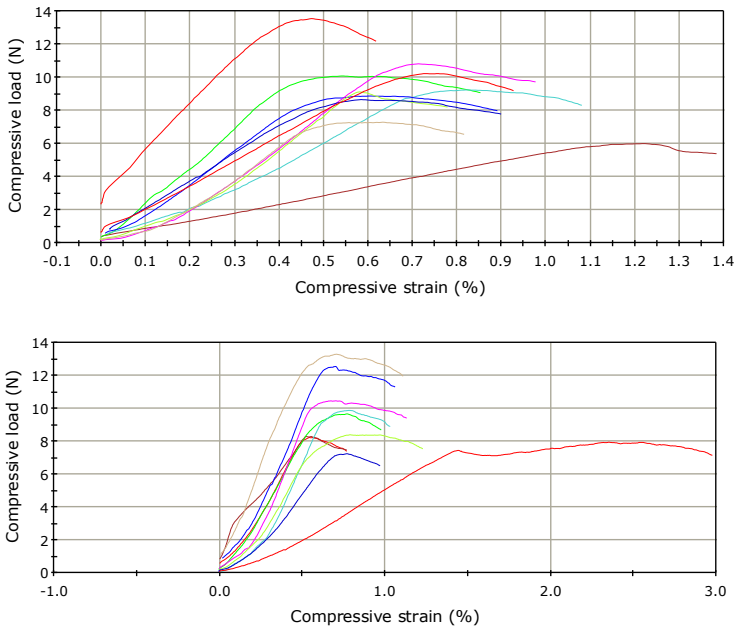

Figure B.14: Load-strain curves from compression test of dry 0.08% Peridur 300 pellets.

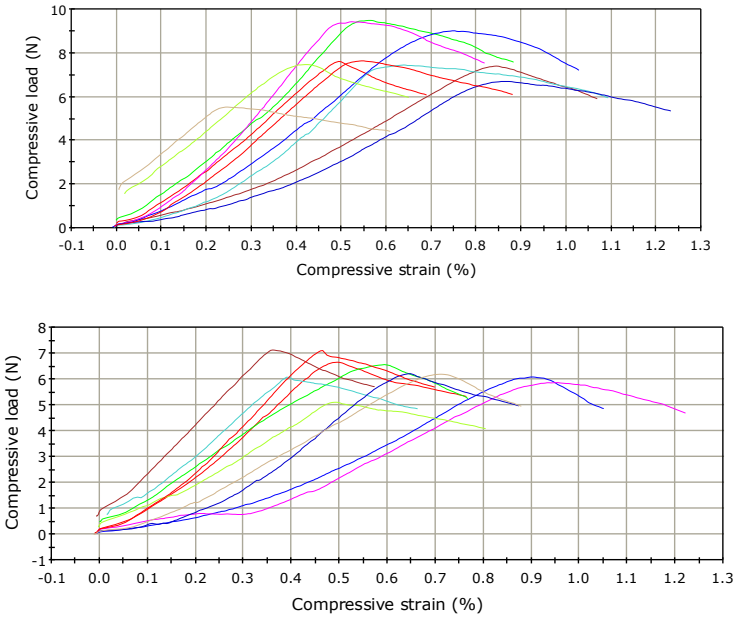

Figure B.15: Load-strain curves from compression test of 0.08% Peridur 300 pellets burnt at 300°C.

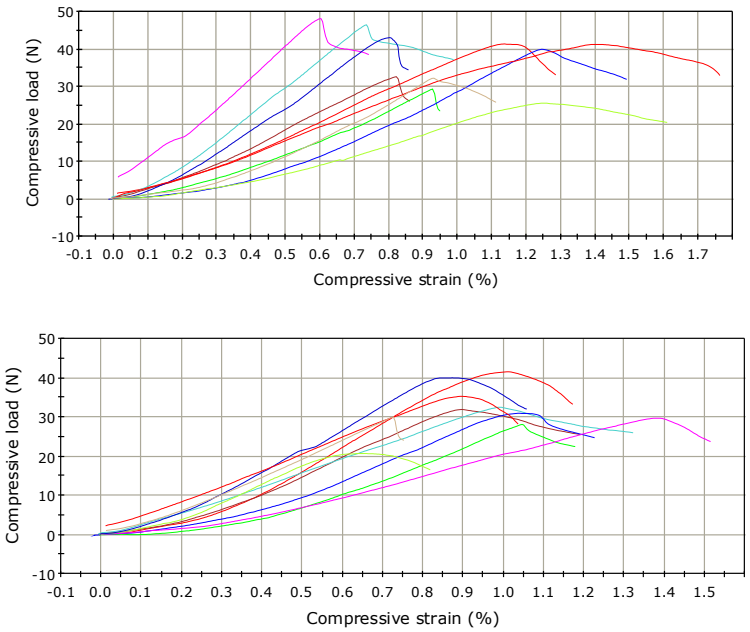

Figure B.16: Load-strain curves from compression test of 0.08% Peridur 300 pellets burnt at 500°C.

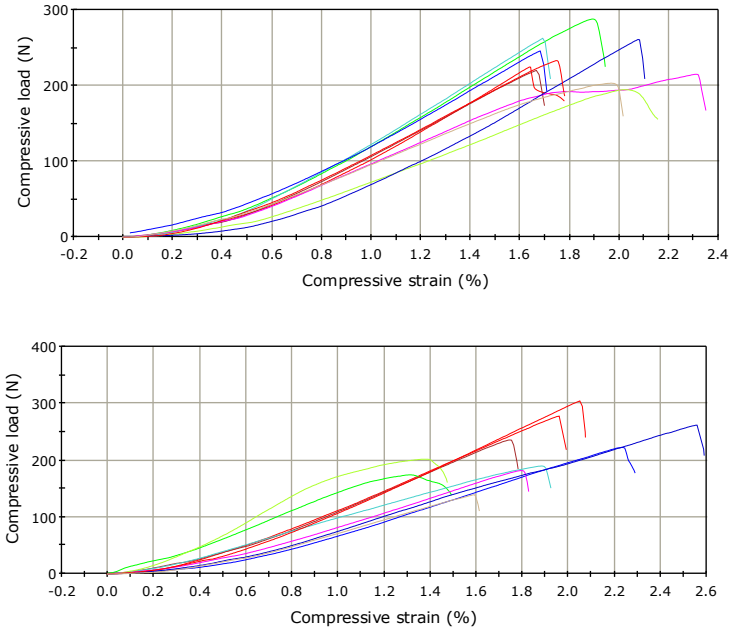

Figure B.17: Load-strain curves from compression test of 0.08% Peridur 300 pellets burnt at 700°C.

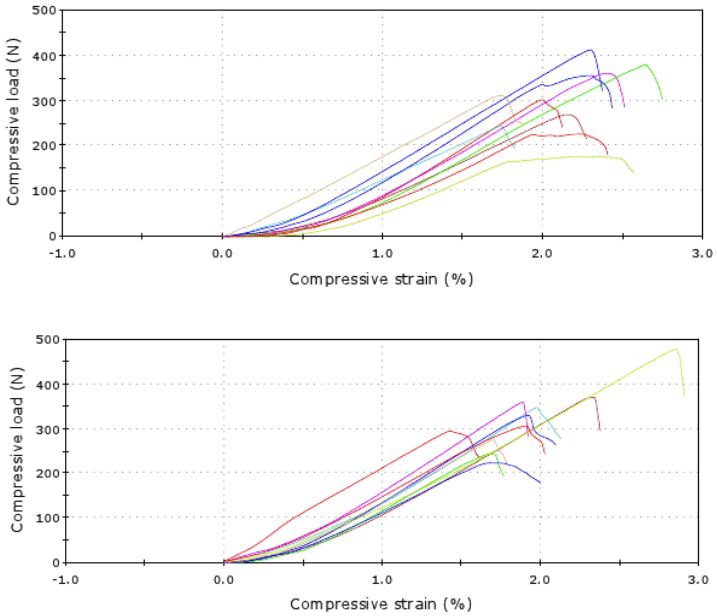

Figure B.18: Load-strain curves from compression test of 0.08% Peridur 300 pellets burnt at 900°C.

B.4 Bentonite

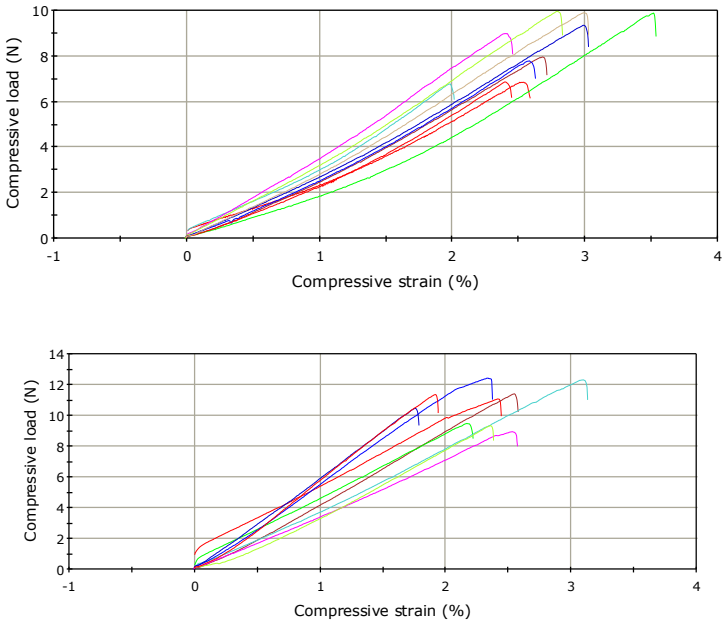

Figure B.19: Load-strain curves from compression test of wet 0.8% bentonite pellets.

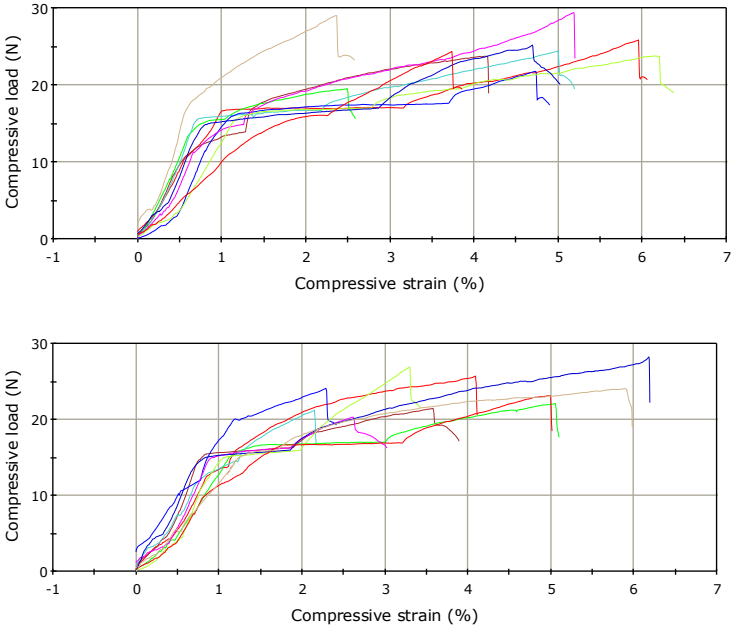

Figure B.20: Load-strain curves from compression test of dry 0.8% bentonite pellets.

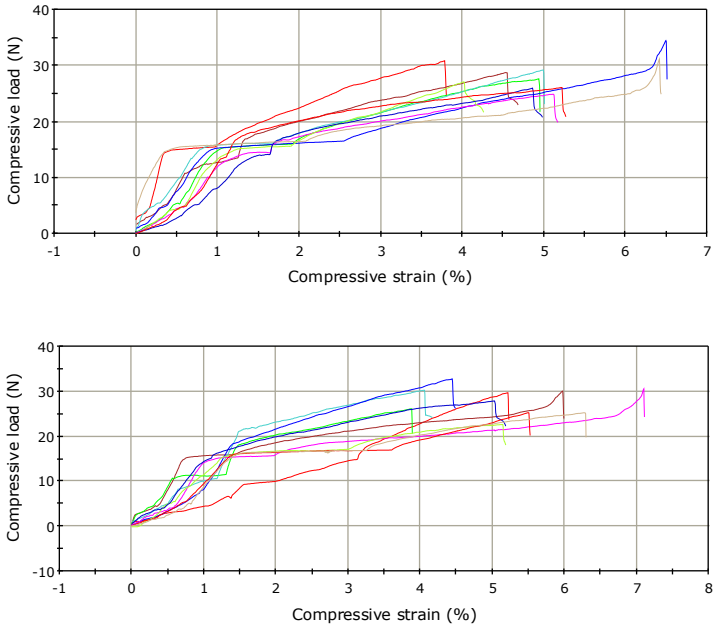

Figure B.21: Load-strain curves from compression test of 0.8% bentonite pellets burnt at 300°C.

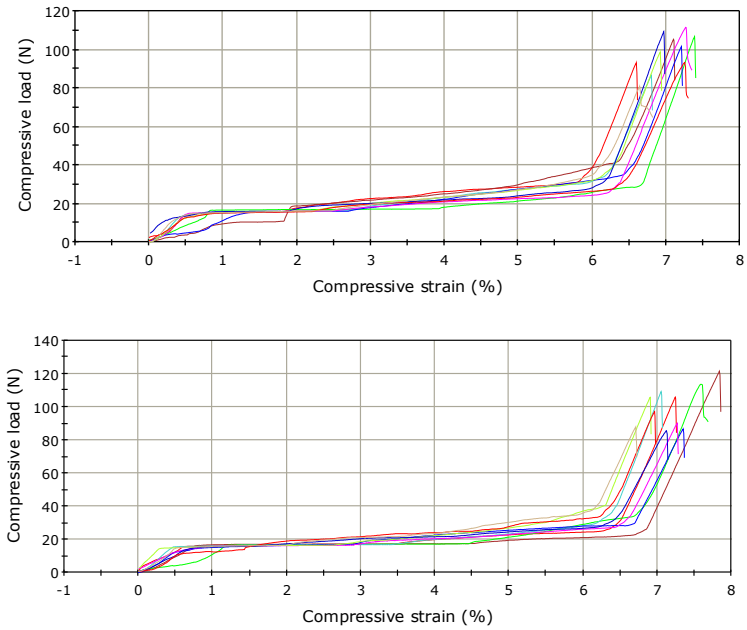

Figure B.22: Load-strain curves from compression test of 0.8% bentonite pellets burnt at 500°C.

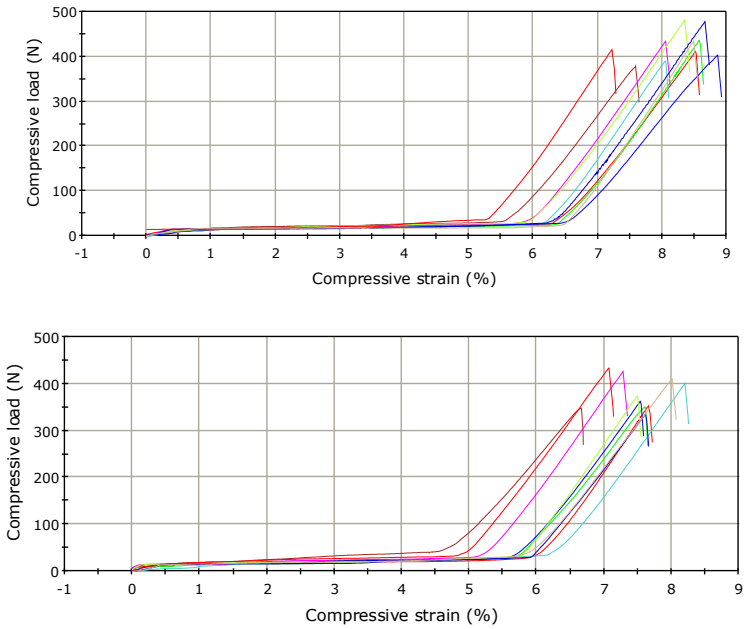

Figure B.23: Load-strain curves from compression test of 0.8% bentonite pellets burnt at 500°C.

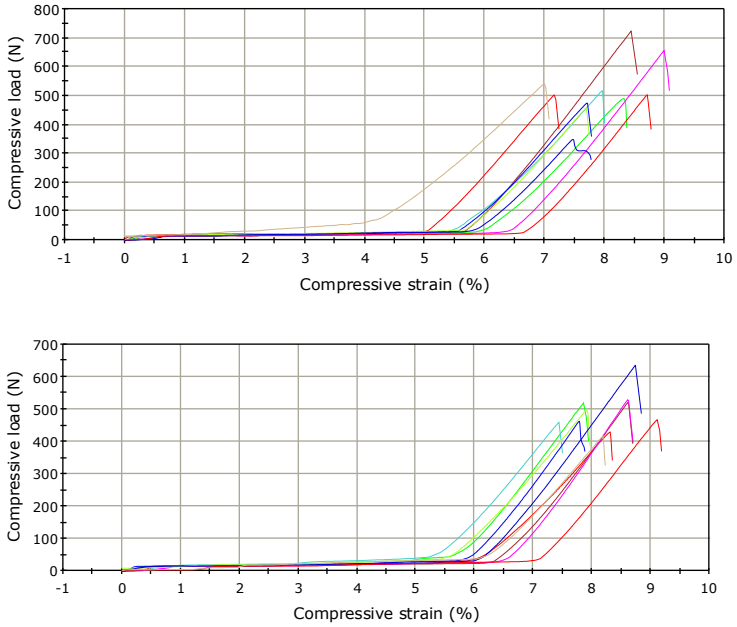

Figure B.24: Load-strain curves from compression test of 0.8% bentonite pellets burnt at 300°C.

B.5 Tyssedal

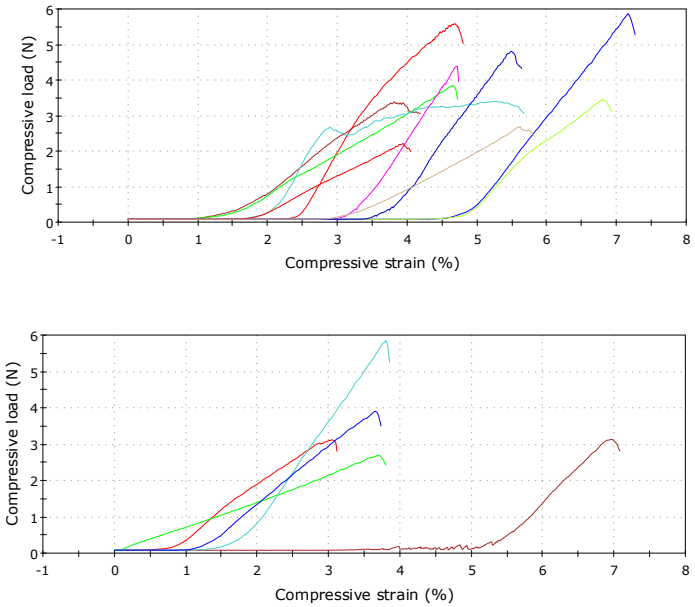

Figure B.25: Load-strain curves from compression test of wet Tyssedal pellets.

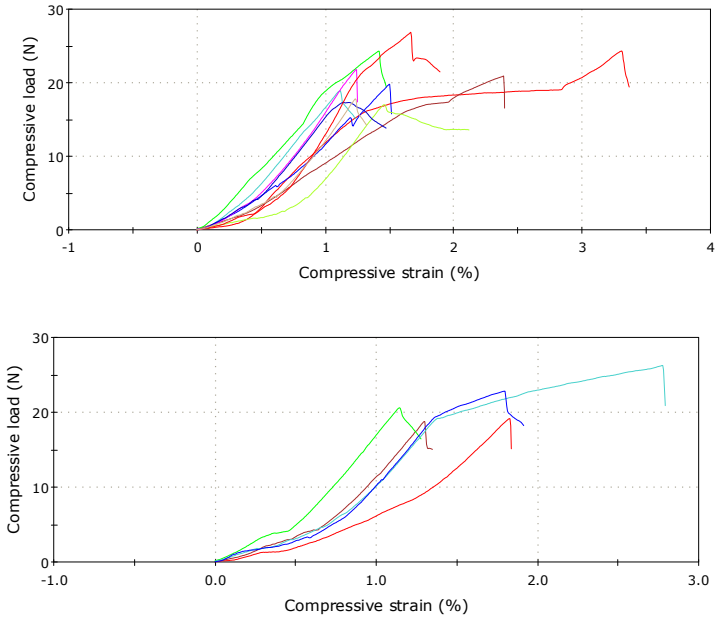

Figure B.26: Load-strain curves from compression test of dry Tyssedal pellets.

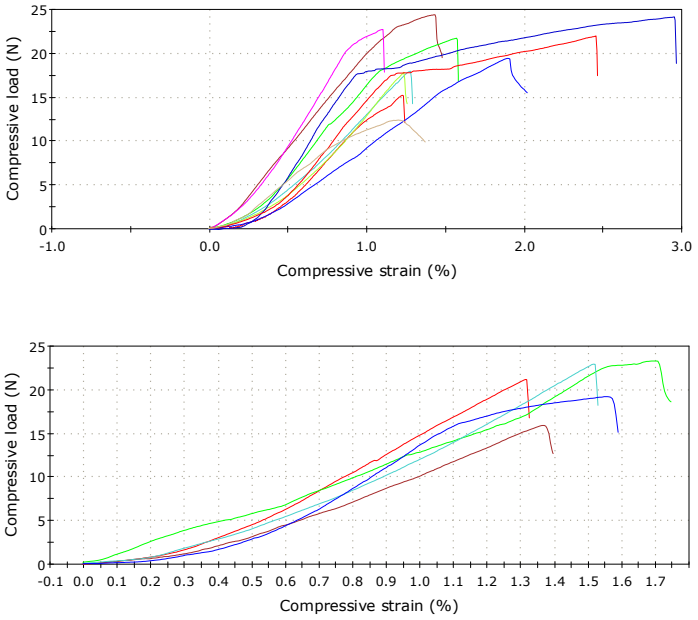

Figure B.27: Load-strain curves from compression test of Tyssedal pellets burnt at 300°C.

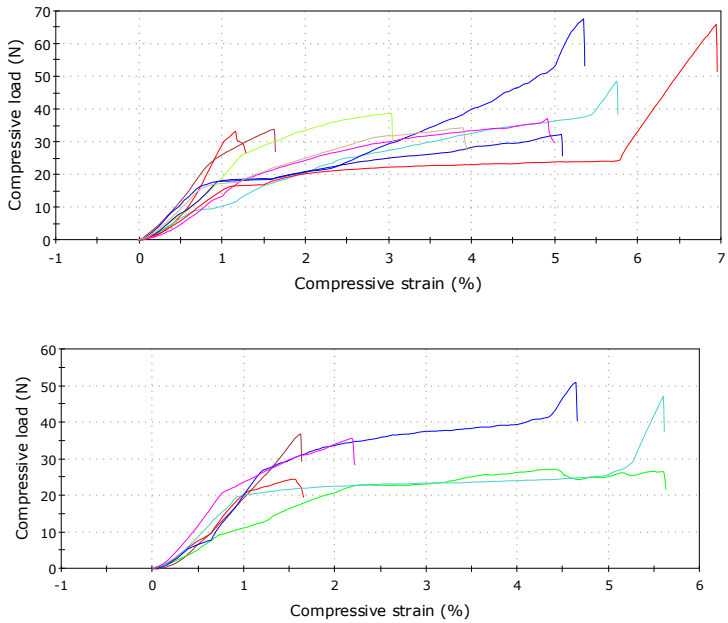

Figure B.28: Load-strain curves from compression test of Tyssedal pellets burnt at 500°C.

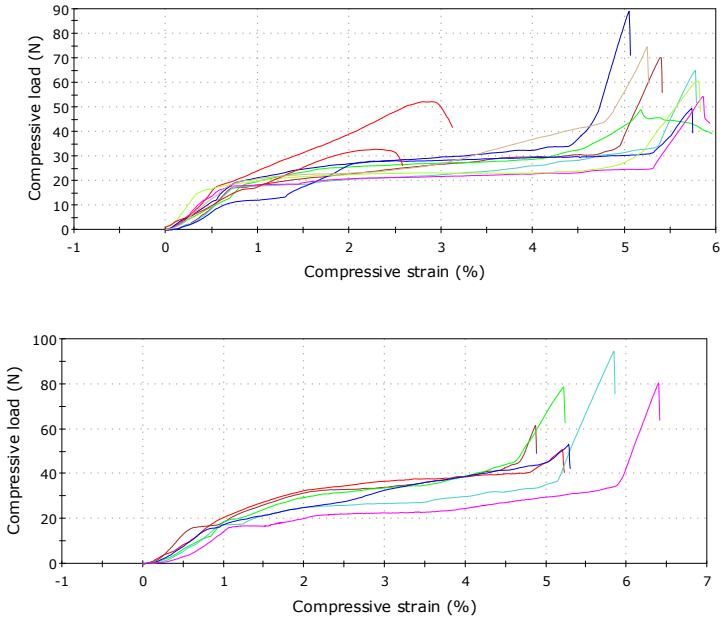

Figure B.29: Load-strain curves from compression test of Tyssedal pellets burnt at 700°C.

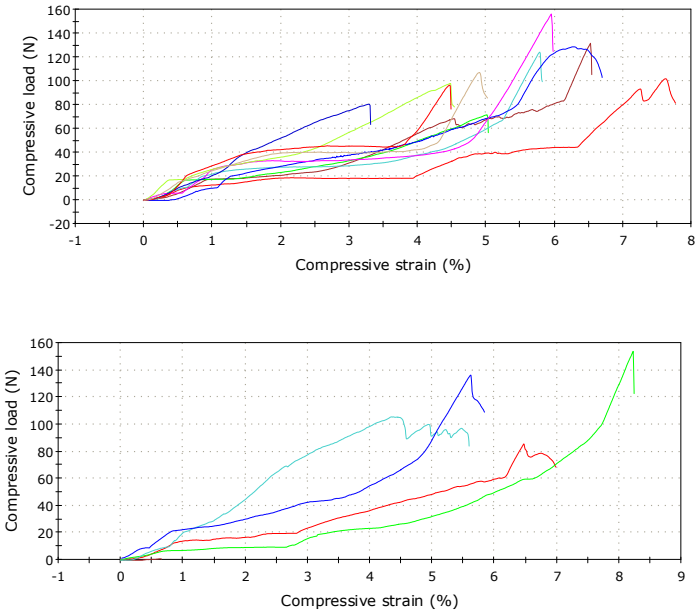

Figure B.30: Load-strain curves from compression test of Tyssedal pellets burnt at 900°C.